Boron, silicon, nitrogen and sulfur-based contemporary precursors for the generation of alkyl radicals by single electron transfer and their synthetic utilization

Vincent Corcé, Cyril Ollivier, Louis Fensterbank

Boron, silicon, nitrogen and sulfur-based contemporary precursors for the generation of alkyl radicals by single electron transfer and their synthetic utilization

Vincent Corcé, Cyril Ollivier, Louis Fensterbank

ARTICLE

Boron, silicon, nitrogen and sulfur–based contemporary precursors for the generation of alkyl radicals by single electron transfer and their synthetic utilization

Received 00th January 20xx,
Accepted 00th January 20xx

DOI: 10.1039/x0xx00000x

Vincent Corcé,*[a] Cyril Ollivier *[a] and Louis Fensterbank *[a]

Recent developments in the use of boron, silicon, nitrogen and sulfur derivatives in single-electron transfer reactions for the generation of alkyl radicals are described. Photoredox catalyzed, electrochemistry promoted or thermally-induced oxidative and reductive processes are discussed highlighting their synthetic scope and discussing their mechanistic pathways.

Introduction

The last decade has witnessed a large number of developments in radical chemistry, mainly based on oxidative or reductive redox processes. This has necessitated the invention of new precursors incorporating a C-heteroatom bond that can readily engage in single-electron transfer (SET) processes and fragment. Consistent with their isodiagonal relationship, boron and silicon derivatives share a lot of common reactivity. More precisely, under an ate form such as for borates or through hypercoordination as in silicates, the resulting low oxidation potentials allow oxidation in very mild photoredox or electrochemistry conditions to generate a variety of alkyl radicals. Of note, activated alkyl trimethysilyl derivatives can also be sources of radicals with stronger oxidants. In contrast, nitrogen- and sulfur-based derivatives depending on their electronic structure can yield to both oxidative and reductive reactivities. This review will focus on the recent development on the engagement of boron, silicon, nitrogen and sulphur derivatives in SET processes. It will restrict to the generation of alkyl radicals and their use in subsequent transformations.

A Alkylboron derivatives

A.1 Alkyl trifluoroborates

Inspired by the seminal work of Kumada and co-workers on the copper(II) oxidation of pentafluorosilicates (see section B for more details), the group of Fensterbank investigated the oxidation of alkyl trifluoroborates.[1] While two previous reports by Nishigaichi[2] and Lemaire[3] suggested the feasibility of this process, it was found that copper(II) was efficient to provide alkyl radicals, as evidenced by the formation of TEMPO adducts from tertiary to primary substrates, the latter requiring harsher conditions (120°C in DMSO instead of rt in Et_2O). The radical character of this transformation was established by radical clocks and Giese type conjugate radical addition was possible. Other oxidants such as Dess-Martin periodinane and tritylium salts[4] proved also to be competent. Recently, the group of Miao showed that silver(I) (Ag_2O) in toluene/H_2O also promotes this type of oxidation.[5] This process could be exploited in radical addition/cyclization tandems on aryl acrylamides[6] and for the synthesis 6-alkylated phenanthridines *via* the addition of alkyl radicals from 2-isocyanobiaryl precursors.[7] A logical step in this chemistry was to devise catalytic oxidation processes. Different approaches have been pursued. For instance, the amount of silver can be rendered catalytic by adding a proper oxidant. This could be applied to the trifluoromethoxylation of alkyl trifluoroborates by using selectfluor as oxidant and trifluoromethyl arylsulfonate as source of OCF_3.[8]

In 2012 and 2013, two seminal reports by Koike and Akita in 2012[9] and by Chen in 2013[10] showed that photoredox catalysis could be used for the oxidation of alkyl trifluoroborates **1** (Scheme 1). In the first one, screening of conditions with benzyl trifluoroborates (E = 0.83 V vs SCE in CH_3CN) in the presence of TEMPO as spin-trapping agent established that $[Ir[dF(CF_3)ppy]_2(bpy)]PF_6$ ($E\ Ir^{III}*/Ir^{II}$ = +1.32V vs SCE in CH_3CN)[11] was the best photocatalyst. Allylic systems gave good results but secondary and primary trifluoroborates reacted very sluggishly, which is consistent with higher oxidation potentials. Interestingly, the corresponding alkyl(triol)borates ($RB(OCH_2)_3CMe^-$) provided better results and Giese type additions could be achieved. The proposed catalytic cycle consists in the reductive quenching of the excited iridium by

[a]Sorbonne Université, CNRS, Institut Parisien de Chimie Moléculaire - 4 Place Jussieu, CC 229, F-75252 Paris Cedex 05, France.
Email : louis.fensterbank@sorbonne-universite.fr ; cyril.ollivier@sorbonne-universite.fr ; vincent.corce@sorbonne-universite.fr

† Footnotes relating to the title and/or authors should appear here.
Electronic Supplementary Information (ESI) available: [details of any supplementary information available should be included here]. See DOI: 10.1039/x0xx00000x

the ate-boron species. The resulting radical is trapped by activated olefin **2** leading to the formation of the Giese-adduct **2a** which is reduced by iridium(II) to recover iridium(III) and generating the anion **2b**. Protonation of this intermediate furnishes the desired addition product **3**. The Koike-Akita group proposed several extensions of this work based on the generation of relatively stabilized radicals, such as the hydroalkoxymethylation[12] or the hydroaminomethylation[13] of electron-deficient alkenes. Nevertheless, as discussed by Molander,[14] because of the irreversible nature of the C-B bond fragmentation, even contra-thermodynamic SETs, meaning mismatched redox potentials, can take place and lead for instance to the generation of cycloalkyl secondary radicals. Moreover, Koike and Akita also showed that the use of a more oxidizing photocatalyst such as the organophotoredox catalyst 9-mesityl-10-methylacridinium salt ([Mes-AcrClO$_4$], Fukuzumi reagent, $E^*_{1/2}$ = +2.06 V vs SCE) allows the oxidation of unactivated primary and secondary substrates and the ensuing radical addition in Giese-type reactions.[15] Meggers and co-workers used a catalytic amount (4 mol%) of chiral bis-cyclometalated indazole rhodium complex (**Λ–RhS**) to perform enantioselective conjugate addition of alkyl radicals, originated from these alkyl trifluoroborates, to electron poor α,β-unsaturated 2-acylimidazoles under blue LEDs irradiation. The chiral rhodium complex acts as both a photocatalyst and a Lewis acid to activate the electron-poor alkenes, and the resulting products exhibit excellent yields (up to 97%) and enantioselectivities (up to 99% ee).[16] In the second study, a deboronative alkynylation was developed based on mixtures of 1.5 equiv of trifluoroborate **1**, 1 equiv of alkynylbenziodoxoles **4**, 0.5 equiv of hydroxybenziodoxole **5** in the presence of Na_2CO_3 and $Ru^{II}(bpy)_3$ as photocatalyst and under blue LEDs irradiation. It relies on the oxidative quenching of $Ru^{II}(bpy)_3$* by the benziodoxole radical **6** ($BI^{\cdot}$). The resulting $Ru^{III}(bpy)_3$ is sufficiently oxidizing to promote the formation of a series of alkyl radicals including unstabilized primary radicals leading to the alkynylation product **7**. Of noticeable value too, the alkynylation process proved to be compatible with physiological conditions and the presence of biomolecules (DNA, proteins, amino acids).

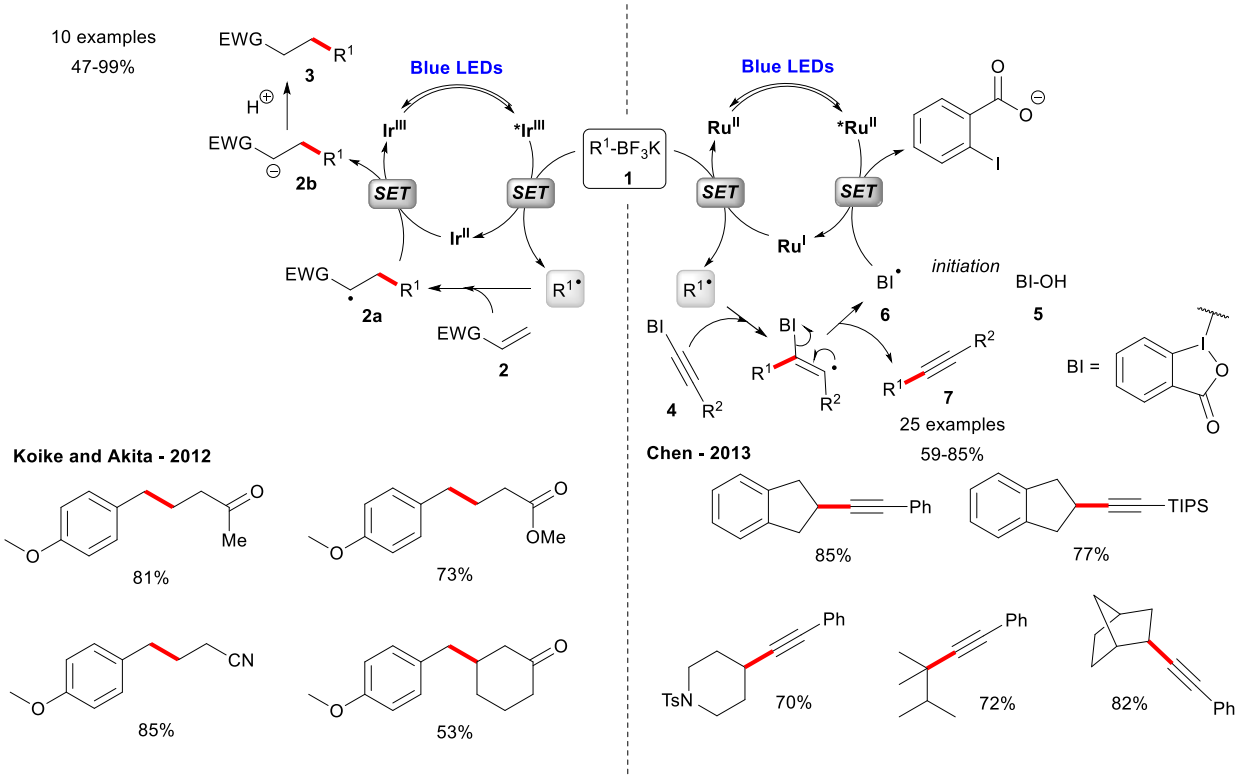

Scheme 1 Giese addition and alkynylation with alkyl potassium trifluoroborates **1**.

Recently, C-H alkylations of heteroarenes such as quinolines, quinazolinones, benzothiazole and purine as well as bioactive compounds (voriconazole, quinine, camptothecin) with organotrifluoroborates by merging photoredox catalysis and electrocatalysis have been developed.[17]

Once these protocols of generation of alkyl radicals have been established, a large number of papers have featured applications notably for radical additions reactions such as the alkylation of benzalaniline[18] This type of reaction could be rendered asymmetric by using α-activated *N*-sulfonylimines or isatin-derived ketimines **8** as radical acceptors as well as easily reduced benzyl trifluoroborates **9** as reagents to give a range of chiral amines **10** featuring a quaternary center with ee's up to 98% (Scheme 2).[19]

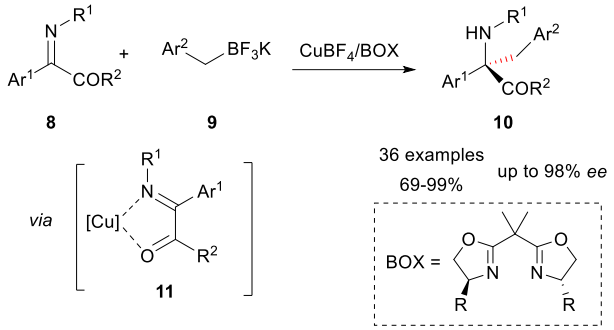

Scheme 2 Copper-assisted asymmetric addition on imine with alkyl trifluoroborate.

The key point of this approach was to use readily available copper(II)-Box complexes **11** which serve as bifunctional catalysts that are involved both in the photoredox process to give the benzyl radicals as well as the asymmetric catalysis through the bidentate N,O complexation of the substrate to copper(II). Presumably, an intermediate Box-Cu(II)-benzyl complex is formed. As suggested by Reiser's work,[20] the latter homolytically cleaves under blue LEDs light which liberates the radical entity and a Cu(I) complex that reduces the aminyl radical originating from the intermolecular addition.

In contrast to the two-electrons multicomponent Petasis reaction involving boronic acids, a photoredox-catalyzed version with alkyltrifluoborates was developed by Molander and co-workers.[21] Thus, a series of primary to tertiary alkyl trifluoroborates could react with aromatic aldehydes and aniline derivatives to provide secondary amines, via the radical addition to an imine. A representative example is given with the preparation of an advanced intermediate of a Pfizer glucagon receptor modulator from aldehyde **12**, amine **13** and cyclohexyl trifluoroborate **14** (Scheme 3).

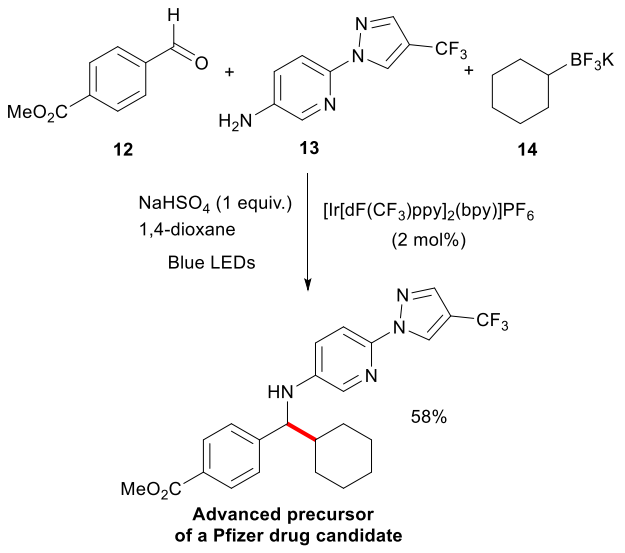

Scheme 3 Multicomponent Petasis reaction for the preparation of advanced drug precursor with cyclohexyl trifluoroborates **14**.

When Ir(III) or 4CzIPN is used as photocatalyst, the generated Ir(II) or 4CzIPN$^{-\bullet}$ radical anion resulting from the SET with the borate is a highly reducing species which can be utilized to generate valuable intermediates that can further react in an interesting manner. For instance, Molander could devise radical/polar cyclopropane formation. The general scheme relies on the initial radical addition derived from alkyl trifluoroborates **15** onto an olefin **16** bearing a leaving group in homoallylic position (Scheme 4).[22] The radical resulting from the addition is reduced by 4CzIPN$^{-\bullet}$ and intramolecular cyclization provides the cyclopropane moiety **17**. It should be noted that this reaction works also with silicates and 4-alkyldihydropyridines.

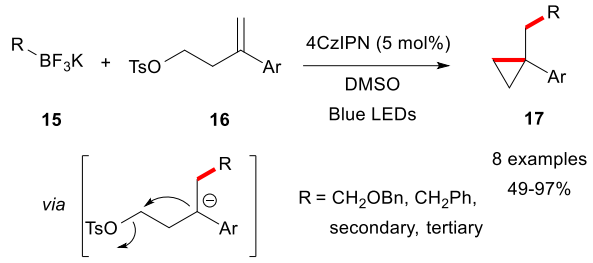

Scheme 4 Formation of cyclopropanes by radical/polar crossover reactions from alkyl trifluoroborates **15** and functionalized alkenes **16**.

Another opportunity provided by the Ir(II) reduction is to generate a ketyl radical anion from ketones **18** that can presumably react through radical coupling with the benzyl radical derived from the organotrifluoroborate **19** leading to coupling adducts **20** (Scheme 5).[23] Of note also, benzyl trifluoroborates can be oxidized to benzaldehydes in flow conditions.[24]

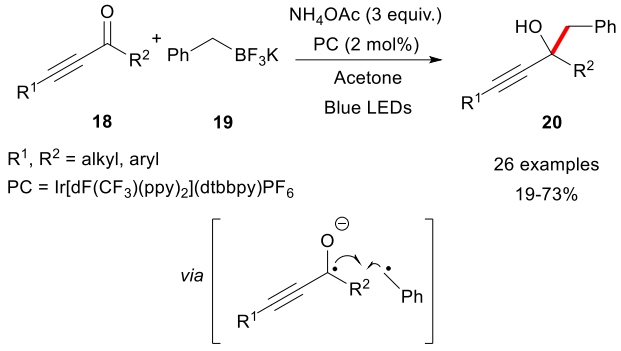

Scheme 5 Radical-radical coupling between ketyl radical anion and benzyl radical derived from benzyl trifluoroborate **19**.

In 2014, two seminal reports by the Doyle and MacMillan groups[25] and the Molander group[26] focused on the merging of photoredox catalysis with nickel catalysis using respectively carboxylate and trifluoroborate precursors **21**. Based on two intertwined catalytic cycles shown on scheme 6, the cross coupling of an alkyl radical **21a** with an aryl halide **22** electrophile is rendered possible, yielding to the cross-coupling product **23**. This single-electron transmetallation as coined by

Molander has been at the origin of intense synthetic developments, however it should be noted that the mechanism of the nickel cycle remains elusive. As drawn, addition of the alkyl radical **21a** onto the intermediate Ar-Ni(II)-X complex **B** to provide a Ni(III) complex **C** that undergoes reductive elimination is a likely pathway. But an alternative pathway involving the oxidative addition of Ar-X **22** onto a R-Ni(I) **E** complex to generate the same Ni(III) complex **C** has also been considered. Calculations by Kozlowski[27] could not distinguish between both pathways. A few selected applications of these new cross-coupling reactions are presented below.

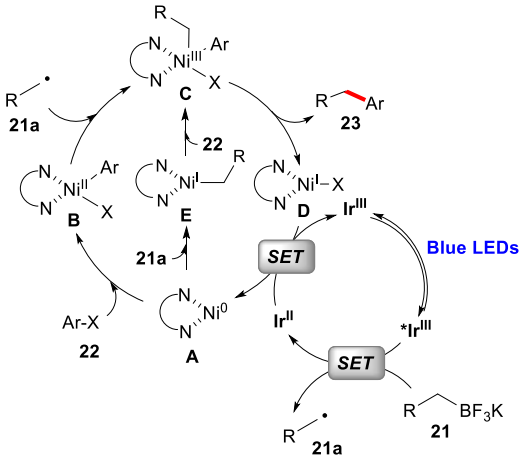

Scheme 6 Proposed mechanistic pathways for the dual photoredox and nickel catalysis.

β-Glycosyl trifluoroborates can serve as precursors for the synthesis of 2-deoxy-α-C-glycosides via α-C glycosylation using aryl- and vinyl-halide electrophiles.[28] Three-component olefin dicarbofunctionalization has been worked out based on the mixing of a tertiary alkyl trifluoroborate **24**, a vinylboronate **25** as radical acceptor and an arylbromide **26** (Scheme 7).[29] The success of this sequence relies on the poor reactivity of tertiary radicals with nickel which suppresses the direct cross-coupling. Instead, the rate of addition of these entities to the vinylboronate partner is high and the resulting secondary radical can engage in the cross coupling. Fair to good yields of cross-coupling products **27** were obtained, featuring also the use of other Giese acceptors such as acrylate and acrylonitrile. Secondary alkyl derivatives were used but showed limited efficiency.

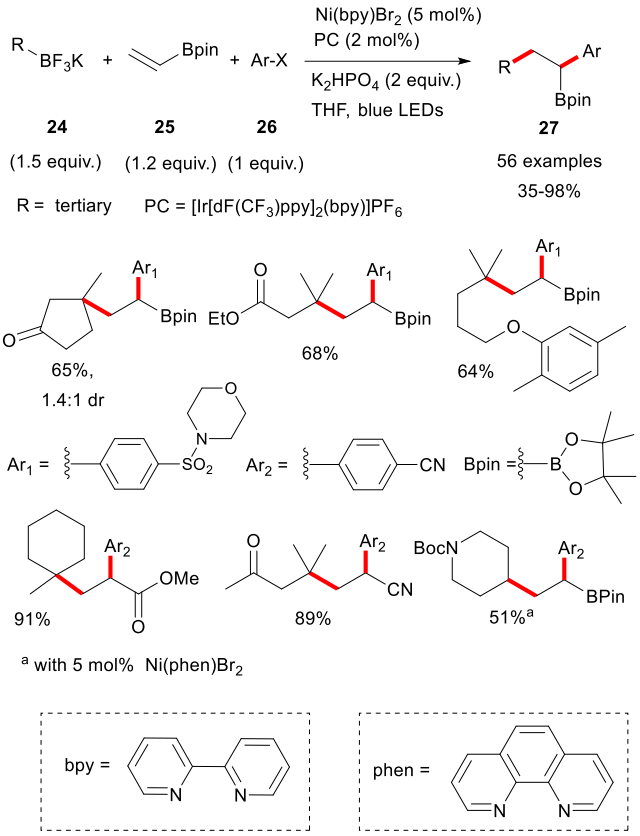

Scheme 7 Three-component dicarbofunctionalization with alkyl trifluoroborates, vinyl boronate and arylbromides.

Recently, bench stable bicyclo[1.1.1]pentane BCP trifluoroborate salts could be prepared in large scale from the corresponding carboxylic acids precursors using flow chemistry and engaged in dual catalysis with complex aryl halides precursors to provide valuable BCP-incorporating products for medicinal chemistry.[30]

A sequence of asymmetric conjugate borylation – trifluoroborate formation – Ni catalyzed cross coupling in photoredox conditions from cyclobutene 1-carboxyesters **28** opens an access to the synthesis of enantioenriched *trans*-heteroaryl cyclobutylcarboxyesters **29** (Scheme 8).[31] The initial borylation is *cis*-selective. High-throughput screening was achieved to determine the best ligand for the copper catalysis. Ligand exchange on boron with KHF_2 provides the trifluoroborate derivative. The radical generated from the cyclobutyl trifluoroborate by photoredox catalysis is then trapped by the nickel *anti* to the ester. Reductive elimination furnishes the *trans*-β-aryl/heteroaryl cyclobutylcarboxyesters.

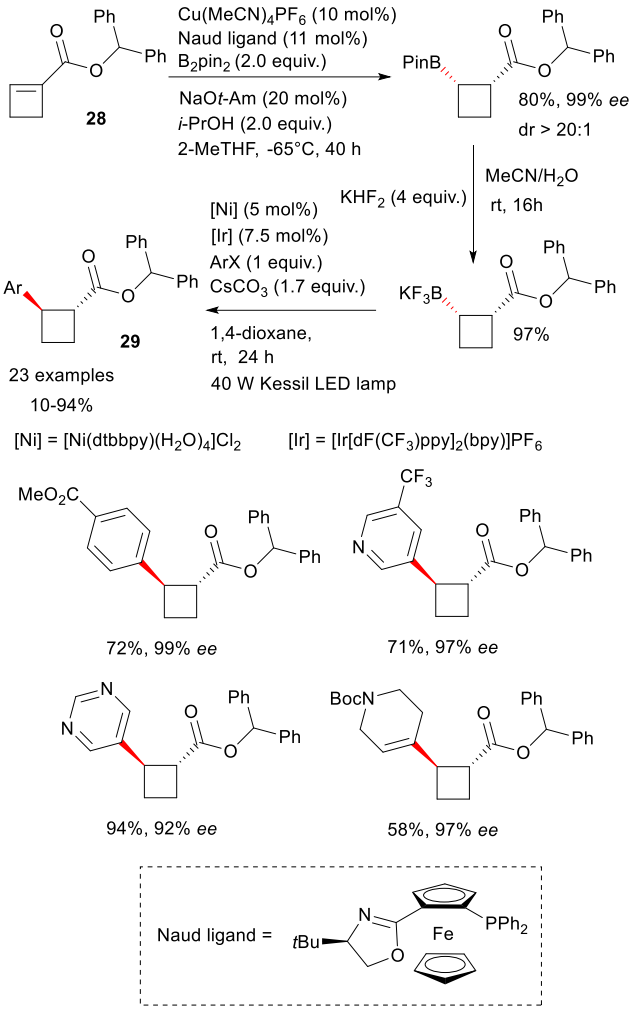

Scheme 8 Enantioenriched cyclobutane synthesis through asymmetric conjugate borylation – trifluoroborate formation – Ni catalyzed cross-coupling reactions.

Recently, mesoporous graphitic carbon nitride could be used as a heterogeneous organic semiconductor photocatalyst for the coupling of allyl- and benzyl trifluoroborates with aryl halides.[32]

Electrosynthesis has also been applied on boronate derivatives. First, anodic oxidation of trifluoroborates has also studied.[33] Second, benzyl trifluoroborates were reacted with aryl halides and bromostyrene in electrochemical conditions.[34] Cathodic reduction of nickel intermediates and anodic oxidation of the benzyl trifluoroborates are invoked as elementary steps of the catalytic cycle.

A.2 Alkyl boronates

Sometimes used as precursors of alkyl trifluoroborates, alkyl pinacol boronates have also been tested to provide radical species by single-electron oxidation under a Lewis base activation for a higher reactivity. In 2014, Aggarwal and co-workers examined the oxidation with manganese triacetate of a preformed ate complex between the alkyl pinacol boronic ester and an organolithiated nucleophile in the presence of the hydrogen donor 4-t-butylcatechol (TBC) as an effective protodeboronation strategy.[35] Recently, this work was extended to the catalytic photooxidation of arylboronate complexes generated *in situ* by reaction of alkyl pinacol boronic esters with phenyllithium. For example, as depicted in scheme 9, cyclohexyl pinacol boronic ester **30** reacts with phenyllithium to afford the ate complex intermediate **31**. After the *in-vacuo* removal of the solvent, treatment with iodide tethered enoate **32** under blue LEDs irradiation leads to the formation of the expected cyclobutane **33**. This methodology was then applied to synthesis of of 3-, 5-, 6-, and 7-membered rings through a sequential deboronation-radical addition–polar cyclization cascade with halide tethered alkenes. Presumably, the intermediate electron-rich boronate complexes **31** undergo a single-electron oxidation by a catalytic amount of the blue LEDs-excited photocatalyst 4CzIPN (5 mol %), as confirmed by the low oxidation potential of arylboronate complexes (+0.31 V vs SCE in CH_3CN for cyclohexyl alkyl pinacol boronic) and the reduction potential of the photocatalyst at its excited state ($E_{1/2}$ (4CzIPN*/[4CzIPN].-) = +1.59 V vs SCE), to give the corresponding alkyl radicals which can add to the activated alkene **32**. Reduction of the resulting radical **32a** by $[4CzIPN]^{\cdot-}$ participates in the regeneration of the photocatalyst and intramolecular alkylation of the stabilized anion **32b** formed leads to the elaboration of the ring systems (Scheme 9).[36] Subsequently, the behaviour of 1,2-bis-boronic esters was also examined. Radical cascade reactions involving mono-deboronation of primary boronate complexes by the excited photocatalyst followed by a 1,2-boron shift affords the thermodynamically favoured secondary β-boryl radicals which can be trapped by an activated olefin.[37] In parallel, Studer and co-workers developed a protocol for the photocatalytic protodeboronation of alkyl pinacol boronic esters using an iridium photocatalyst $[Ir[dF(CF_3)ppy]_2(dtbbpy)]PF_6$ and thiophenol as hydrogen donor. The authors combined this methodology with a Matteson homologation that was subsequently used successfully in several total syntheses, including δ-(*R*)-coniceine and indolizidine 209B.[38]

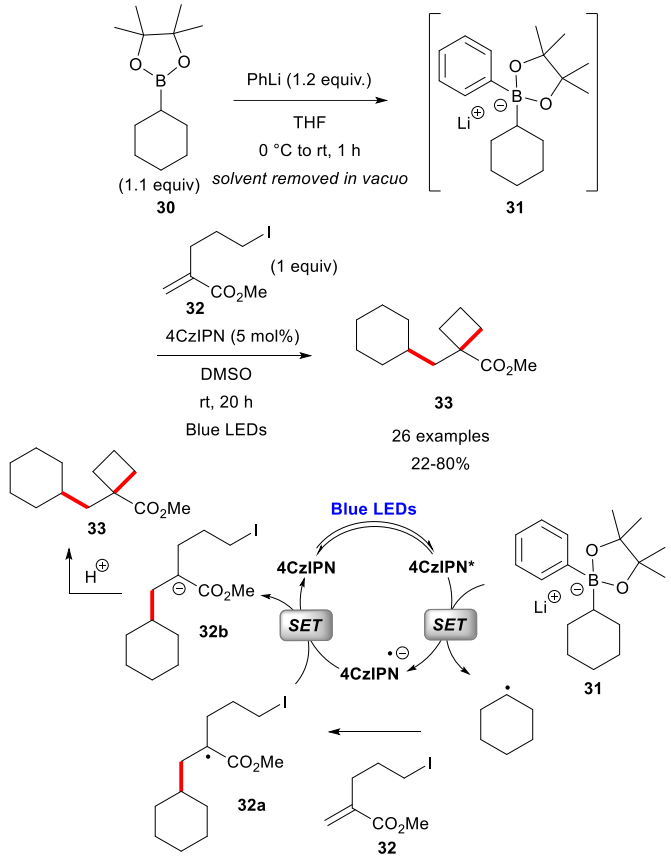

Scheme 9 Photoredox-catalyzed cyclobutane synthesis by reaction of cyclohexyl boronic acid pinacol ester **30** with iodide-tethered **32** enoate and the proposed mechanism.

Inspired by these works, Liu and co-workers proposed recently to use sodium methoxide (NaOMe) or sodium hydroxide (NaOH) as a valuable alternative Lewis base for the activation of alkyl pinacol boronates **34**, and apply them in alkynylation processes with alkynyl phenyl sulfones **35** to furnish to alkynylation adduct **36**. The mixture of alkyl pinacol boronate and NaOMe (1.285 V vs SCE in THF) shows a lower oxidation potential than the corresponding trifluoroborate salt (+1.56 V vs SCE in THF) but higher than the arylboronate complex (+0.98 V vs SCE in THF). Upon treatment with 4CzIPNunder blue LEDs irradiation, the alkyl-Bpin/NaOMe complexes **34a** react with alkynylsulfones in good to moderate yields. A similar mechanism as before has been proposed except that alkyl radicals generated by photooxidation adds to alkynylsulfones. Then, the fragmentation provides alkynylation adducts and the expelled sulfonyl radical can participate in the regeneration of the photocatalyst (Scheme 10).[39]

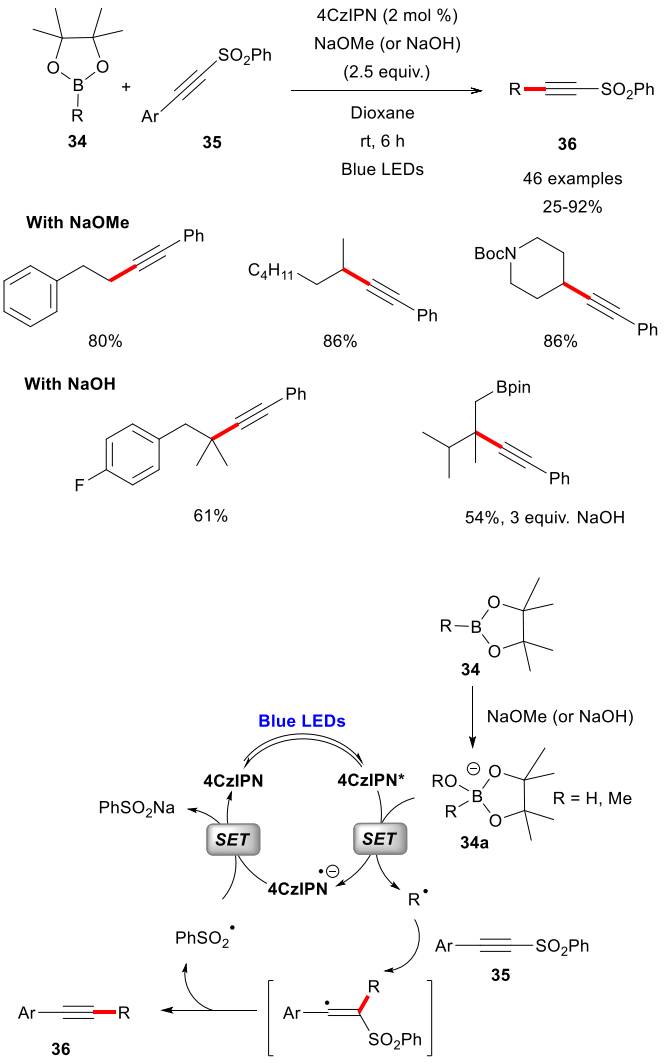

Scheme 10 Photocatalytic alkynylation of alkyl pinacol boronates and the proposed mechanism.

Based on their studies already carried out since 2016,[40,41] Ley and co-workers have employed different Lewis base catalysts, such as 4-dimethylaminopyridine (DMAP) or 3-hydroxy-quinuclidine or triphenylphosphine, to activate alkyl pinacol boronic esters and achieve their photocatalytic oxidation by the iridium photocatalyst $[Ir[dF(CF_3)ppy]_2(dtbbpy)]PF_6$ or Fukuzumi-type organic photocatalyst, 10-(3,5-dimethoxyphenyl)-9-mesityl-1,3,6,8-tetramethoxyacridin-10-ium tetrafluoroborate (Mes-Acr-4, $E^*_{1/2}$ = +1.65 V vs SCE)). Particularly, a variety of γ-amino butyric acids analogues were formed from Boc-protected amino boronic esters **37** and dimethyl malonate-derived olefins **38** as radical trap in moderate to good yields under either batch or continuous flow conditions (Scheme 11).[41,42]

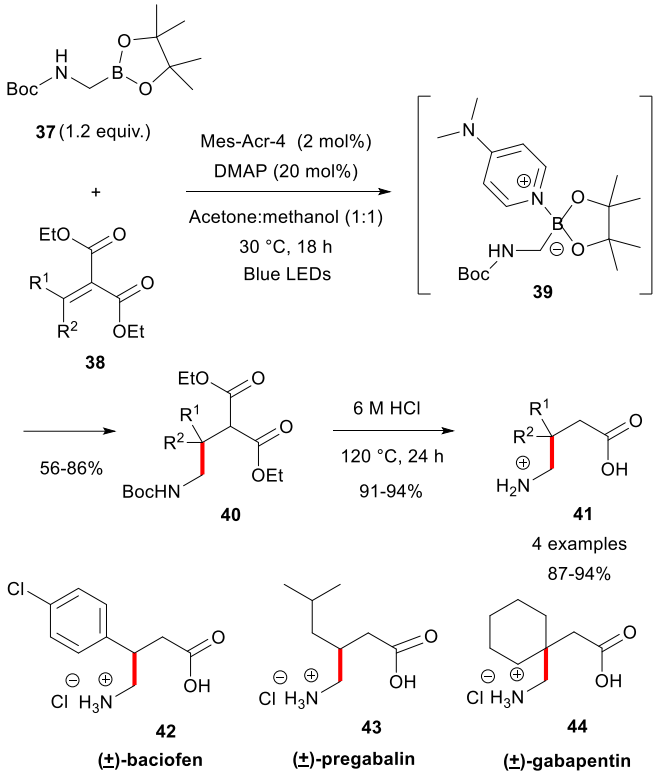

Scheme 11 Application of photoredox activation of pinacol boronic ester **37** to γ-amino butyric acids analogues synthesis in batch.

As described by Lennox, Stahl and co-workers, direct electrochemical oxidation of benzylpinacol boronic ester in the presence of sodium hydroxide as an anionic activator gives rise to the corresponding benzyl radical which can be trapped by TEMPO. The same results can be obtained by using a catalytic amount of ferrocenium derivative as an electrochemical mediator.[43]

Boracene-based alkylboronates have recently been reported as effective precursors of alkyl radicals under direct visible-light irradiation. These original molecular structures were readily obtained by reaction of organolithium or Grignard reagents with 8,9-dioxa-8a-borabenzo[fg]-tetracene, so-called boracene, and were successfully involved in carbon-carbon bond formation processes upon blue LEDS activation, such as spin trapping experiments, dimerizations, 4-cyanopyridine decyanoalkylations, Giese-type reactions and nickel-catalyzed alkyl-aryl cross-couplings.[44]

A.3 Alkyl boronic acids

The presence of Lewis base is generally required for the activation of alkyl boronic acids to generate alkyl radicals by oxidative SET, such as in the case of the previously mentioned boronates. The group of Ley used similar photooxidative conditions (*vide supra*), in the presence of 3-hydroxy-quinuclidine or 4-dimethylaminopyridine (DMAP) as activating additive and an iridium photocatalyst $[Ir[dF(CF_3)ppy]_2(dtbbpy)]PF_6$ (or the Fukuzumi's organic photocatalyst) under blue LEDs irradiation, to efficiently access Giese-type conjugated radical additions in both batch and flow regimes.[41,42] Very recently, this methodology has been extended to the synthesis of substituted trifluoromethyl olefins by Li, Xu and co-workers. Activation of boronic acids **45** by complexation with 1,4-diazabicyclo[2.2.2]octane (DABCO) affords the ate complex **45a** species which undergoes SET oxidation with a blue LEDs-photoexcited iridium photocatalyst $[Ir[dF(CF_3)ppy]_2(dtbbpy)]PF_6$ to form carbon-centered radicals that can add to *tert*-butyl carbonate (1-phenyl-2-(trifluoromethyl)allyl) **46**. The radical adducts **46a** are reduced by the iridium complex reduced to anions **46b**. Finally, $E1_{CB}$ elimination of the OBoc group provides the trifluoromethyl olefin **47** in moderate to good yields (Scheme 12).[45]

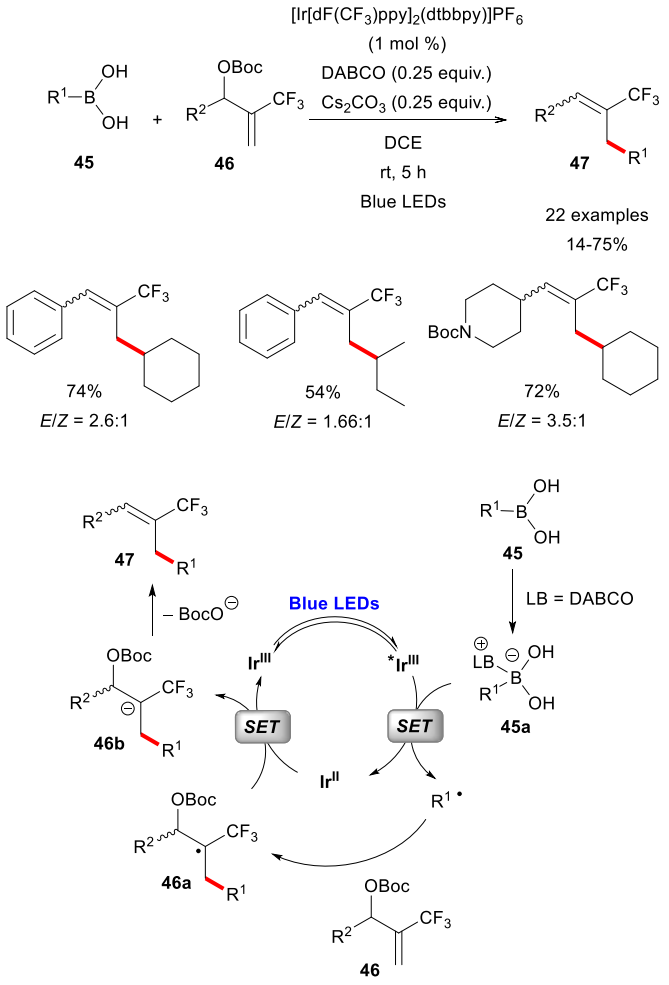

Scheme 12 Synthesis of trifluoromethyl olefins by visible light catalysis from DABCO-activated alkyl boronic acids **45** and the proposed mechanism.

An example of activation by a sulfinate anion was reported by Wang and co-workers for the photocatalyzed alkenylation of organoboronic acids **48** with alkenyl sulfones **49**. This transformation involves sequential formation of a benzenesulfinate/boronic acid complex **50**, generation of an alkyl radical by a photoexcited iridium(III) photocatalyst

followed by an addition-elimination reaction with an alkenyl sulfone to yield the alkenylation product **51**. The process does not require the presence of an external Lewis base but utilizes the sulfinate anion by reduction of the expelled phenylsulfonyl radical by the reduced form of the photocatalyst (Scheme 13).[46]

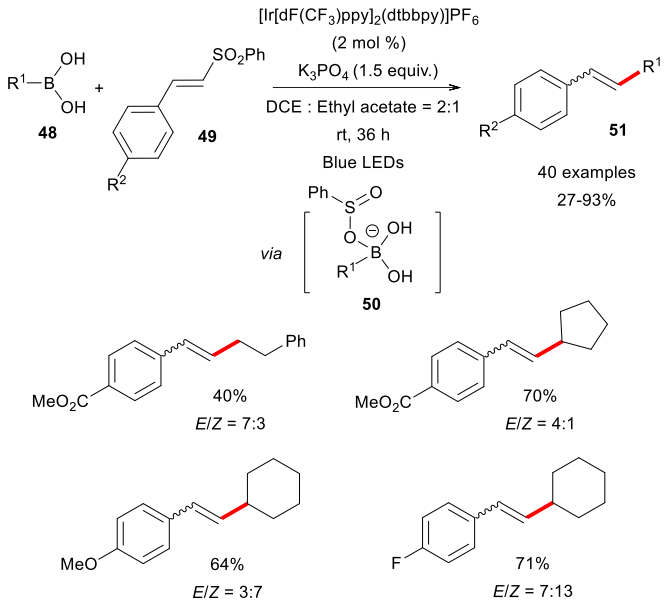

Scheme 13 Visible-light–mediated alkenylation of benzenesulfinate-activated alkyl boronic acids.

In the same vein, activation by complexation with sodium hydroxide (NaOH) has also been studied. Yoshimi *et al.* examined the reaction of aryl, alkenyl, or alkyl boronic acid **52** with electron-deficient alkenes **53** under photoredox activation. The photocatalytic system consists of a mixture of phenanthrene (Phen) and 1,4-dicyanobenzene (DCB) where the excited state of Phen (Phen*) reduces DCB to the radical anion (DCB.-) and releases the radical cation of Phen (Phen-+). Photo-oxidation of the NaOH-based alkylborates **52a** by Phen-+ leads to the corresponding radical which can be trapped by the olefin in satisfactory yields (Scheme 14).[47]

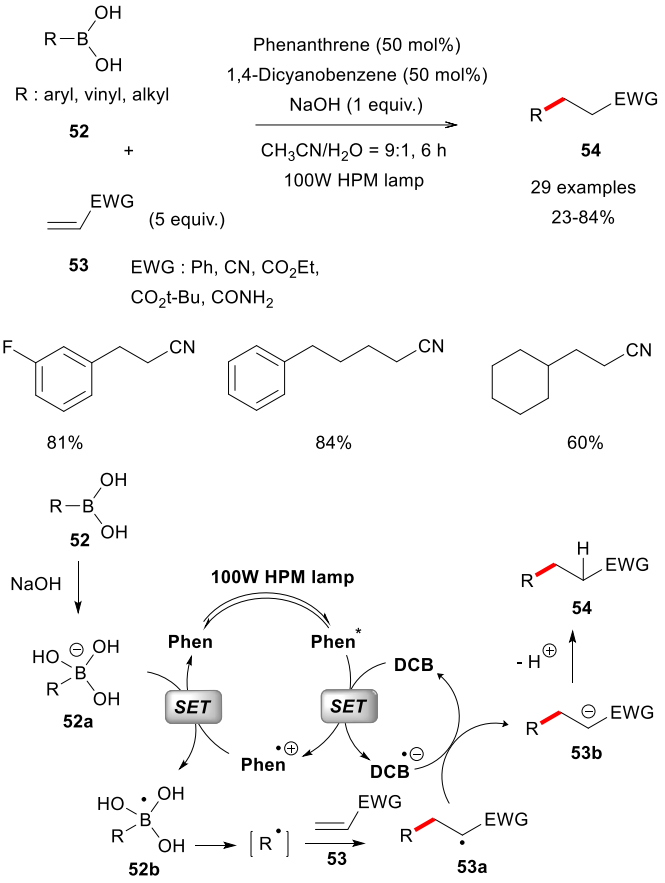

Scheme 14 Photooxidation of NaOH-based alkylborates and the proposed mechanism.

Hydrogen-bonding interactions between alkyl boronic acids and amide-based solvents such as *N*,*N*-dimethylacetamide (DMA) can activate the organoborane making it prompt to undergo visible-light-induced photocatalytic oxidation by 4CzIPN. The radical liberated was readily engaged in a Giese-type reaction. Complexation and hydrogen bonds with DMA have been shown to modulate the high oxidation potential of boronic acids (BA) (Potential of > 2.0 V for BA vs SCE compared to 1.13 V vs SCE in CH_3CN for BA+DMA) and may explain this increase in reactivity. An efficient scale-up strategy involving a continuous flow mode extended the interest of this work (Scheme 15).[48]

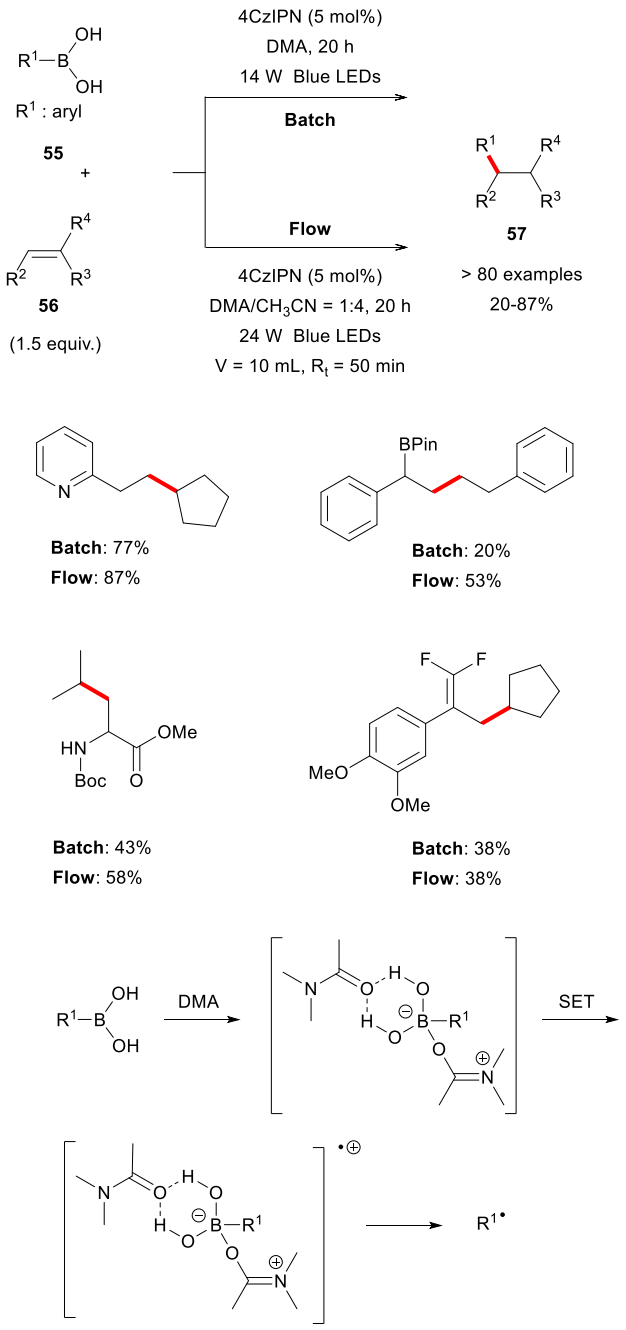

Scheme 15 DMA-Assisted organophotoredox activation.

Homolytic substitution at the boron atom is an original approach to generate carbon-centered radicals from organoboronic acids. The benzoyloxy radical (BI-O•), obtained by photoreduction of the hypervalent compound acetoxylbenziodoxole (BI-OAc) with eosin Y, was found to be particularly efficient in this elementary step for the generation of alkyl radicals. Cascade reactions involving sequential formation of inter- and intramolecular carbon-carbon bonds *via* radical addition/cyclization reaction of acrylamides were published by Han, Wang and co-workers. The SET mechanism described in scheme 16 is consistent with the photocatalytic reaction conditions used and results in 3,3-disubstituted oxindoles in moderate to good yields (Scheme 16).[49]

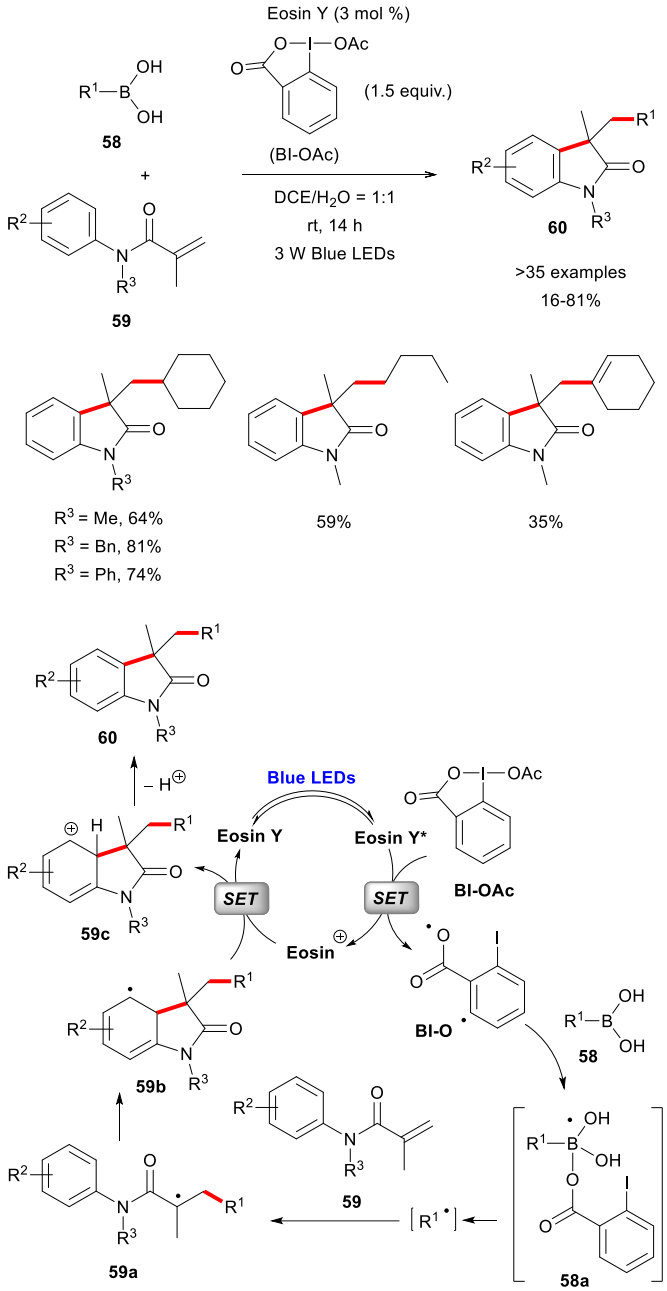

Scheme 16 Visible-light-induced deboronative alkylarylation with organoboronic acids and the mechanism proposed.

Treatment of alkyl boronic acids **61** and vinyl cyclobutanols **62-64** with the system $[Ir(dtbbpy)(ppy)_2]PF_6$/BI-OAc leads to the formation of substituted cylopentanones **65**, dihydrofuranones **66** and cyclohexanones **67** with α-quaternary centers. A mechanism involving a radical addition to the vinyl group and a semi-pinacol rearrangement is operating (Scheme 17).[50]

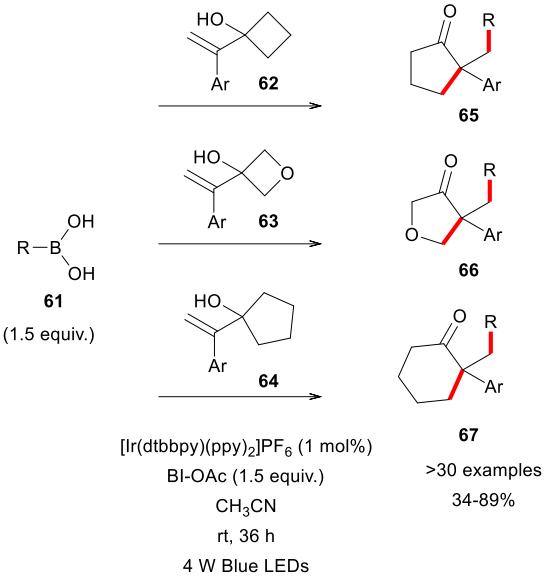

Scheme 17 Synthesis of ketones with α-quaternary centers by alkyl boronate addition/rearrangement reactions under photoredox conditions.

Lei and co-workers reported the first example of electrochemical oxidative generation and conversion of alkyl radicals from alkyl boronic acids. The synthesis of a series of benzo[4,5]imidazo[2,1-*a*]isoquinilin-6[5*H*]-one and indolo[2,1-*a*]isoquinoline derivatives **70** has been accomplished by Mn-catalyzed electrochemical radical cascade reactions, including radical addition/annulation steps, from alkyl boronic acids **68** as radical precursors with N-methacryloyl 2-arylbenzoimidazoles or N-methacryloyl 2-aryl indoles **69** in satisfactory yields (Scheme 18).[51]

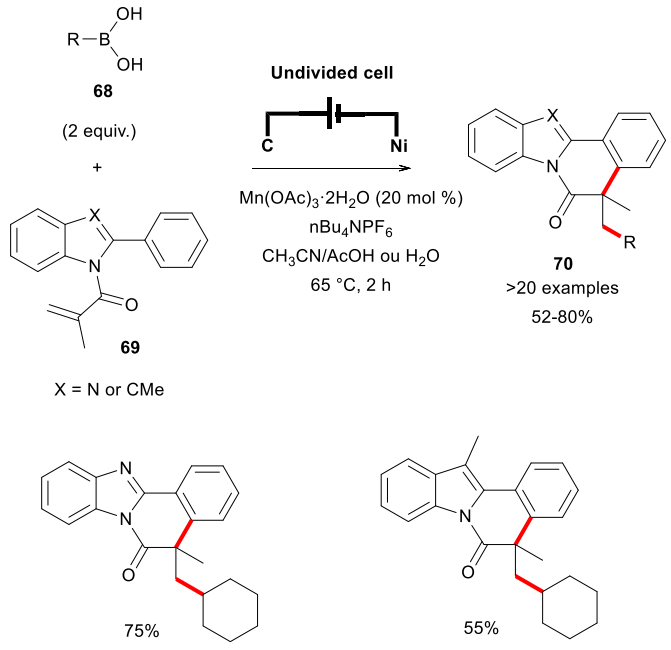

Scheme 18 Manganese-catalyzed electrochemical radical cascade cyclization toward the synthesis of benzo[4,5]imidazo[2,1-*a*]isoquinolin-6(5*H*)-one and Indolo[2,1-*a*]isoquinoline derivatives.

B. Alkylsilicate derivatives

The chemistry and reactivity of organic silicon compounds including its hypercoordinated derivatives have been known for a long time and are mainly governed by anionic and cationic chemistries.[52] However, in 1982, Kumada reported the stoichiometric copper(II) oxidation of organopentafluorosilicates to provide organic radicals *via* a single electron transfer (SET) process. This seminal work paved the way for the use of these electron-rich penta- and hexavalent silicon species to generate alkyl radicals upon oxidative SET conditions. Similarly, the oxidative cleavage of alkyl tetramethylsilanes is also possible but much more limited due to their higher oxidative potential.

B.1 Alkyl bis-catecholatosilicates

The first use of alkyl bis-catecholatosilicates in radical chemistry was performed by Nishigaishi in 2007 with the allyl derivative **71** (Scheme 19).[53,54] The generation of the corresponding radical was performed by photoinduced electron transfer (PET) between silicate **71** and carbonyl compound **72** (or a mixture of dicyanoarene **73** and anthracene as photosensitizer) at 400 nm (or 330 nm). The resulting allyl radical was coupled with the radical anion of carbonyl compounds **72** (or dicyanoarenes **73**) formed after PET, leading to the formation of allylated compounds **74** (or **75**).

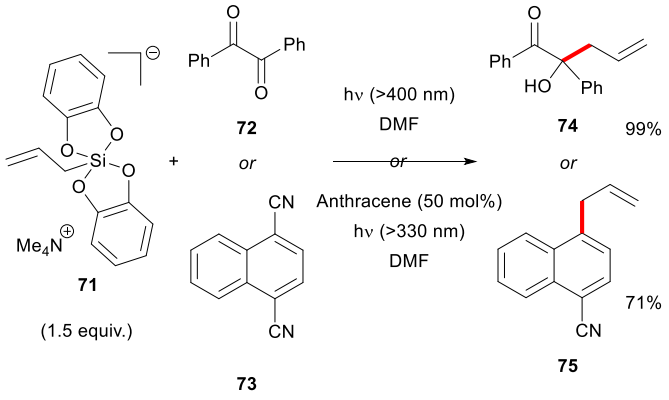

Scheme 19 Seminal work of Nishigaishi on PET processes with allyl bis-catecholatosilicates **71**.

In 2015, Fensterbank and co-workers introduced the use of alkyl bis-catecholatosilicates **76** as sources of alkyl radicals under photocatalytic conditions (Scheme 20).[55] The low oxidation potentials of silicates (from +0.34 V to +0.89 V vs SCE) allowed the use of mildly oxidative photocatalysts and represent a convenient access to unstabilized primary radicals. A large number of silicates have been engaged in allylation reactions with allylsulfones **77** or Giese-type additions to electron-deficient alkenes **78** such as dimethyl maleate, methyl vinyl ketone, vinyl sulfone or cyclopentenone in good yields, including the challenging primary radicals. Addition product **79** and **80** are obtained in good to excellent yield. Mechanistic

studies based luminescence quenching,[55] quantum yield determination[56] and calculations[55] suggest that the reaction proceeds through a reductive quenching pathway by the silicate. The silicate is oxidized by the iridium(III) photocatalyst $[Ir[dF(CF_3)ppy]_2(bpy)]PF_6$ (Ir^{III}) at its excited state (Ir^{III*}) (E Ir^{III*}/Ir^{II} = +1.32V vs SCE in CH_3CN) followed by the addition of the alkyl radical to the appropriate alkene. The catalytic cycle is closed by oxidation of the generated Ir^{II} complex by a sulfonyl radical (or a stabilized C-centered radical). It should be noted that metal-free oxidation with organic dyes such as Ledwith–Weitz salt was also performed with these substrates.[4] However, a stoichiometric amount of reagent was needed.

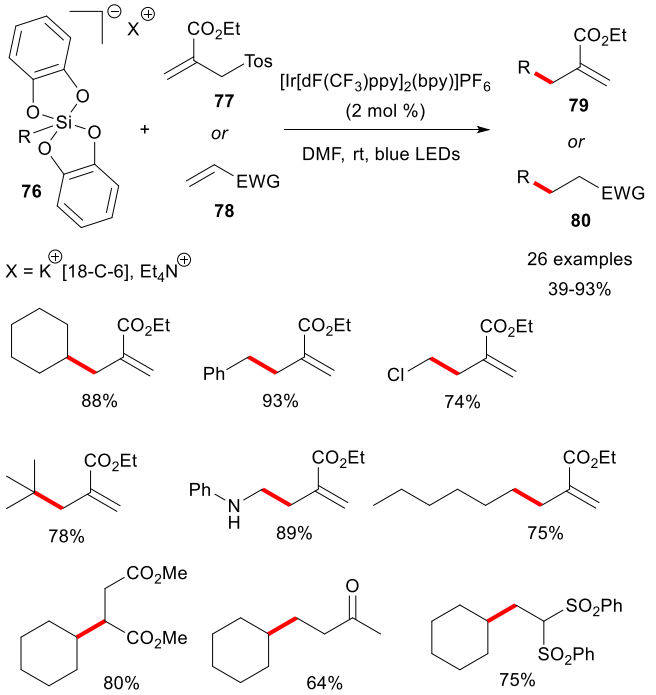

Scheme 20 Allylation and Giese-type reactions with alkyl bis-catecholatosilicates **76**.

Goddard, Ollivier, and Fensterbank *et al.* - 2015

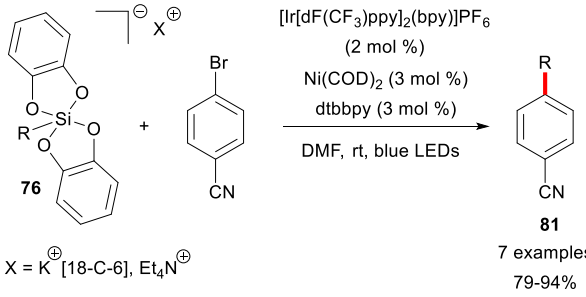

Molander *et al.* - 2016

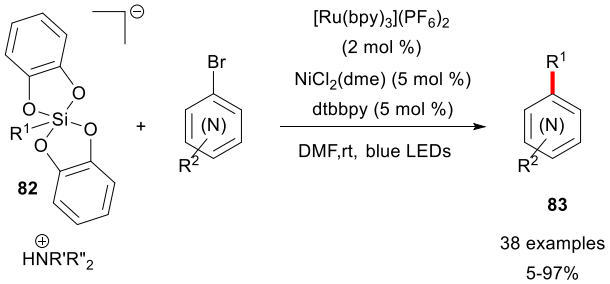

Goddard, Ollivier and Fensterbank *et al.* - 2016

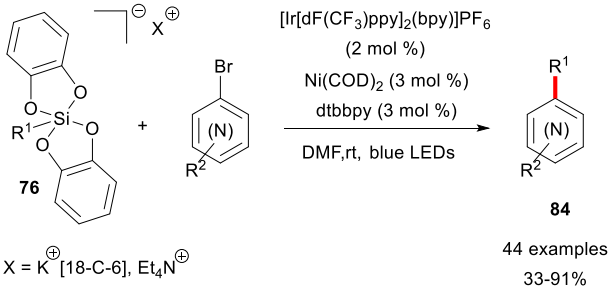

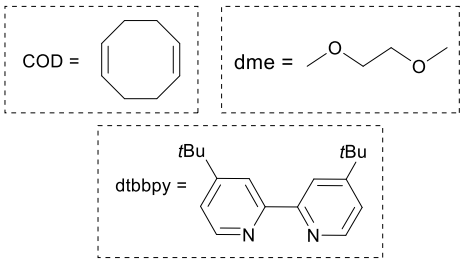

Scheme 21 Alkyl bis-catecholatosilicates in photoredox Ir/Ni dual catalysis.

As exposed in section A.1, the merging of photocatalysis and Ni catalysis opened a new paradigm for cross-coupling reactions, but with the limitation of the use of stabilized radicals.[25,26] In 2015, Fensterbank and co-workers achieved a milestone with the use of primary alkyl silicates **76** in dual iridium/nickel cross-coupling reactions for the formation of $C(sp^2)$-$C(sp^3)$ cross coupling products **81** with 4-bromobenzonitrile (Scheme 21).[55] This finding was further extended by Molander[57] and Fensterbank[58] and, in both cases, the reaction displayed a wide substrate scope in primary and secondary bis-catecholatosilicates (**76** and **82**) and also in (hetero)aryl bromides leading to the cross coupling adducts **83**

and **84** in moderate to excellent yield. Other electrophilic partners have been successfully applied such as alkenyl halides,[59] phenol derivatives[60] or borylated (hetero)aryl bromides.[61] A particular behaviour has been observed for 3-mercaptopropyl silicate **85** under dual catalysis conditions (Scheme 22).[62] The formation of a carbon-sulphur bond was obtained instead of the expected carbon-carbon bond. Indeed, oxidation of silicate **85** provides a primary alkyl radical which undergoes an intramolecular hydrogen atom transfer (HAT) and generates the corresponding thiyl radical. The latter adds to the (hetero)aryl-Ni(II) complex and a reductive elimination closes the catalytic cycle. Several aryl- and heteroaryl bromides can be engaged with mercaptosilicate affording the S-arylated products **86** in good to excellent yield. In the same paper, the authors improved their methodology by using thiols and isobutyl bis-catecholatosilicate **87** acting as a hydrogen atom abstractor. Under these conditions, the photooxidation of silicate **87** leads to the formation of isobutyl radical which can abstract hydrogen from thiols producing isobutane and the corresponding thiyl radicals (scheme 23). A wide range of aryl- and heteroaryl bromides, as well as primary, secondary, and tertiary thiols are efficiently coupled to deliver thioethers **88** under these mild reaction conditions.

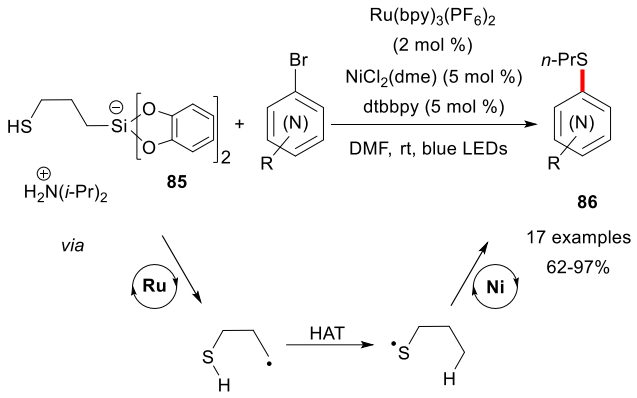

Scheme 22 Thioetherification with 3-mercaptopropyl bis-catecholatosilicate.

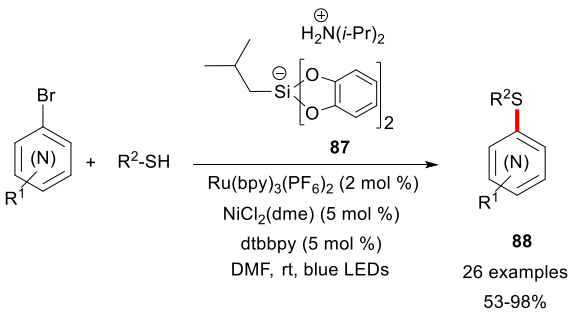

Scheme 23 Thioetherification with a thiol and isobutyl bis-catecholatosilicate as an H atom abstractor.

In addition to the formation of C(sp^2)-C(sp^3) carbon bonds, Fensterbank and co-workers have described C(sp^3)-C(sp^3) cross-coupling reactions of alkyl silicates with alkyl halides (Scheme 24).[63] After a screening of nickel sources, the ancillary ligands and photocatalysts, the authors found that $Ni(COD)_2$, bipyridine, and $[Ir[dF(CF_3)ppy]_2(bpy)]PF_6$ offer the best combination to perform this cross-coupling reaction. Alkyl bromides remain the best electrophilic partners, while iodide derivatives react poorly and no reaction was observed with alkyl chlorides or tosylates. A series of alkyl silicates **89** and alkyl bromides **90** gave coupling product **91** in low to moderate yields, which could be explained by the simultaneous formation of homocoupling products between two alkyl bromide molecules. Radical clock experiments tend to support a radical pathway where a SET takes place between Ni and alkyl bromides but the full details of the mechanism remain unknown and are still under investigation.

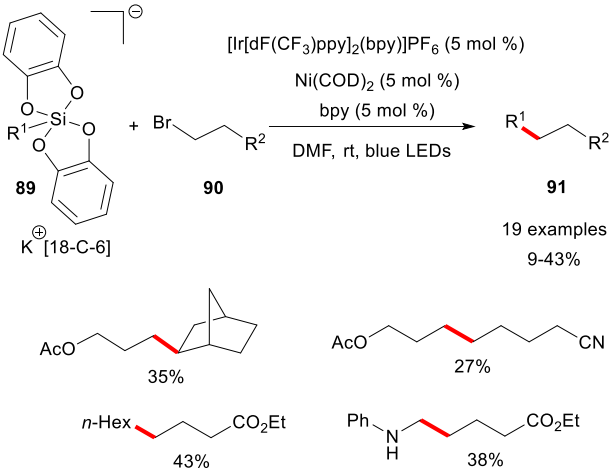

Scheme 24 C(sp^3)-C(sp^3) Cross-coupling reactions of alkyl bis-catecholatosilicate with alkyl bromides.

In 2016, Fensterbank and co-workers introduced the use of the high oxidizing organic dye 1,2,3,5-tetrakis-(carbazol-yl)-4,6-dicyanobenzene (4CzIPN)[64] for the oxidation of bis-catecholatosilicates.[65] This dye displayed promising features for photoredox catalysis: a high photoluminescence quantum yield (94.6%), a long life-time in the excited state (5.1 μs) and a high reduction potential at its excited state ($E_{1/2}$ (4CzIPN*/[4CzIPN]$^{\bullet-}$) = +1.59 V vs SCE)[66]. Furthermore, Zhang et al. successfully applied 4CzIPNin dual photoredox/nickel catalysis with aminocarboxylates and benzyl trifluoroborates.[67] Therefore, the use of this organic photocatalyst was extended to alkyl silicates **76** (Scheme 25). A large panel of reactions could be performed from Giese-type additions on various radical acceptors to photoredox/nickel dual-catalyzed cross-coupling reactions with aryl bromides or alkenyl halides.

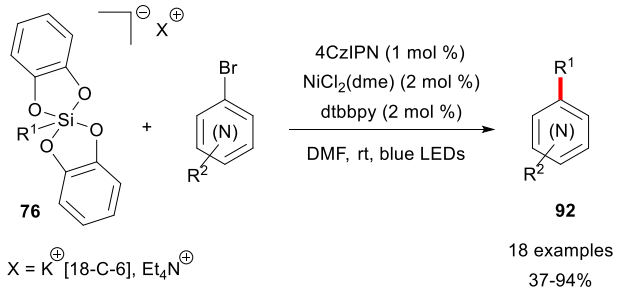

Scheme 25 4CzIPNas a photocatalyst in photoredox/nickel dual-catalyzed cross-coupling reactions of alkyl bis-catecholatosilicates with aryl bromides.

In 2017, Molander and co-workers disclosed the addition of alkyl radicals, issued from the photooxidation of alkyl silicates **93** by 4CzIPN, to imines **94** (Scheme 26).[68] Several aryl imines and sulfonyl imines were used as radical acceptors and could generate the corresponding secondary amines **95** in good yields. A broad scope of silicates was described and this very simple procedure proved to be chemoselective towards aldehydes and could be combined with Ru/Ni dual catalysis in a sequential two-step manner.

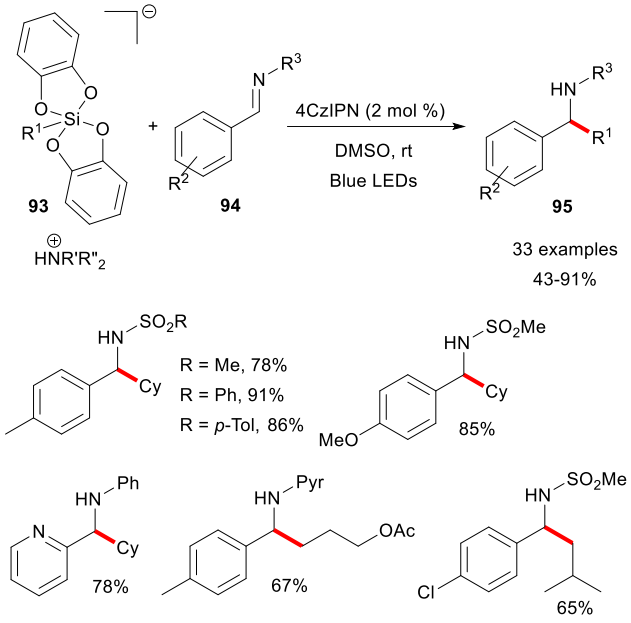

Scheme 26 Addition of alkyl bis-catecholatosilicates to imines under photocatalytic conditions.

Mechanistically, the most likely pathway for *N*-arylimines is shown in scheme 27. First, 4CzIPNplaced under irradiation would be engaged in a SET process with silicates **93** to produce a C-centered radical **93a** that adds to the imine **94** and provides an aminyl radical **94a**. This one is reduced to the anion **94b** by another SET from 4CzIPN$^{\bullet-}$ regenerating the photocatalyst to its ground state. Finally, amines **95** are obtained by protonation of the corresponding amides **94b**.

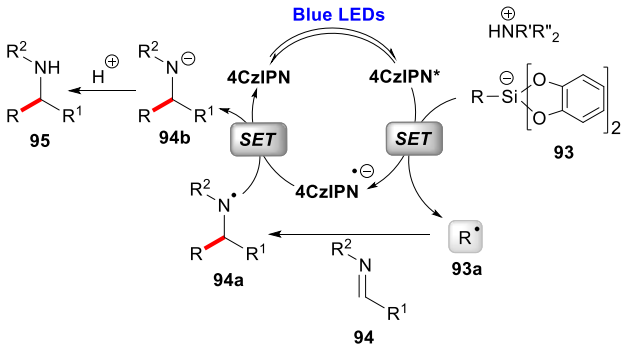

Scheme 27 Mechanism proposal of addition of alkyl bis-catecholatosilicates **93** to *N*-arylimines **94**.

The same approach was developed by Friestad using aliphatic and aromatic *N*-acylhydrazones as radical acceptors, in the presence of $MgCl_2$ as a Lewis acid activator.[69]
In 2018, Molander and co-workers developed a radical/polar crossover cyclopropanation procedure from iodomethyl bis-catecholatosilicate **96** and trifluoromethylalkenes **97** for the formation of the corresponding trifluoromethylcyclopropanes **98** (Scheme 28).[70] These particular cyclopropanes represent valuable structures that are highly valued in medicinal chemistry because of their bio-isosteric properties.

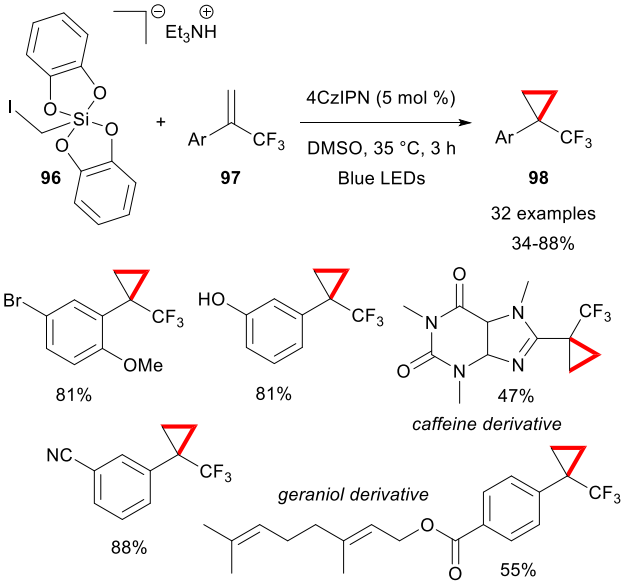

Scheme 28 Formation of trifluoromethylcyclopropanes by radical/polar crossover reactions from iodomethyl bis-catecholatosilicate **96** and trifluoromethylalkenes **97**.

Comprehensive mechanistic studies were performed by the authors including DFT calculations and photophysical experiments. After irradiation, iodomethylsilicate **96** is presumably oxidized by the excited photocatalyst generating the iodomethyl radical **96a** (Scheme 29). The latter adds to the activated olefin and the radical formed **96b** is then reduced by a SET process allowing the regeneration of the photocatalyst

and the formation of the anion **96c**. Finally, cyclopropanes **98** are obtained after a 3-*exo*-tet cyclization.

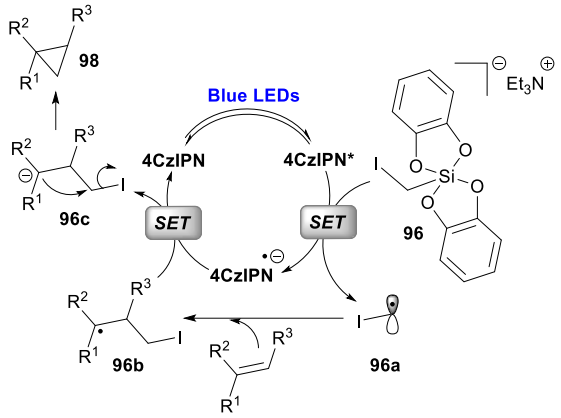

Scheme 29 Proposed mechanism for the synthesis of trifluoromethylcyclopropanes under photocatalytic conditions.

This protocol has been further extended to the reactivity of other silicates.[71–74] An original application to a radical/polar crossover annulation involving a sequential addition of bromoalkylsilicates **99** to imine **100** followed by nitrogen alkylation has also been performed by Molander and co-workers leading to the formation of various saturated nitrogen heterocycles **101** (Scheme 30).[75]

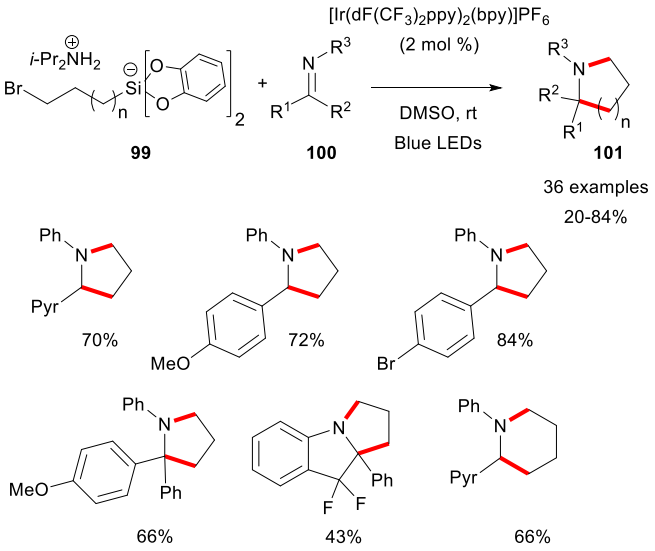

Scheme 30 Formation of saturated nitrogen heterocycles by a radical/polar crossover annulation from silicates **99** and imines **100**.

In 2019, the Ollivier-Fensterbank group developed an approach for the synthesis of ketones via a Ir/Ni dual catalysis involving alkyl bis-catecholatosilicates **76** and acyl chlorides **102** as electrophiles (Scheme 31).[76] Unsymmetric ketones **103** were obtained in poor to excellent yield. This method proved to be effective with reactive and/or stabilized benzyl or secondary radicals but remained limited with primary radicals and highly electrophilic acyl chlorides. In these cases, acylation of catechol was found to be a competitive reaction leading to poor yields in cross-coupling products.

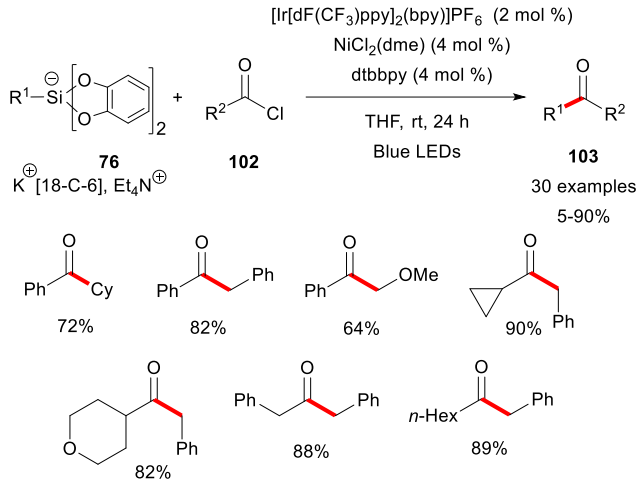

Scheme 31 Synthesis of ketones via a Ir/Ni dual catalysis with alkyl bis-catecholatosilicates and acyl chlorides.

An alternative approach to the synthesis of ketone was disclosed by Ryu and Fensterbank and is based on the photoredox carbonylation of alkyl bis-catecholatosilicates **76** under oxidative conditions (Scheme 32).[56] This multi-component approach allows the formation of a range of substituted ketones **104** from primary and secondary alkylsilicates and activated alkenes, placed together under CO atmosphere (80 bars). In this process, the key alkyl radical, generated by a conventional reductive quenching of the photoactivated photocatalyst (4CzIPN) by the silicate, adds to carbon monoxide. The acyl radical formed was engaged in a Giese-type addition to the activated olefin and provided a α-stabilized radical that was then reduced, thus closing the catalytic cycle. After protonation of the resulting carbanion intermediate, various ketone products were isolated.

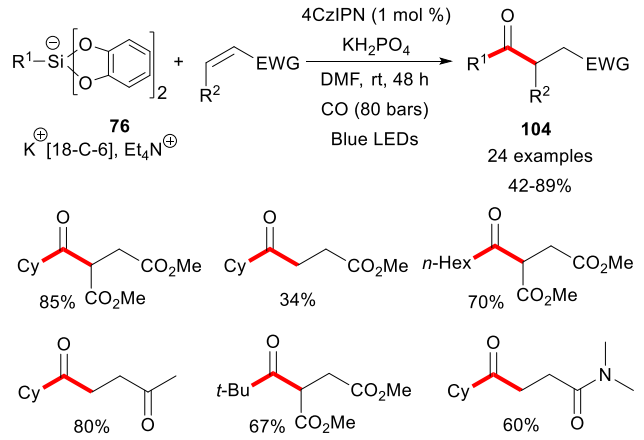

Scheme 32 Synthesis of substituted ketones by carbonylation/Giese addition of alkyl bis-catecholatosilicates under photocatalytic redox conditions.

As an extension of this carbonylation work, Ryu and Fensterbank reported the formation of amides from alkylsilicates **76**, and amines **105** under CO atmosphere (Scheme 33).[77] Primary, secondary and tertiary alkylsilicates were competent substrates and a large range of primary and secondary amines was successfully employed in this transformation yielding to the formation of multiple functionalized amides **106**.

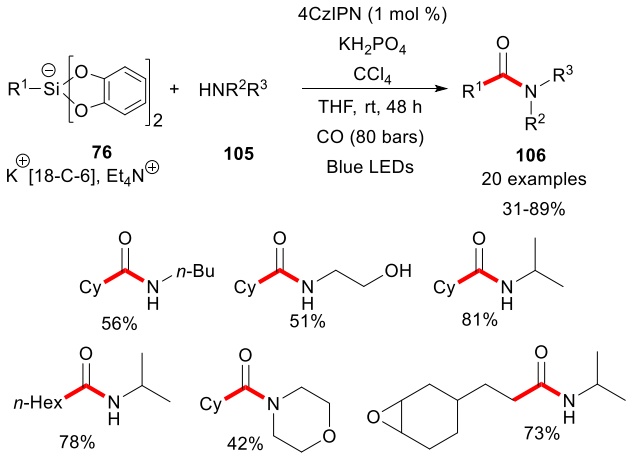

Scheme 33 Synthesis of amides by carbonylation of alkyl bis-catecholatosilicates **76** in the presence of amines under photocatalytic redox conditions.

Mechanistically, the formation of the acyl radical intermediate **107** presumably takes place as above in scheme 34. Chlorine abstraction from CCl_4 would then generate *in situ* the acyl chloride **108** and the trichloromethyl radical intermediate **109**. Acyl chloride **108** is then trapped by the amine to furnish the desired amide **106**. The trichloromethyl radical **109** acts as a sacrificial electron acceptor for $[4CzIPN]^{\bullet-}$ leading to the anion **110**, and allowing the regeneration of the photocatalyst in its ground state. The anion **110** would be protonated by KH_2PO_4 or by the protonated amide to form chloroform as a byproduct.

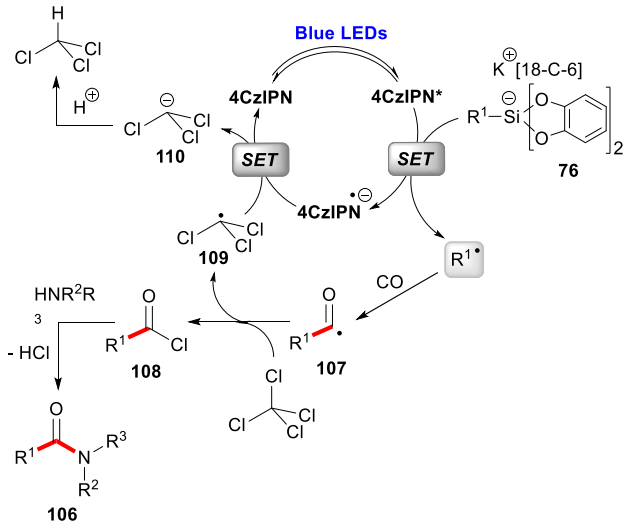

Scheme 34 Mechanism proposal for the synthesis of amides by carbonylation of alkyl bis-catecholatosilicates **76**.

B.2 Martin's spirosilane derivatives

In 2020, Kano and co-workers introduced alkylsilicates derived from Martin's spirosilane as new alkyl radical source upon SET.[78] These silicates **111** were conveniently synthesized by addition of alkyllithium or alkyl Grignard reagents to Martin's spirosilane (Scheme 35) and proved to be stable to water and particularly resistant to acidic conditions. However, unlike their bis-catecholatosilicate counterparts, Martin's silicates present higher oxidation potentials (for instance: E_{red} = +1.47 versus E_{red} = +0.69 vs SCE for Martin's cyclohexyl silicate and cyclohexyl biscatecholatosilicate respectively).

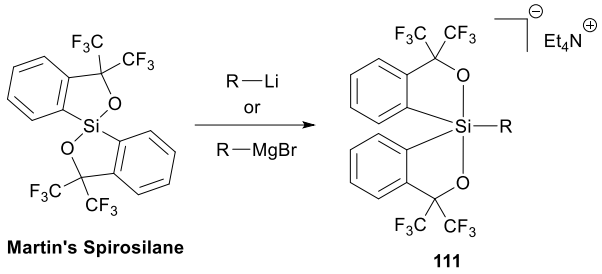

Scheme 35 Synthesis of alkylsilicates **111** derived from Martin's spirosilane.

During their investigations, Kano and co-workers showed that silicates **111** could be engaged in a C-H alkylation of heteroarenes under photocatalytic redox conditions (Scheme 36). Although silicates **111** possess a rather high oxidative potential, a SET takes place with the Mes-acridinium photocatalyst (Fukuzumi reagent, Mes-AcrClO$_4$) in its excited state leading to the formation of a *C*-centered radical that can add onto the electron-deficient heteroarenes **112** following a classical Minisci-type reaction. The photocatalyst is regenerated to its ground state by reduction of the radical cation from the radical addition. A wide range of alkyl and heteroarene partners were engaged affording the Minisci-type products **113** in modest to excellent yields.

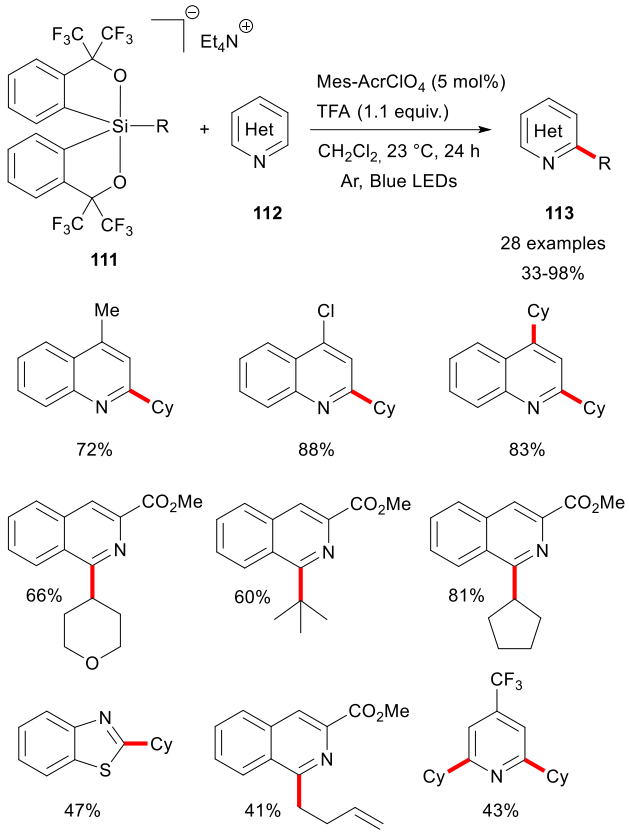

Scheme 36 Minisci-type addition of Martin's silicates under photocatalytic redox conditions.

In 2021, the same authors applied the use of silicates **111** in Giese-type additions with several activated olefins **114** in the presence of a catalytic amount of di-tBu-Mes-Acridinium photocatalyst ([di-tBu-Mes-AcrBF4], $E^*_{1/2}$ = +2.08 V vs SCE) under blue light irradiation (Scheme 37).[79] The reaction proceeds smoothly through reductive quenching between the photocatalyst and the silicates. A wide range of primary, secondary and tertiary alkyl radicals could be generated and efficiently coupled with olefins affording the Giese adduct **115** in good to excellent yields. It is noteworthy that under these conditions, the methyl radical, a very challenging radical, could be generated smoothly and trapped in good yield, representing a major breakthrough in radical chemistry.

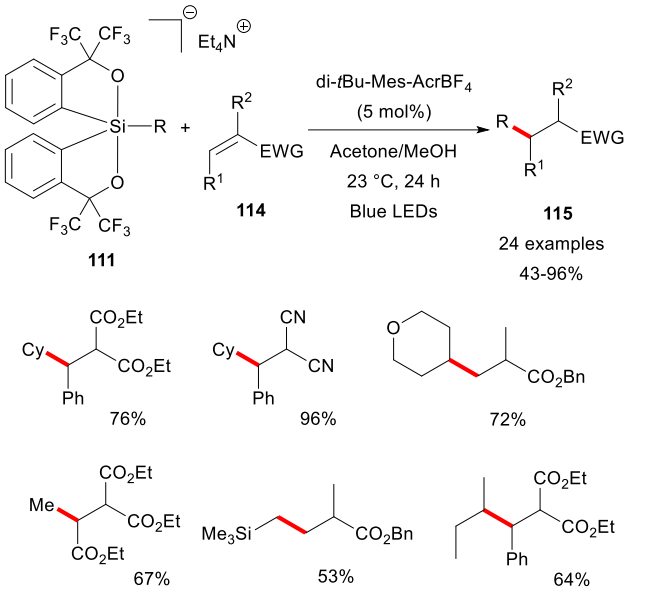

Scheme 37 Giese-type addition of Martin's silicates **111** *via* a photocatalytic SET process.

Another interesting feature of this approach is that during photocatalysis, Martin's spirosilane is produced at the end of the photoreaction and can be recovered as the hydroxy silicate derivative by simple precipitation with hexane. Further acidic treatment furnishes Martin's spirosilane that could be engaged in the synthesis of a new alkyl radical precursor by addition of an organolithium or a Grignard reagent.

B.3 Alkyl pentafluorosilicates

Inspired by the previously mentioned work of Kumada on pentafluorosilicates,[80] Wang and co-workers, very recently, used these substrates (**116**) as a source of primary alkyl radicals in the presence of copper(II) triflate, diethylamine, and a catalytic amount of TBAF for the C-1 alkylation of tetahydroisoquinolines **117** (Scheme 38).[81] Several radical precursors and tetrahydroisoquinoline substrates were engaged, leading to a wide range of C-1 functionalized products **118** in moderate to excellent yields.

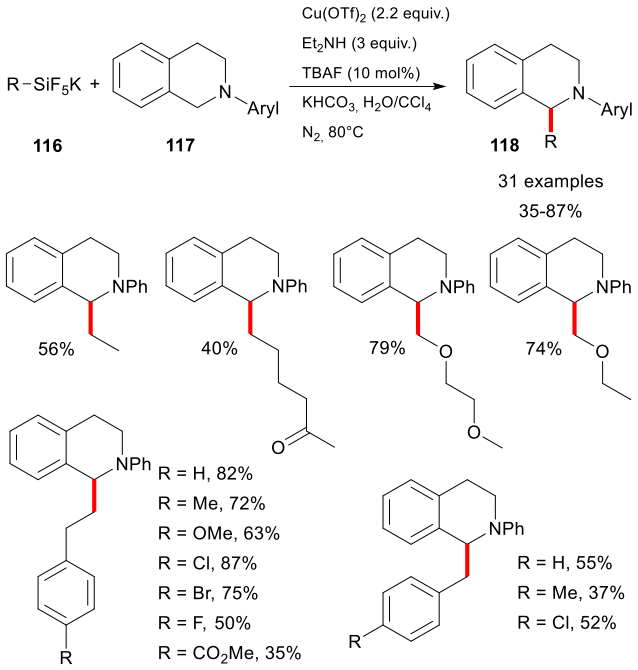

Scheme 38 C-1 alkylation of tetrahydroisoquinoline with alkylpentafluorosilicates **116**.

Several experiments were conducted to elucidate the mechanism of the reaction, including spin trapping and EPR approaches and the authors proposed a SET pathway for this transformation (Scheme 39). First, tetrahydroisoquinoline **117** would be oxidized by the copper(II) salt, leading to the radical cation **117a**. The latter is then converted to the iminium salt **117b**. At the same time, organopentafluorosilicate **116** is oxidized by copper(II) *via* SET to generate the radical anionic species **116a**. The *C*-centered radical **116b** is formed after cleavage of the Si-C bond of the pentafluorosilicate moiety. Attack of the alkyl radical on the iminium salt yields a new radical intermediate cation **119**, which is then reduced by diethylamine, which acts as a sacrificial electron donor, giving the final product **118**.

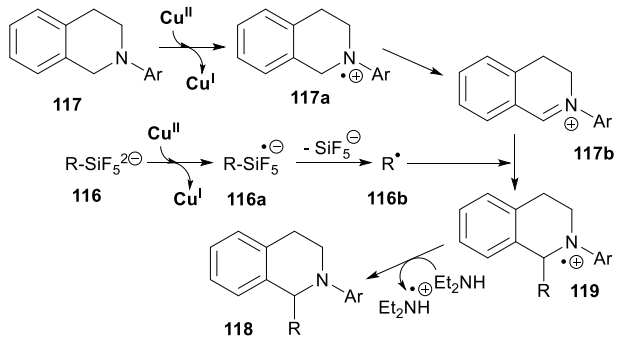

Scheme 39 Proposed mechanism for the copper(II)-mediated oxidation of pentafluorosilicate **116**.

B.4 Alkyl trimethylsilanes

Despite the high oxidation potential of benzyl trimethylsilanes (+1.68 V vs SCE for benzyl trimethylsilane), the reactivity of these more accessible organosilanes in visible-light photoredox catalysis has recently been tackled by Garcia Mancheño and co-workers. Upon oxidation with the photoexcited Fukuzumi 9-mesityl-10-methylacridinium salt (Mes-AcrClO$_4$, +2.06 V vs SCE), under aerobic conditions, a series of benzyl trimethylsilane derivatives **120** reacted with various Michael trapping reagents (such as maleimides, maleic anhydride, dimethyl fumarate and sulfonylethylene) and allyl sulfone to form the desired adducts **121** in good yields (Scheme 40). Mechanistic investigations have suggested that the reaction proceeds through a SET from the organosilane to the singlet excited state of the acridinium salt (Mes-Acr^{+}*), producing a putative radical cation intermediate which can release the benzyl radical **120a**. Its addition to the activated double bond provides another radical **120b** which can be reduced to anion **120c** by Mes-Acr$^{\bullet}$ and regenerates the photocatalyst. Protonation of the anionic intermediate gives rise to the Giese-type reaction product **121**. Finally, the process was shown to require the presence of oxygen to achieve better yields, which can participate either in the reduction of the conjugated adduct radical or in the regeneration of the photocatalyst. A few examples with α-TMS-substituted (thio)ethers or amino derivatives have also been reported.[82]

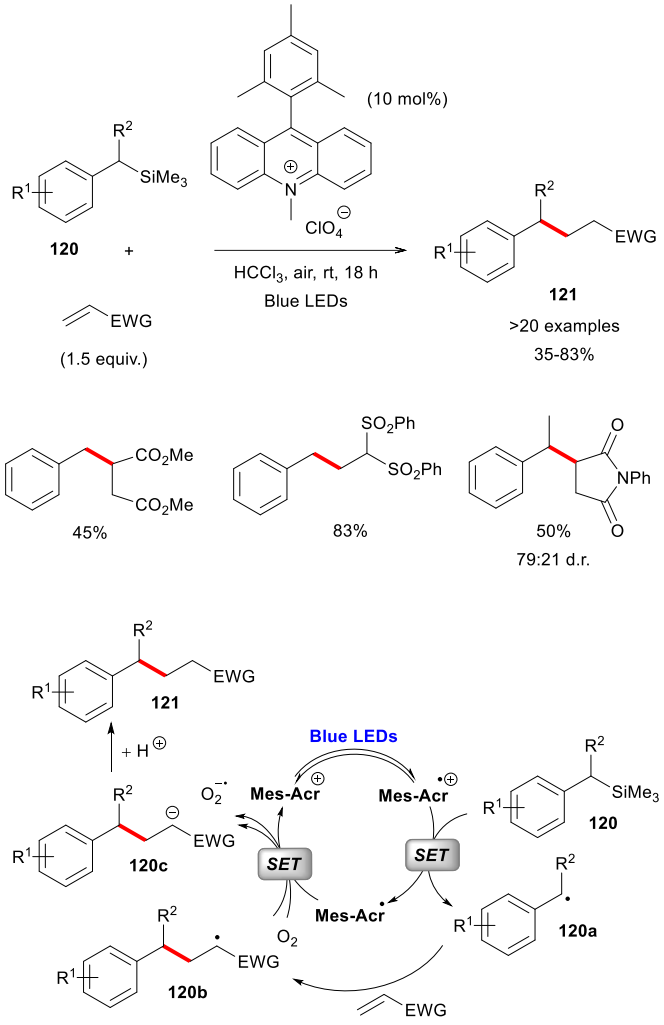

Scheme 40 Photooxidation of benzyl trimethylsilanes by visible-light photoredox catalysis and Giese-type reactions.

An extention to the fluoroalkylselenolation was proposed last year by Monnereau, Tlili and co-workers with the use of fluoroalkyltolueneselenosulfonate reagents as effective radical traps (Scheme 41). Similarly, fluoroalkyl selenyl products **122** were obtained by the action of the Fukuzumi catalyst mainly with benzyl trimethylsilanes **120**. A similar mechanism supported by luminescence and EPR spectroscopy has been postulated except that potassium persulfate is required to regenerate the photocatalyst.[83]

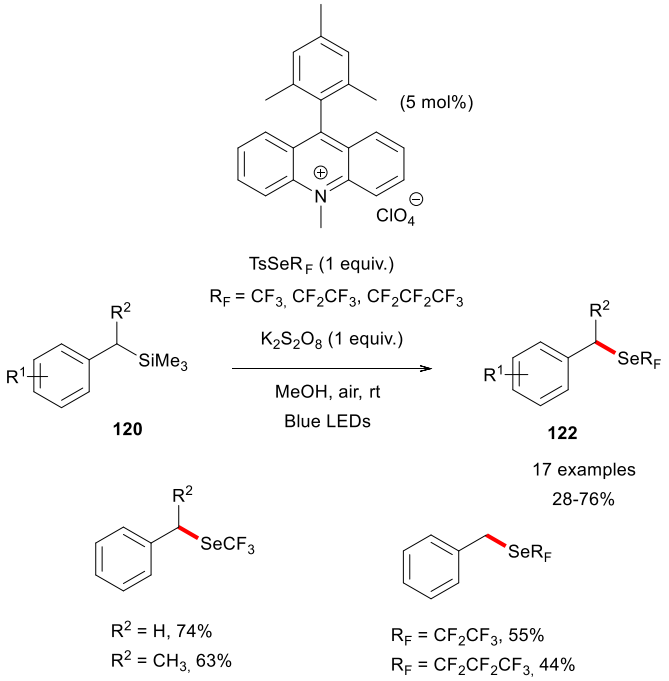

Scheme 41 Fluoroalkylselenolation of benzyl trimethylsilanes by visible-light photoredox catalysis.

In the same vein, Woo and co-workers explored in 2018 the generation of α-alkoxymethyl radicals from α-TMS-substituted ethers **123** by visible-light photooxidation with the Fukuzumi catalyst or $Ru(bpz)_3(PF_6)_2$, followed by their addition to various activated alkenes **124** (Scheme 42). The alkoxymethylated adducts **125** were isolated in good to moderate yields. The authors suggested a similar radical pathway as in scheme 40 with the formation of radical cations of the α-silyl ethers obtained through a photocatalyzed electron transfer and cleavage of the C-Si bond to liberate the α-alkoxymethyl radicals as key steps.[84]

Merging of photoredox catalysis with chiral Lewis acid catalysis creates opportunities to develop new asymmetric processes. In 2005, Yoon and co-workers used this approach in enantioselective 1,4-additions of α-amino radicals to α,β-unsaturated *N*-acyl pyrazoles promoted by (*i*BuPybox)$Sc(OTf)_3$ as an optimized chiral Lewis acid. α-Amino radicals were generated by photooxidation of α-silylmethyl amines with a 23W fluorescent light-activated ruthenium complex $Ru(bpy)_3Cl_2$ and the expected radical conjugated addition products were obtained with enantioselectivities up to 96% ee.[85]

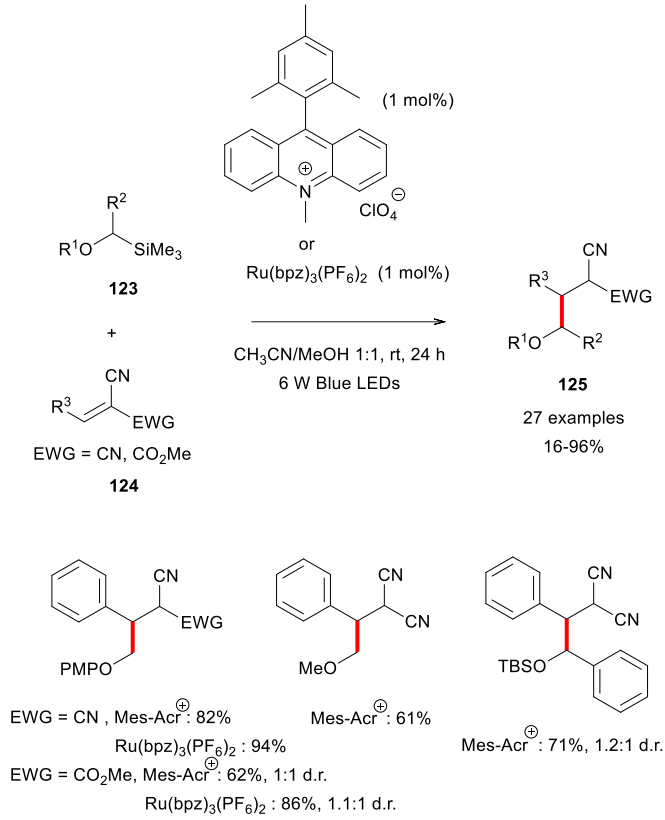

Scheme 42 Visible-light photoredox-catalyzed hydroalkoxymethylation of activated alkenes with α-TMS-substituted ethers.

Melchiorre and co-workers have devised a very elegant photocatalyst-free approach to the enantioselective β-alkylation of α,β-unsaturated aldehydes **126** involving SET processes from an alkyl trimethysilane **127** to a direct visible-light photoexcited chiral iminium ion **126b**, easily obtained by treatment of an enal with a chiral secondary amine catalyst (20 mol%) catalysed by TFA (40 mol%) (compound **126a,** scheme 43). A diradical coupling between the β-enaminyl **127a**, generated by reduction of the photoactivated iminium ion **126b** with the alkyl trimethysilane **127**, and the released alkyl radical allowed the carbon-carbon bond formation and thus the formation of β-substituted aldehydes **128**.[86] A series of enals was exposed to various types of alkyl trimethysilanes including benzyl trimethysilane and α-TMS-substituted ethers, thioethers or amines under the same conditions.[86]

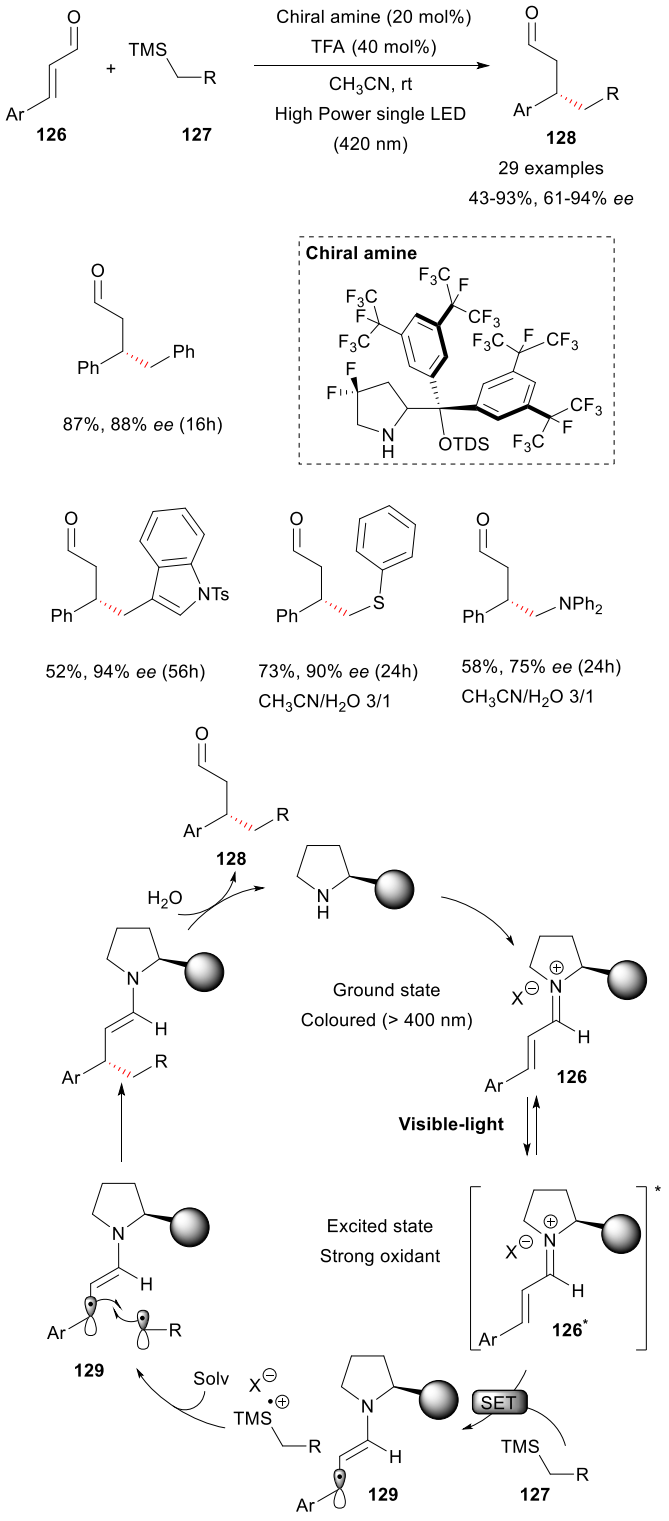

Scheme 43 Enantioselective organocatalytic β-alkylation of enals by visible-light activation of iminium.

Dual nickel/photoredox-catalyzed cross-coupling reactions of α-TMS-substituted amines **130** and functionalized (het)aryl halides **131** were performed by Molander and co-workers to construct aminomethylated (het)aryl adducts **132**. The authors showed that a mixture of nickel complex, Ni(dtbbpy)Br_2, and

the 4CzIPN photocatalyst under blue LEDs irradiation was able to promote the sequential photo-oxidation of secondary and tertiary α-silylamines and the cross-coupling with (het)aryl bromides in good yield with a high tolerance of functional groups. The following mechanism was suggested (Scheme 44).[87] Formation of radical cation **130a** by the photoexcited catalyst is followed by TMS loss to generate α-amino radical **130b** that is intercepted by Ni(0) to give **133**. After oxidative addition (**134**), reductive elimination delivers products **132**.

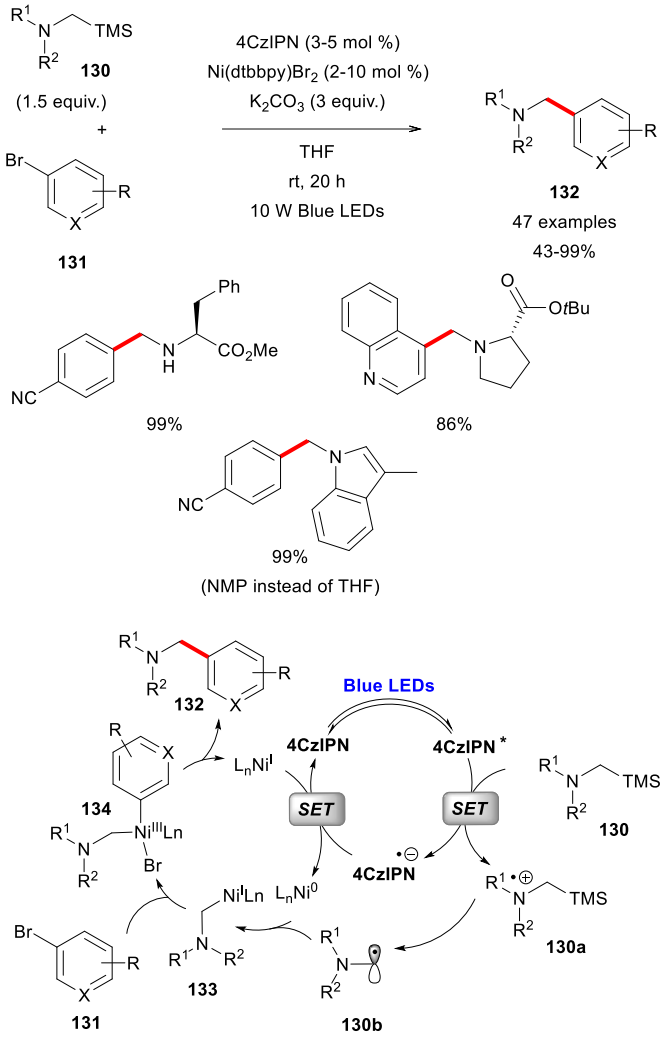

Scheme 44 Aminoalkylation of aryl halides by photoredox/nickel dual catalysis using α-TMS-substituted amines **130**.

C pyridine derivatives

Pyridine derivatives can be seen as electron-rich species and therefore sensitive to oxidation or as electron-poor compounds and so prompt to accept an electron. We will see that this dual reactivity can be selectively driven depending on the precursors used.

C.1 4-Alkyl 1,4-dihydropyridine derivatives

The 1,4-dihydropyridine (DHP) motif is a long-known structure found in the NADH cofactor, which is involved in many biological redox processes. Similarly, 1,4-dihydro-2,6-dimethyl-3,5-pyridinedicarboxylic acid diethyl ester, known as Hantzsch ester (HE), is a 1,4-dihydropyridine derivative and a synthetic analog of NADH. Therefore, HE has been widely used as a source of hydride or hydrogen in radical abstraction processes.[88,89]

Pioneering works have recently demonstrated that 4-alkyl-dihydropyridines (4-alkyl-DHPs) can be envisioned as alkylating reagents initiated by polar or radical C-C bond cleavage under photochemical[90] or thermal[91–93] reaction conditions. Chemically, 4-alkyl-DHPs are easily synthesized in a one pot manner from aldehyde precursors by different methods.[91] Due to their electron-rich structures, alkyl-DHPs exhibit a low oxidation potential (+0.89 V vs SCE for Bn-DHP)[94] suggesting their favourable behaviour towards oxidizing agents. In 2016, Nishibayashi and co-workers developed a photocatalyzed method for the alkylation of dicyanoarenes **135** from 4-alkyl-DHP derivatives **136** (Scheme 45).[95] The reaction proceeded smoothly in the presence of *fac*-Ir(ppy)$_3$ as a photocatalyst, sodium acetate as a base in 1,3-dimethyl-2-imidazolidinone (DMI) as a solvent under visible light irradiation. Stabilized radicals such as benzyl or α-alkoxymethyl radicals and unstabilized radicals reacted efficiently with dicyanoarenes affording the addition product **137** in poor to excellent yields. This reaction worked with 1,4- or 1,2-dicyanoarenes but also with electron-deficient cyanoheteroarenes. The authors noticed a mixture of addition products (2- vs 4-position) with a ratio largely in favour of position 4.

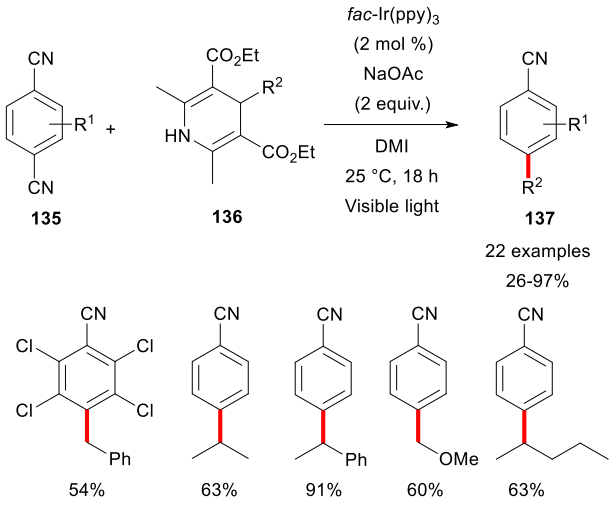

Scheme 45 Photoredox-catalyzed addition of 4-alkyl-DHPs on dicyanoarenes.

A reaction mechanism was proposed by the authors as depicted in scheme 46. After excitation of the Ir-based photocatalyst by light, reductive quenching takes place

between alkyl-DHPs **136** and Ir(III)* leading to the radical cations **136a**. After fragmentation, a C-centered radical and the pyridinium salt **138** are obtained. Concomitantly, the oxidation of the Ir(II) species by the dicyanoarene partner **135** affords the radical anion **135a** and regenerates the Ir(III) photocatalyst. A radical-radical coupling would occur between **135a** and the *C*-centered radical giving the corresponding anion intermediate **139**. Finally, cyanide elimination affords the alkylation product **137**.

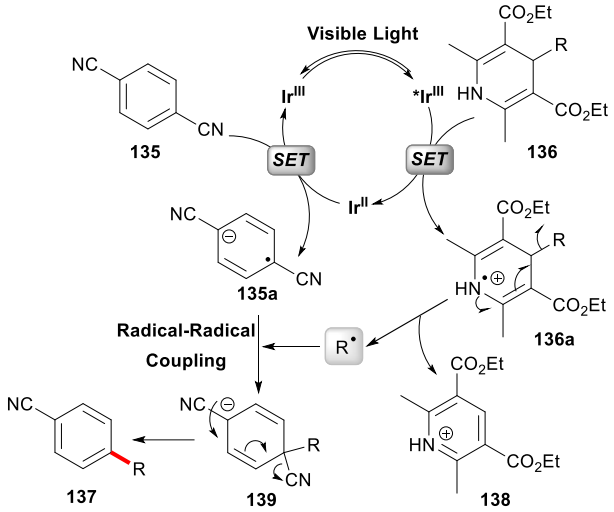

Scheme 46 Proposed mechanism for the photoredox-catalyzed addition of 4-alkyl-DHPs **136** on dicyanoarenes.

Similarly, Cheng and Ma reported a protocol for the photocatalyzed radical-radical coupling between α-bromoketones **140** and 4-alkyl-DHPs **136** leading to congested ketones **141** in good yields (Scheme 47).[94] The reaction showed compatibility with a wide range of α-bromoketones bearing several functional groups while the radical precursor is limited to benzyl (or substituted) radicals. The reaction mechanism is similar as previously proposed. Reductive quenching occurs between the photocatalyst in its excited state and the 4-alkyl-DHP derivative resulting in the formation of a *C*-centered radical. The photocatalyst returns to its ground state by reducing the α-bromoketone. The two radicals formed couple to give the expected product.

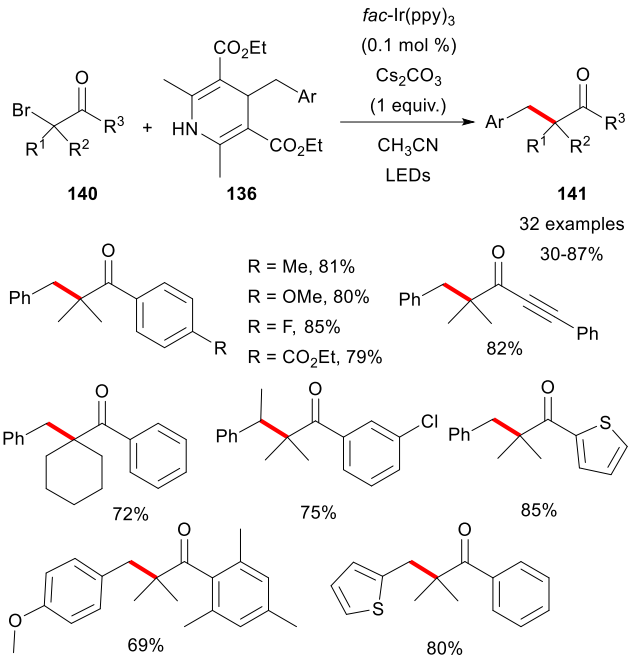

Scheme 47 Photocatalyzed coupling of 4-alkyl-DHPs with α-bromoketones.

A major breakthrough was achieved by Nishibayashi and co-workers with the use of 4-alkyl-DHPs in dual Ir/Ni cross-coupling reactions.[96] The authors found that aryl iodides **142** and alkyl-DHPs **136** reacted smoothly in the presence of *fac*-Ir(ppy)$_3$ as a photocatalyst, $NiCl_2$ as a catalyst, 4,4'-di-*tert*-butyl-bipyridine (dtbbpy) as an ancillary ligand and sodium acetate as a base in DMI as a solvent under visible light irradiation (Scheme 48). Cross-coupling products **143** were obtained in poor to very good yields. The mildness of the reaction conditions allows a wide diversity of functional groups through this classical dual Ir/Ni catalytic cycle.

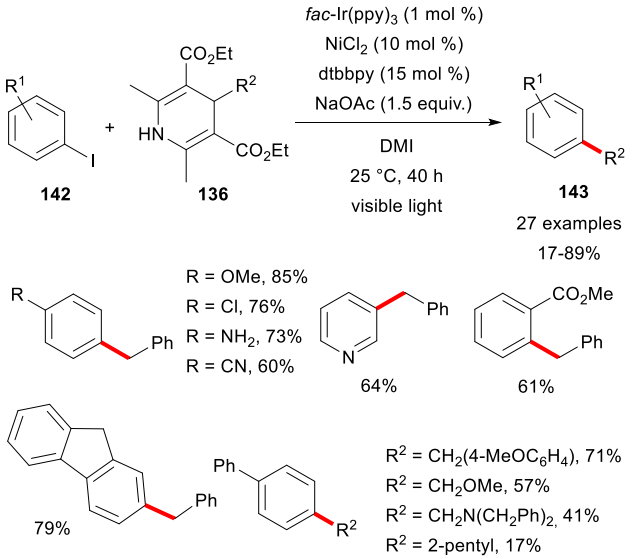

Scheme 48 Dual Ir/Ni cross-coupling reactions with 4-alkyl-DHPs.

It is noteworthy that this protocol was also applied to vinyl iodide derivatives by the same research group.[97] Under these conditions, retention of stereochemistry for alkyl-substituted alkenyl iodides was observed, while an isomerisation of the double bond occurred with aryl-substituted alkenyl iodides. In the same vein, a cross-coupling reaction protocol with aryl bromides was reported by Molander and co-workers using 4CzIPNas photocatalyst.[98]

Minisci-type reactions are also possible with 4-alkyl-DHPs and have been mainly applied for late-stage functionalization of complex structures. For instance, this approach has been explored by Molander and co-workers for the functionalization of natural products and drugs such as (-)-nicotine, caffeine, quinine or (+)-camptothecin.[99] Chen and Wang reported a specific peptide modification to histidine with 4-alkyl-DHPs by visible light irradiation and thus modified peptides such as angiotensin II, ubiquitin or secretin were successfully synthesized and isolated.[100] Very recently, Wang and co-workers proposed an interesting protocol for the photocatalyzed alkylation of heteroarenes **144** with 4-alkyl-DHP **136** using molecular oxygen as oxidant (Scheme 49).[101] Several heteroarenes were engaged with primary, secondary and tertiary alkyl-DHP leading to the Minisci adducts **145**. Poly-substituted drugs such as quinoxyfen or milrinone were also efficiently modified at an advanced stage. The reaction mechanism follows an identical reductive quenching and the photocatalyst is regenerated by oxidation with molecular oxygen instead of the heterocycle adduct.

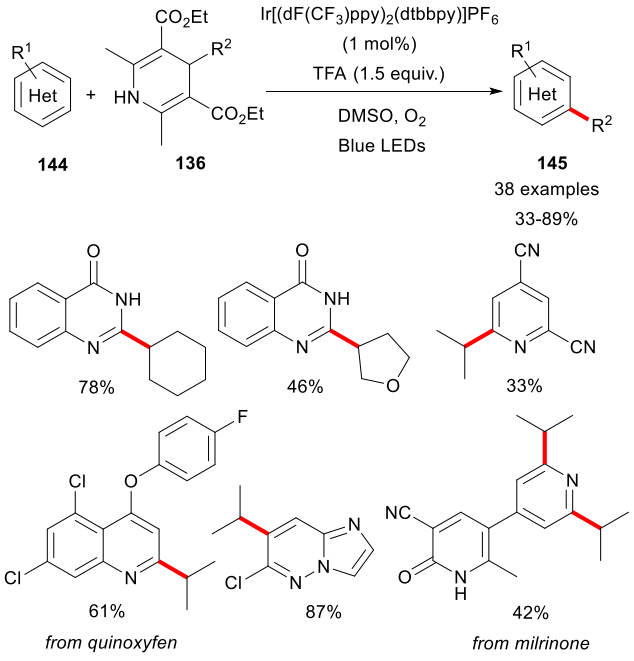

Scheme 49 Wang's protocol for Minisci addition.

Similar protocols have been developed for the photo-induced generation of alkyl radicals from alkyl-DHPs for addition to different substrates such as imines[102], 1-trifluoromethyl alkenes[103], brominated alkynes[104] or diazonium salts[105].

In continuation of their work on dual Ni/photoredox cross-coupling reactions, Molander and co-workers proposed a convenient strategy for ketones synthesis (Scheme 50).[106]

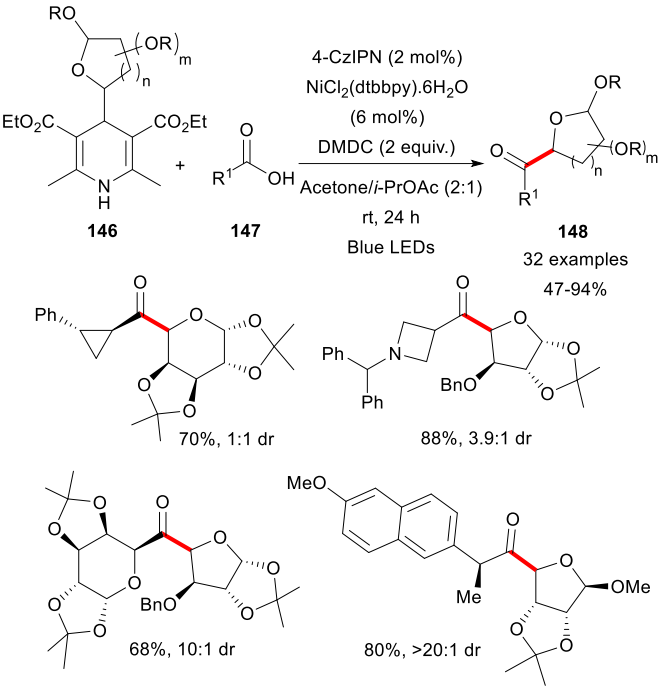

Scheme 50 Ketones synthesis through carboxylic activation.

Alkyl-DHPs **146** and carboxylic acid **147** reacted smoothly in the presence of $NiCl_2(dtbbpy).6H_2O$ complex and 4CzIPNas photocatalyst in a mixture of acetone/isopropyl acetate (2:1) under blue LEDs irradiation to give the products **148**. *In-situ* activation of the carboxylic acid was performed by the addition of 2 equivalents of dimethyldicarbonate (DMDC). The authors applied this methodology mainly for the synthesis of several C-acyl glycosides but they also reported that non-glycoside substrates could be engaged allowing the formation of unsymmetrical dialkyl ketones in good yield. The reaction mechanism follows a traditional Ni/photoredox catalytic cycle.

Very recently, a similar Ni-free approach has been proposed by Scheidt and co-workers by merging photoredox and *N*-heterocyclic carbene (NHC) catalysis (Scheme 51).[107] In this procedure, acyl imidazole **149** and alkyl-DHPs **136** would react in the presence of 1,4-dimethyl-4H-1,2,4-triazolium iodide as NHC precursor, caesium carbonate as base and $[Ir[dF(CF_3)ppy]_2(dtbbpy)]PF_6$ as photocatalyst in acetonitrile under blue LEDs irradiation to afford ketones **150** in moderate to good yields.

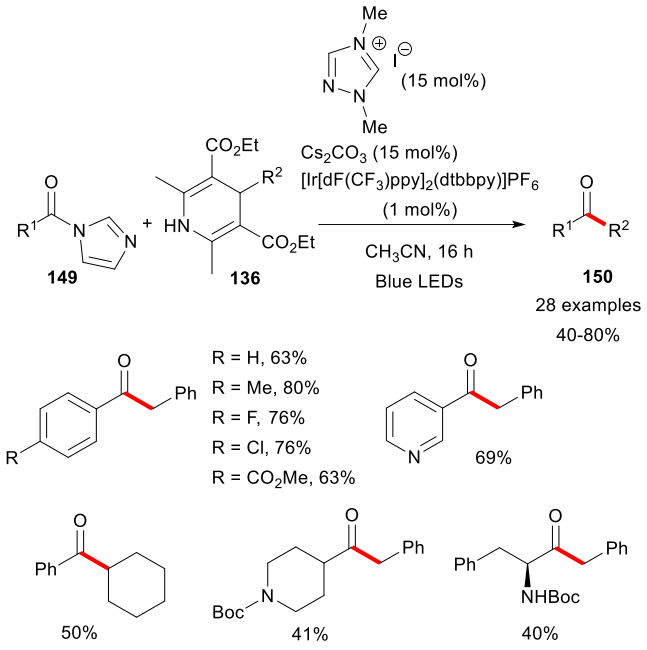

Scheme 51 Ketone synthesis assisted by NHC catalysis.

A wide range of acylimidazoles with multiple functional groups are engaged with alkyl radical precursors (mainly benzyl-DHPs.) Improvement of the protocol is also mentioned with the direct one-step alkylation of carboxylic acid. Preliminary treatment with carbonyl diimidazole (CDI) led to the *in-situ* formation of acyl imidazole intermediates that would react under the reaction conditions mentioned above. This method allowed a late-stage functionalization of pharmaceutical compounds such as telmisartan, repaglinide and dehydrocholic acid derivatives.

A mechanism scenario was proposed. Concomitant with the formation of a C-centered radical *via* the corresponding radical cation **136a**, acyl imidazole **149** is converted to an acyl triazolium species **151**. Single electron reduction of the latter by Ir^{II} would furnish the triazole radical **151a** while regenerating the photocatalyst in its ground state (Scheme 52). C-centered radical then reacts under the ketyl radical resonance form **151b**, which allows radical-radical coupling. The desired ketone **150** is obtained after loss of the NHC motif.

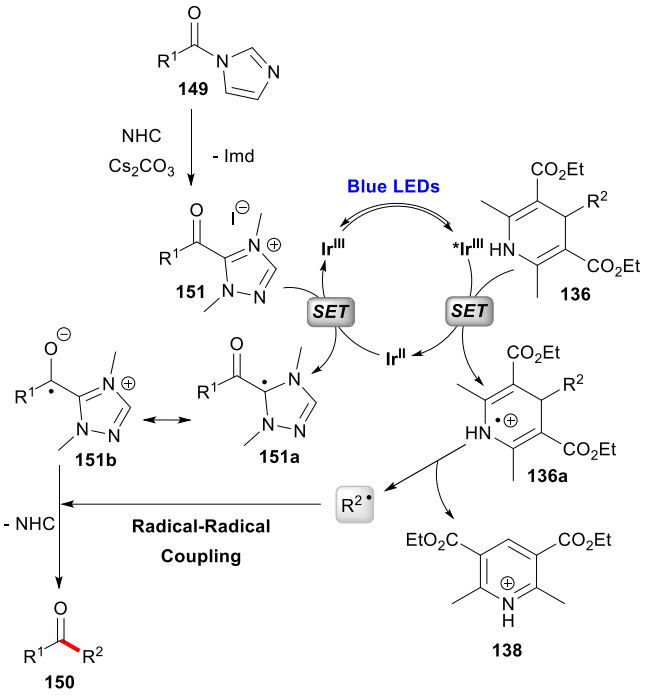

Scheme 52 Proposed mechanism for the merging of photoredox and *N*-heterocyclic carbene (NHC) catalysis.

In the same article, an experiment was made with acylimidazole **152**, alkyl-DHP **153** and a chiral carbene in order to control the enantioselectivity of the addition. A modest result was obtained with an e.r. of 66:34 for **154** but remains very encouraging for the future of this catalysis (Scheme 53).

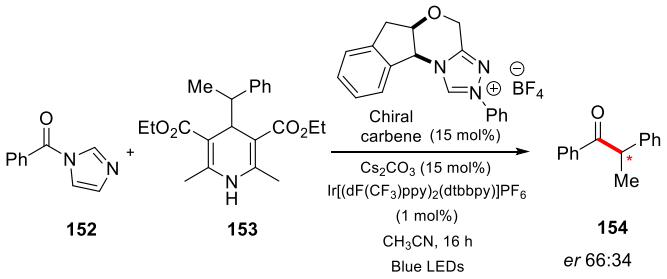

Scheme 53 Ketone synthesis assisted by a chiral NHC catalysis.

In this quest for selective addition, Yu and co-workers reported an asymmetric allylic alkylation (AAA) by merging palladium and photoredox catalysis, opening a new field in the use of alkyl-DHPs (Scheme 54).[108] The developed protocol involves racemic allylic esters **155** as electrophiles, alkyl-DHPs **136** as radical source, $Pd_2(dba)_3$ as catalyst, $[Ir(dtbbpy)(ppy)_2]PF_6$ as the photocatalyst, K_2CO_3 as the base in acetonitrile under blue LEDs irradiation to afford alkylation products **156**. After screening, (*R*)-DTBM-GARPHOS proved to be the best chiral ligand for this catalysis and very high enantiomeric ratios (*er*) were obtained. Similarly, a very good regioselectivity was observed during this AAA reaction and only branched adducts were obtained. A significant range of allylic esters is represented but only stabilized radicals were engaged (with

one exception for isopropyl radical). Mechanistically, conventional oxidative addition of allyl ester from Pd^0 leads to a Pd^{II}-π-allyl intermediate. The alkyl radical generated as above would combine with the π-allylpalladium complex to generate a Pd^{III} complex, which undergoes reductive elimination to give the allylic alkylation product **156**. The photoredox catalytic cycle is closed by reduction of the Pd^{I} with the Ir^{II} species regenerating simultaneously the photocatalyst to its ground state.

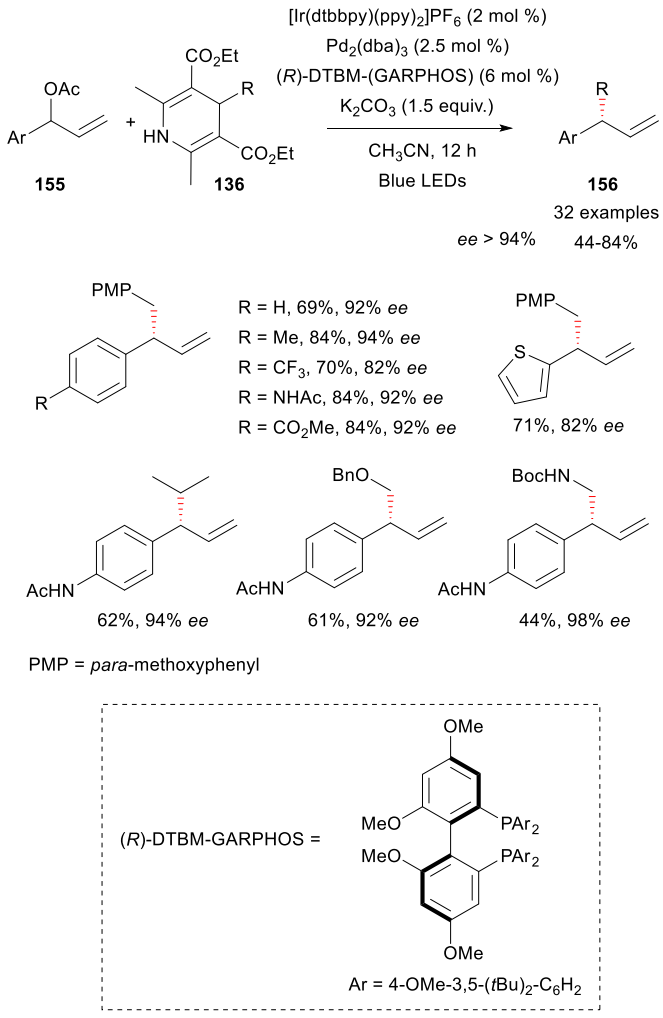

Scheme 54 Asymmetric allylic alkylation by dual Pd/Ir catalysis.

Very recently, a close protocol of dual Pd/Ir catalysis was also developed with vinyl cyclic carbonates allowing the asymmetric synthesis of homoallylic alcohols.[109]

In addition to this AAA reaction, Xiao and co-workers reported an enantioselective photocatalyzed Giese addition on activated alkenes **157** with alkyl-DHPs **136** in the presence of mesityl acridinium perchlorate (Mes-$AcrClO_4$) as photocatalyst, a cobalt complex as chiral inducer in acetonitrile under blue light irradiation to afford β-alkylated ketones **158** in good yields (Scheme 55).[110]

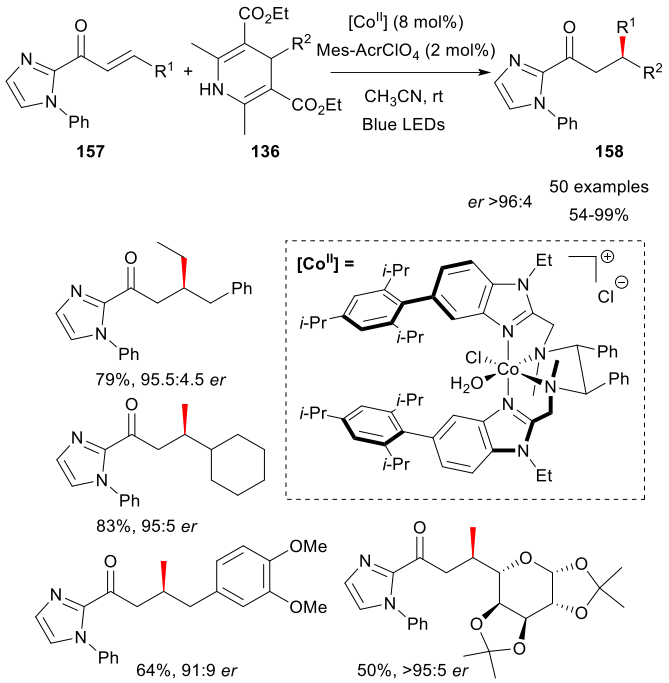

Scheme 55 Cobalt-catalysed stereoselective addition of alkyl-DHPs on enone.

Based on the Meggers' catalysts[111,112], the authors developed a series of chiral octahedral cobalt complexes as chiral Lewis acid for Giese-type addition. During their investigations, the authors found that the directing group appended on the alkene is critical for the outcome of the reaction and ultimately determined that *N*-phenyl imidazole proved to be the most suitable for this reaction. Primary and secondary alkyl-DHPs were efficiently added on different enones in moderate to very good yields with a high degree of enantioselectivity. A plausible mechanism proposed by the authors is depicted in scheme 56. The photocatalytic cycle is initiated by reductive quenching of the Ir-based photocatalyst with alkyl-DHP **136** giving the radical cation **136a** which expels a *C*-centered radical. In parallel, enone **157** is activated by the cobalt catalyst leading to the chiral complex **157a**. The stereoselective addition of the radical on **157a** affords the Co^{II} intermediate **159** which is in equilibrium with its Co^{III} form **159a**. Its reduction by the Ir^{II} species enables the formation of the Co^{II} intermediate **159b** and closes the photocatalytic cycle. A ligand exchange assisted by the pyridinium salt **138** furnishes the desired alkylation product **158**.

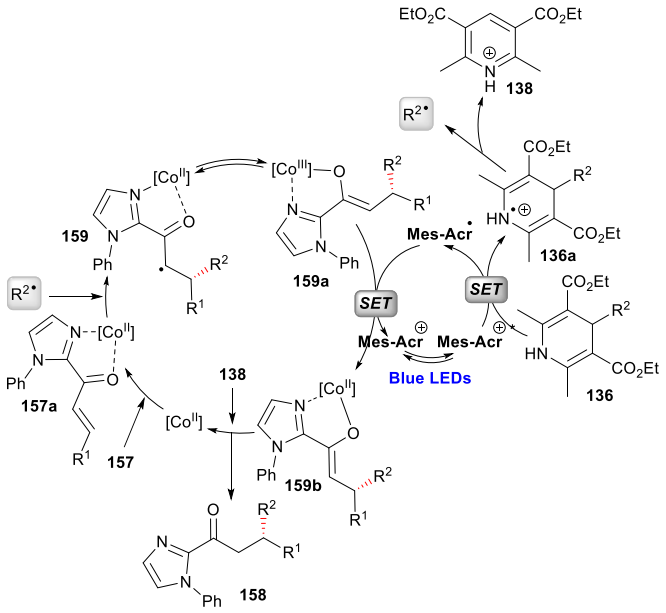

Scheme 56 Proposed mechanism for the cobalt-catalysed stereoselective addition of alkyl-DHPs on enone.

Very recently, Melchiorre and co-workers disclosed an elegant approach for the asymmetric photochemical allylation from allylic alcohol derivatives **160** and alkyl-DHPs **161** in the presence of $[Ir(cod)Cl]_2$ and a (*S*)-phosphoramidite-olefin ligand.[113] The allylated products **162** were obtained in good yields with good selectivities (Scheme 57).

In this method, the catalytic cycle is initiated by the formation of the chiral allylic Ir(III) complex from the mixture of $[Ir(cod)Cl]_2$, chiral ligand and the allylic alcohol precursor. This complex exhibits redox properties upon irradiation leading to a SET with the alkyl-DHPs to generate an alkyl radical. The latter intercepts the metal centre *via* radical-metal crossover. The final reductive elimination step affords the cross-coupling product and regenerates the chiral Ir(I) catalyst.

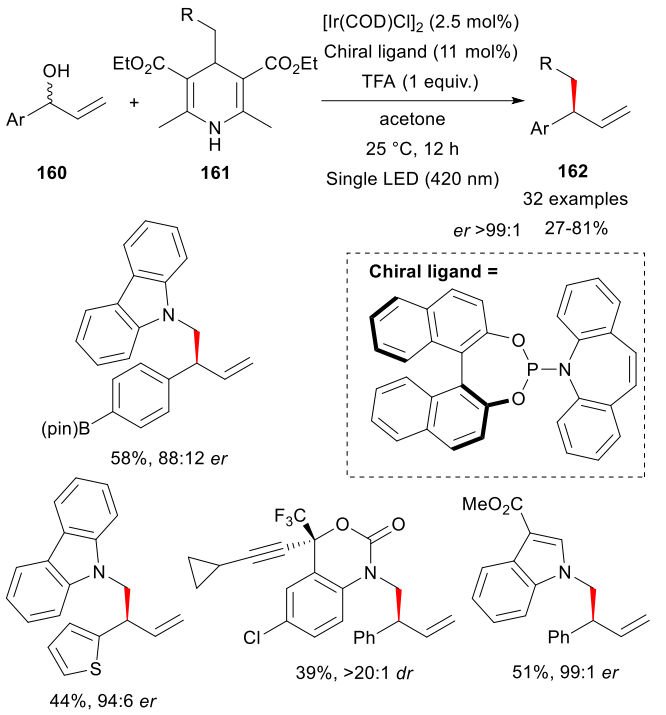

Scheme 57 Iridium-catalysed stereoselective addition of alkyl DHPs

An important study was carried out by Melchiorre and co-workers by developing a photocatalyst-free Ni cross-coupling with alkyl-DHPs (Scheme 58).[114] During their investigations, the authors found that the DHP motif could be directly excited by visible light leading to strong reductive properties (E_{red}^* = -1.955 V vs SCE in CH_3CN) and could be embedded in a metal catalytic cycle.[114] The light-triggered cross-coupling process operates at ambient temperature using $NiCl_2$·DME as the metal catalyst, bipyridine as the ligand and 2,6-lutidine as the base in acetonitrile with high-powered LED (λ_{max} = 405 nm, irradiance of 50 mW.cm^{-2}) as irradiation source. A variety of aryl bromides **163** were successfully coupled with alkyl-DHPs **136** to afford the corresponding cross-coupling products **164** in good to excellent yields. The reaction tolerated a wide range of functional groups, including cyano, aldehyde, ester, and chloride moieties. For the radical counterpart, both linear and cyclic alkyl-DHPs could be successfully engaged with aryl bromides as well as primary stabilized radical precursors.

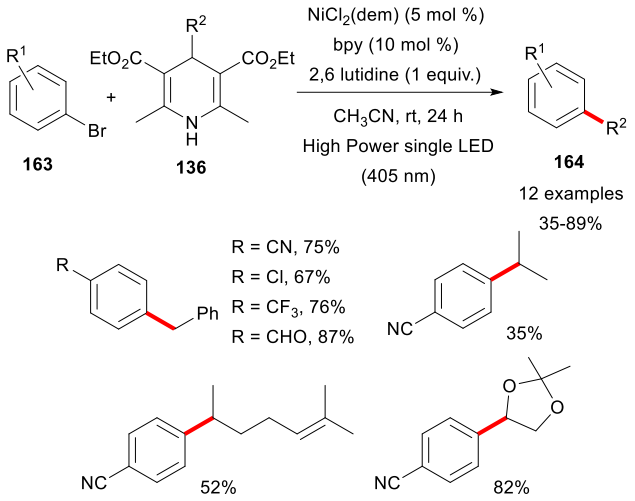

Scheme 58 Light-triggered nickel-catalyzed cross-coupling reactions with alkyl-DHPs.

An in-depth study of the reaction mechanism was made and allowed the authors to propose the following explanation (Scheme 59). The catalysis would start with the photoexcitation of alkyl-DHP **136** and the resulting excited-state intermediate **136*** reduces the Ni^{II} precatalyst through two SET events to give the active Ni^{0} intermediate. The formation of the radical cation **136a** leads to the formation of the alkyl radical, which would combine with the formed Ni^{0} complex. The Ni^{I} species undergoes oxidative addition with the aryl bromide **163** resulting in the formation of the intermediate Ni^{III}. After reductive elimination, the desired cross-coupling product **164** is obtained. The catalytic cycle is completed by a SET reduction of the generated Ni^{I} complex with the excited alkyl-DHPs **136***.

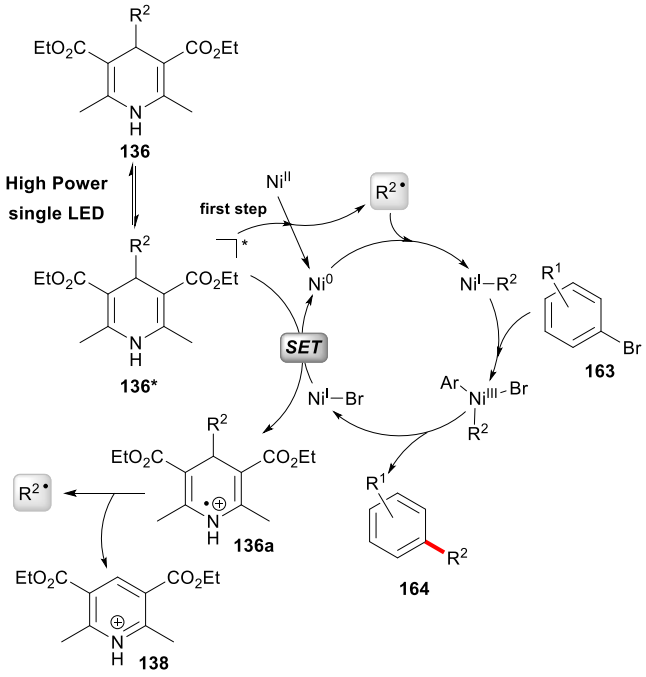

Scheme 59 Melchiorre's mechanism for the light-triggered cross-coupling with alkyl-DHPs.

As an extension of his work on iminium chemistry[86], an elegant approach was disclosed by the Melchiorre group using the photochemistry of chiral iminium cations to generate C-centered radicals from alkyl-DHPs (Scheme 60).[115] Enals **165** and alkyl -DHPs **136** react smoothly in the presence of trifluoroacetic acid (TFA), a chiral amine, in a mixture of acetonitrile and perfluorohexane at -10°C under high power single LED (λ_{max} = 420 nm) to give the β-alkylated products **166** in good yields. The stereoselectivity obtained via the chiral amine organocatalyst proved to be very high. Mechanistically, a reductive quenching would be involved between the strongly oxidizing excited iminium ions (+2.355 V vs SCE) and alkyl-DHPs, causing the formation of the radical cation and the alkyl radicals respectively. Radical-radical coupling followed by hydrolysis of the iminium would deliver the expected β-alkylated products.

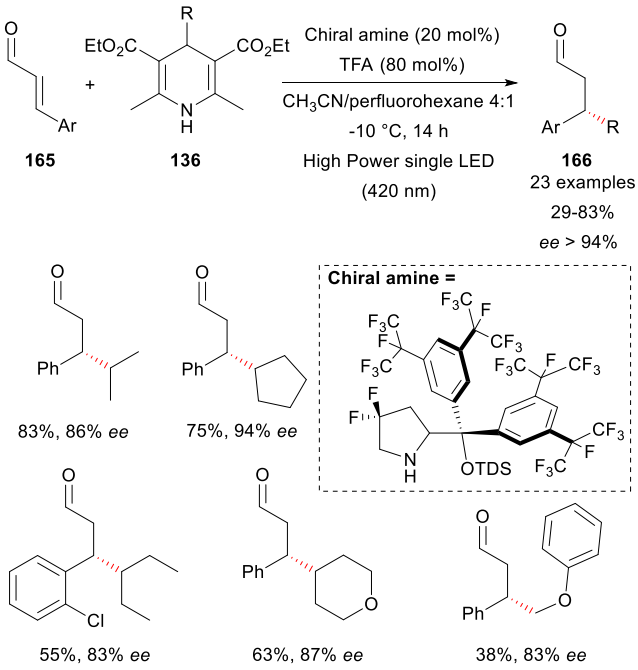

Scheme 60 Stereoselective β-alkylation of enals with alkyl-DHPs.

Recently, a photocatalyst-free version of Giese-type addition was also reported by Melchiorre and co-workers.[116] Activated olefin **167** and alkyl-DHPs **136** reacted in the presence of $Ni(bpy)_3(BF_4)_2$ in acetonitrile with high-powered LED (λ_{max} = 405 nm) as irradiation source to afford the addition product **168** (Scheme 61). A variety of α,β-unsaturated nitriles or esters and substrates with secondary, benzyl or α-heterosubstituted alkyl fragments are well tolerated in this transformation.

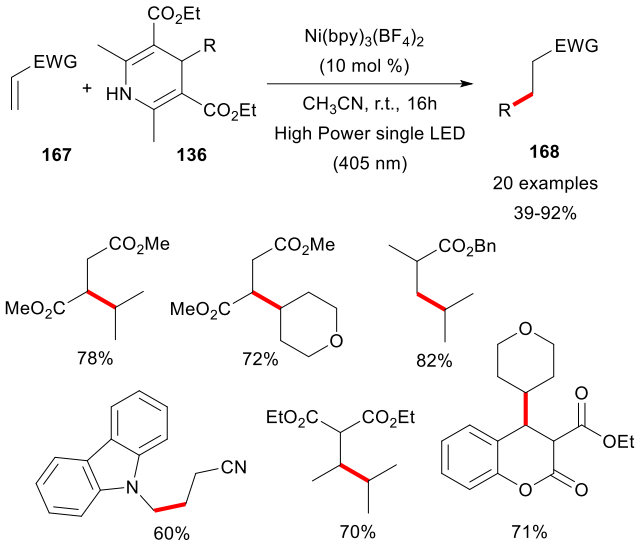

Scheme 61 Photocatalyst-free Giese-type addition with alkyl-DHPs.

In an attempt to elucidate the reaction mechanism, the authors demonstrated that the catalytic amount of $Ni(bpy)_3(BF_4)_2$ is mandatory for the course of the reaction and proved its role as an electron mediator (Scheme 62**).** After excitation of alkyl-DHP **136**, the excited state of alkyl-DHP **136*** is oxidised by $Ni(bpy)3^{2+}$ producing the alkyl radical through the generation of the radical cation **136a**. Giese addition takes place on activated alkenes **167** producing the corresponding radical **167a**. The Ni^{I} intermediate reduces **167a** to the anion **167b** which delivers the Giese addition product **168** after protonation.

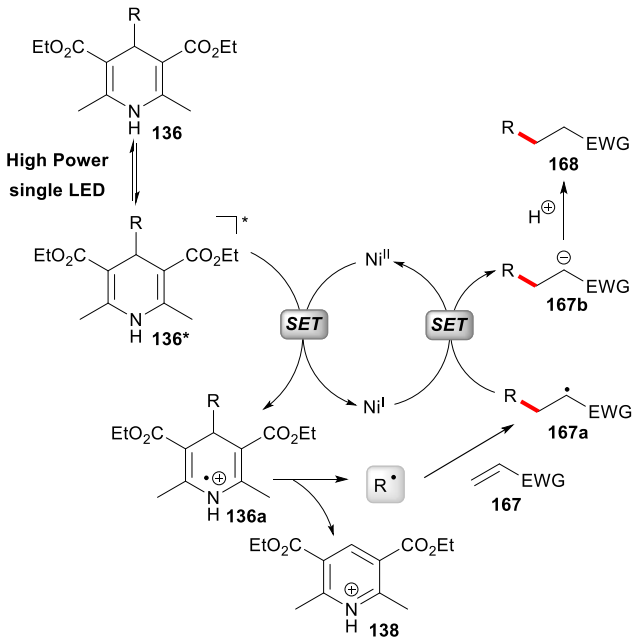

Scheme 62 Melchiorre's mechanism for the photocatalyst-free Giese-type addition.

Very recently, Hong and co-workers have developed a procedure for the alkylation of pyridinium salts **169** with alkyl-DHP **136** allowing through an electron donor-acceptor complex (EDA) the formation of alkylated pyridines **170** (Scheme 63).[117] An EDA complex results in the association between an electron-rich species (named Donor) and an electron-deficient entity (named Acceptor). This association lead to a complex that can absorb light and exhibit photochemical properties.[118,119] A wide range of radicals could be engaged including primary, secondary, tertiary or amino acid-derived radicals. A broad scope of pyridinium salts has been covered and complex molecules such as vismodegib, or bisacodyl have been efficiently transformed.

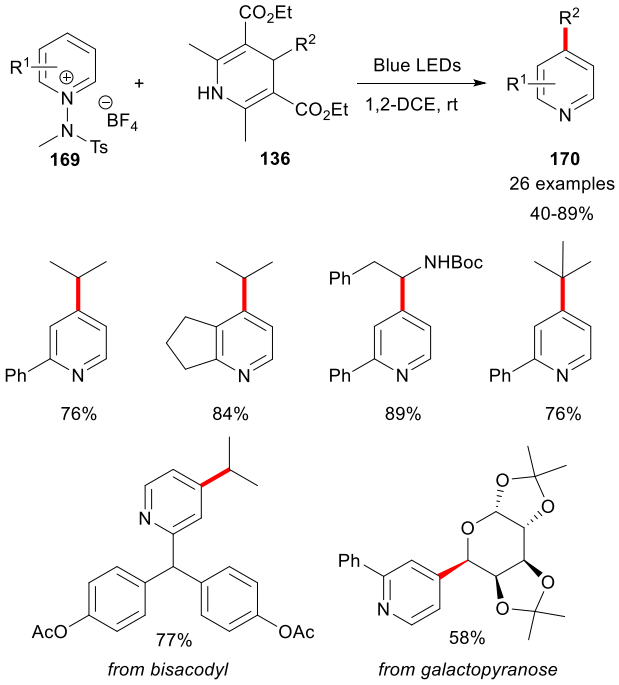

Scheme 63 Alkylation of pyridinium mediated by EDA complex.

The authors described a plausible mechanism divided in two steps (Scheme 64). The initiation step is triggered by the interaction of **169** and **136** to form an EDA complex. Once formed, the EDA complex **171** is excited and a photo-induced SET provides the fragmentation and the formation of a C-centered radical. In the second step of the mechanism, the radical adds regioselectively to the C-4 position of the pyridinium salt **169** affording the radical intermediate **172**. Deprotonation and cleavage of the N-N bond allow the release of the aminyl radical **173** and the expected product **170**. The expelled *N*-centered radical **173** is reduced by the alkyl-DHP **136** to give a new radical cation **136a** and the anion **174** allowing the propagation of the radical chain.

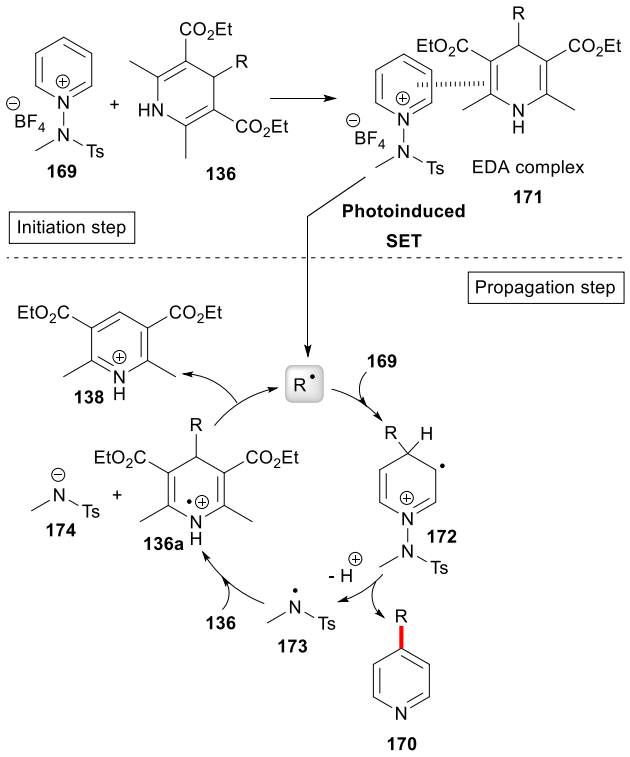

Scheme 64 Proposed mechanism of the alkylation of pyridinium salts **169** with alkyl-DHP **136**.

C.2 alkyl pyridinium salts

Pyridinium salts represent an important class of compounds in organic chemistry and display considerable applications. In 1977, Katritzky synthesized 2,4,6-triphenylpyridinium salts from primary amines and the 2,4,6-triphenylpyrylium cation (scheme 65).[120] These salts, named Katritzky salts are electron-deficient structures and therefore are therefore easily reduced ($E_{1/2}$~ -0.90 V vs SCE).[121]

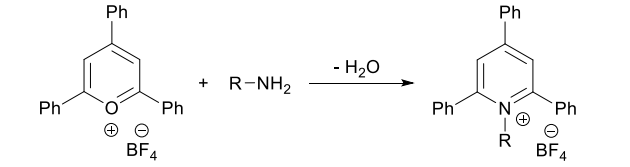

Scheme 65 formation of Katritzky salt from 2,4,6-triphenylpyrylium cation and primary amines.

Forty years later, there is renewed interest in the use of these salts in radical chemistry and their applications as a source of alkyl radicals have recently been reviewed.[122–124]
In 2017, the Watson group demonstrated that Katritzky salts **175** could be engaged with aryl boronic acid **176** in a nickel-catalyzed Suzuki–Miyaura reaction in the presence of $Ni(OAc)_2$, bathophenanthroline (Bathophen) and potassium *tert*-butoxide leading to the formation of cross-coupling product **177** (Scheme 66).[125] This method allows for a cross-coupling reaction through a C–N bond activation of alkyl amines and it exhibits a broad reaction field with a high degree of tolerance of functional groups.

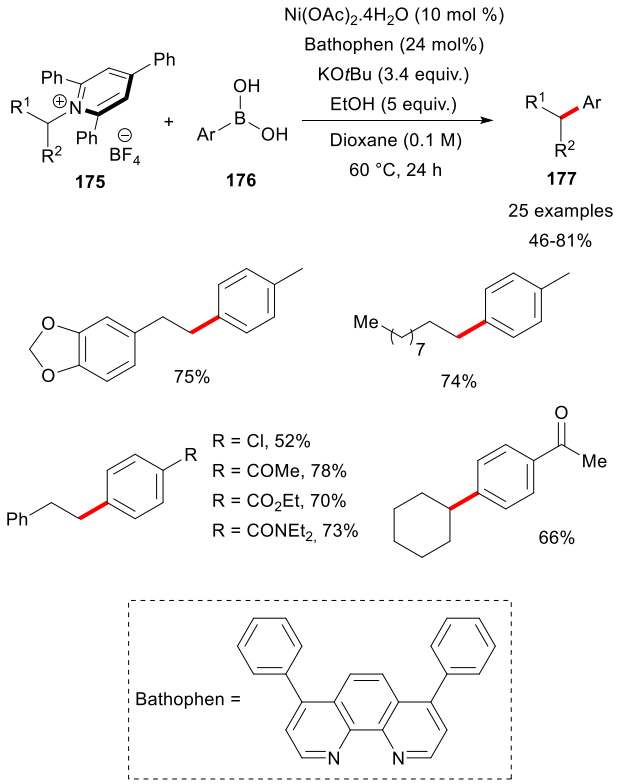

Scheme 66 Suzuki-Miyaura cross-coupling with Katritzky salts **175**.

From a mechanistic point of view, investigations by Watson suggested a Ni(I)/Ni(III) cycle (Scheme 67). In this scenario, the Katritzky salt **175** is reduced by a SET with a ArNi(I) intermediate to generate the radical intermediate **175a** which after fragmentation expels the respective alkyl radical, a ArNi(II) species and 2,4,6-triphenylpyridine (TPP). The two partners combine together and lead to a new ArNi(III) complex. Reductive elimination furnishes the desired cross-coupling product **177** and restores an active Ni(I) intermediate.

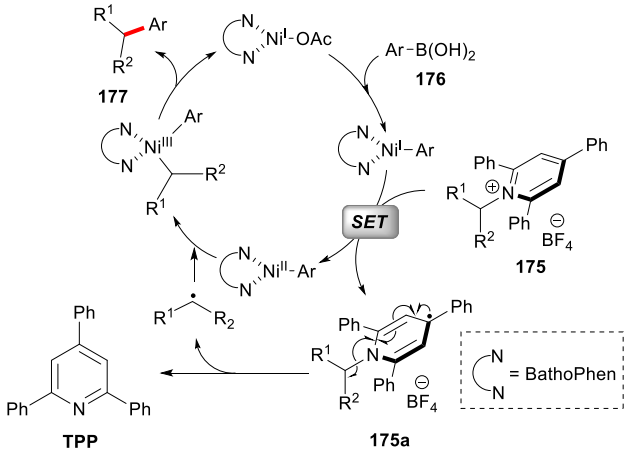

Scheme 67 Proposed mechanism by Watson for Suzuki-Miyaura cross-coupling with Katritzky salts **175**.

In the same year, the Glorius group succeeded in generating alkyl radicals under visible light irradiation from various Katritzky salts **175** and heteroarenes **178** in the presence of an iridium-based photocatalyst. The generated radicals were engaged in Minisci-type reaction with several heteroaryl partners affording functionalized heteroarenes **179** (Scheme 68).[126]

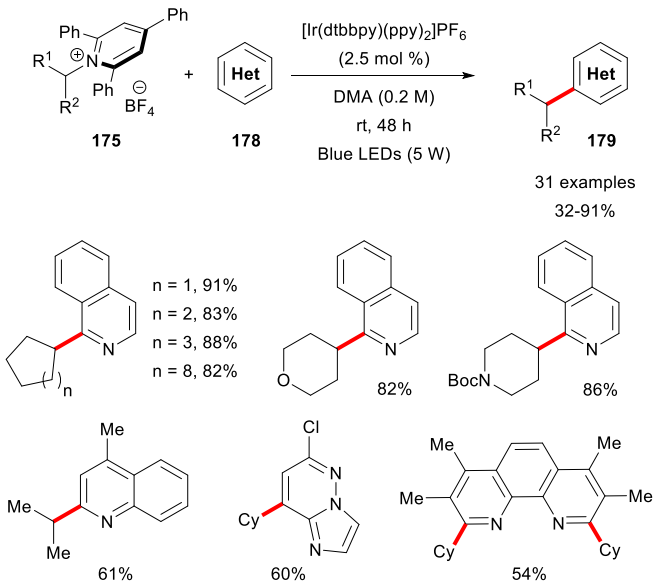

Scheme 68 Minisci-type reaction with heteroaryl and Katritzky salts **175**.

This method presents a wide range of amine precursors for the regioselective alkylation of heteroarenes. Interestingly, Glorius employed nucleophilic alkyl radicals for the Minisci-type reaction with electron-deficient heteroarenes, but also electrophilic α-carboxyl radicals (from amino acids) for the reaction with electron-rich heteroarenes. In its excited state, the Ir photocatalyst reduces Katritzky salt **175** by SET (Scheme 69). Homolytic cleavage of the C-N bond leads to the formation of a C-centered radical that trapped by the heteroarene **178**. The catalytic cycle is closed by oxidation of the radical **178a** by the Ir(IV) intermediate leading to a carbocation intermediate **178b**. Subsequent re-aromatization by deprotonation gives the Minisci-type product **179**. After these seminal findings, other approaches and substrates were explored.

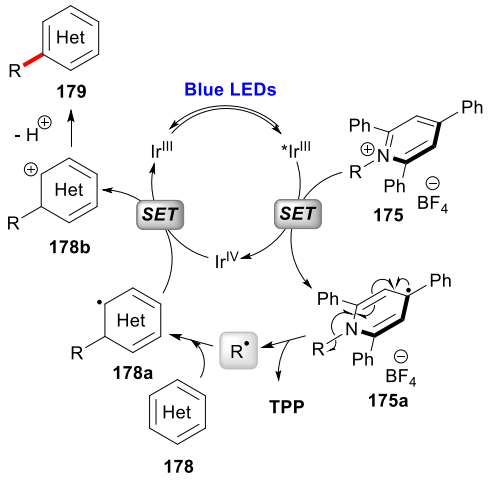

Scheme 69 Proposed mechanism for Glorius's Minisci-type reaction with Katritzky salts **175**.

In 2018, Liu and co-workers disclosed a photoredox allylation with Katritzky salts **175** and an iridium-based photocatalyst (Scheme 70).[127] This methodology displays a large substrate scope in radicals that could be allylated in good yields with allylsulfones **180**. The allylic counterpart can possess a large variety of substituents such as methyl, cyano, ester and substituted aryl moiety allowing a consequent diversity in terms of products **181**.

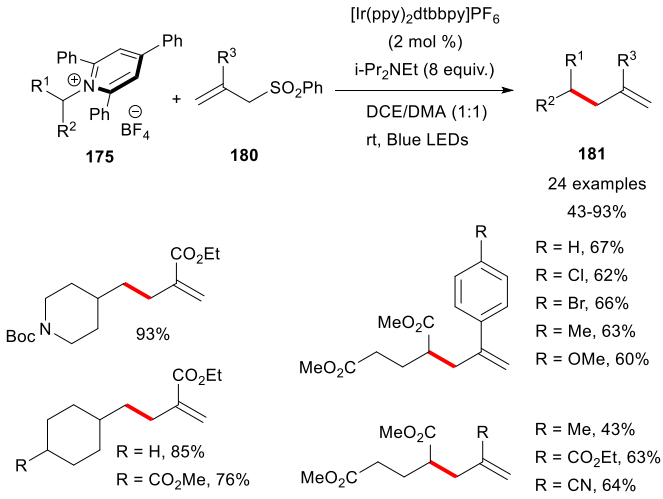

Scheme 70 Photoredox allylation of Katritzky salts **175**.

The next year, Xiao and co-workers reported a photo-induced Heck-type coupling between Katritzky salts **175** and alkenes **182** (Scheme 71).[128] This strategy provides a mild alternative to the palladium-catalyzed Heck coupling which often needs harsh conditions and overcomes the instability encountered with alkylpalladium species. Mechanistically, an oxidative quenching takes place between the excited Ir(III) and a pyridinium salt. The expelled radical reacts with the alkene creating a more stable radical. The catalytic cycle is completed by reduction of the Ir(IV) intermediate to Ir(III) by the C-

centered radical. The resulting carbocation leads to the corresponding alkene **183** through a base-assisted deprotonation. It is interesting to note that the outcome of the reaction strongly depends on the nature the alkenes involved. Of course, simple alkenes afforded Heck-type products, but enol ethers **184** furnished the homologated ketones **185**. Moreover, if a CO atmosphere is applied with the same reaction conditions, this strategy permits a carbonylative Heck-type reaction and the corresponding enones **186** are obtained in good yields (Scheme 72).

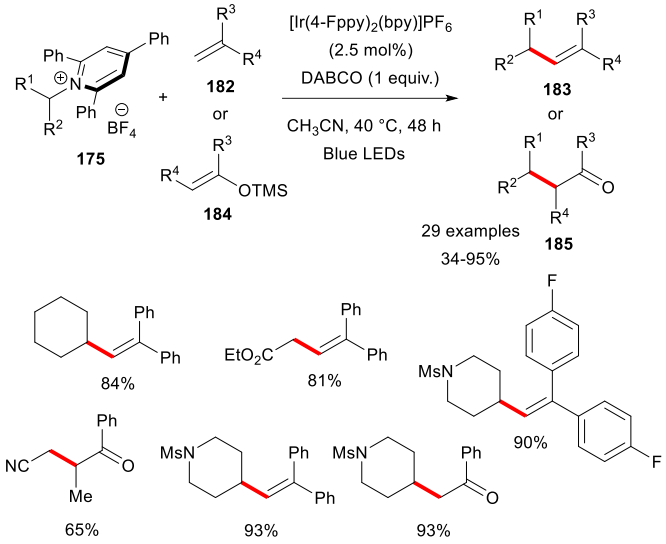

Scheme 71 Heck-type cross coupling with Katritzky salts **175**.

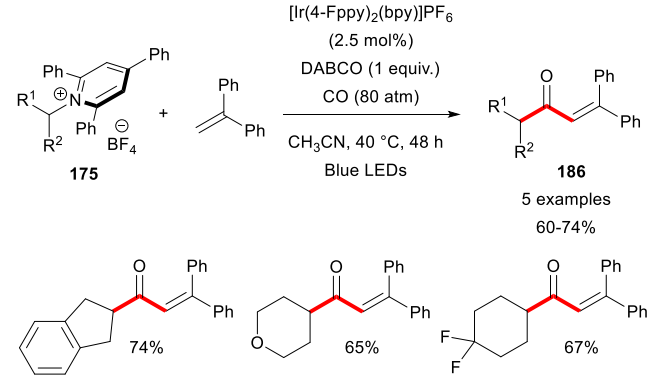

Scheme 72 Carbonylative Heck-type cross coupling with Katritzky salts **175**.

Uchiyama and co-workers reported a similar photocatalyzed Heck-type coupling with Katritzky salts **175** and alkenes **187** in a stereoselective manner (Scheme 73).[129] The reaction mechanism is the same that outlined above, but in this case the authors designed the methodology to obtain the desirable diastereomer. During their investigation, they found that the E-isomer **188** could be selected using $Ru(bpy)_3(PF_6)_2$ as photocatalyst, whereas the Z-isomer **189** is obtained with *fac*-$Ir(ppy)_3$ as photocatalyst. The authors attributed this selectivity to *E–Z* isomerization promoted by the Ir-based photocatalyst.

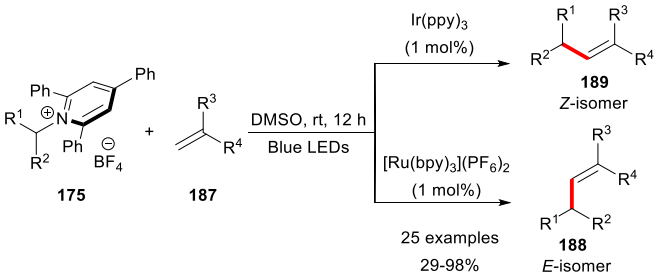

Scheme 73 Stereoselective Heck-type coupling with Katritzky salts.

As an extension of this work, the groups of Glorius and Lautens reported three component reactions between Katritzky salt **175**, functionalized indoles **190** and styrene derivatives **191** (Scheme 74).[130] This dicarbofunctionalization methodology displays a large scope especially in terms of styrenes and radicals formed from Katritzky salts, even if limited to stabilized ones. The first step of the reaction starts with a classical SET from the oxidative quenching pathway, expelling a benzyl radical. This adds onto the styrene double bond creating another stable benzyl radical which is then oxidized by the photocatalyst. Finally, the electron-rich indole reacts with the benzyl carbocation and delivers the expected compound **192** after a deprotonation step.

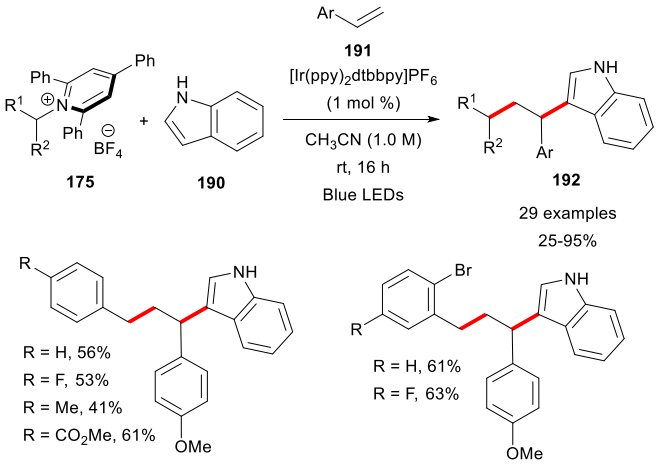

Scheme 74 Three component reactions between Katritzky salt, styrene derivatives and functionalized indoles.

Alongside all these methods, an elegant C(sp)–C(sp^3) and C(sp^2)–C(sp^3) bonds formation was disclosed by Gryko from Katritzky salts (Scheme 75).[131] In their approach, a metal-free photoredox protocol was proposed from alkyl Katritzky salts **175** and sulfonylated alkynes/alkenes **193** as radical traps using eosin Y as photocatalyst. The developed method has been extended to a plethora of pyridinium precursors and a wide variety of substrates bearing multiple functional groups. In addition, complex targets such as indomethacin or mexiletine (commercially available pharmaceuticals) were selectively functionalized, demonstrating the strong synthetic potential of this method. From a mechanistic point of view, the

authors evoke a classical oxidative quenching route of eosin Y with Katritzky salts. The addition of the alkyl radical to the alkenyl/alkynyl sulfone is followed by the fragmentation of the sulfonyl radical affording the alkynyl-alkenylated products **194**. The photocatalyst is restored by reduction with a sacrificial electron donor (e.g. DIPEA).

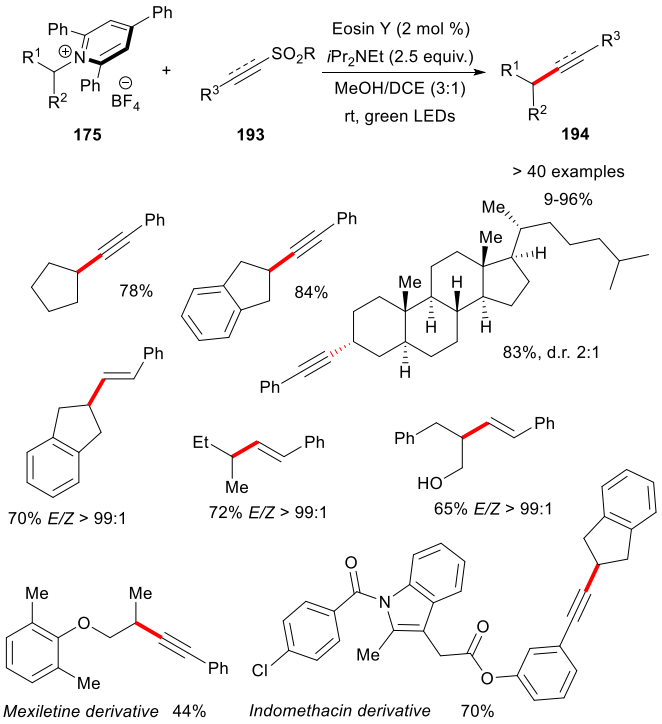

Scheme 75 Gryko's desulfurative alkenyl- and ethynylation with Katritzky salts.

In the line of her seminal work, Watson reported the first Csp^3-Csp^3 cross-coupling between Katritzky salts **175** and alkylzinc reagents **195** (Scheme 76).[132] In this study, a wide range of amines was successfully engaged with alkylzinc halides in the presence of $Ni(acac)_2$ leading to the formation of Csp^3-Csp^3 cross coupling products **196**. Interestingly, Watson found that the ancillary ligand has a dramatic effect on the reaction outcome. For primary pyridinium salts, 4,4',4''-tri-*tert*-butyl-2,2':6',2''-terpyridine (ttbtpy) appears to be the ligand of choice, while secondary Katritzky salts must resort to 2,6-bis(N-pyrazolyl)pyridine (1-bpp). Concerning the organozinc counterparts, only primary alkylzinc reagents are effective, secondary and tertiary substrates failed to react. Despite this limitation, this methodology represents a major breakthrough in cross-coupling reactions and has been applied to natural products such as pinanamine, Mexiletene, Tamiflu or Mosapride intermediate. In terms of reaction mechanism, the authors hypothesize that the reaction proceeds by SET of Ni(I) to the alkyl pyridinium salt from a Ni(I) intermediate. The expelled radical recombines with a Ni(II) intermediate to subsequently deliver the product. A similar protocol was disclosed by Ni and Li in the same year.[133]

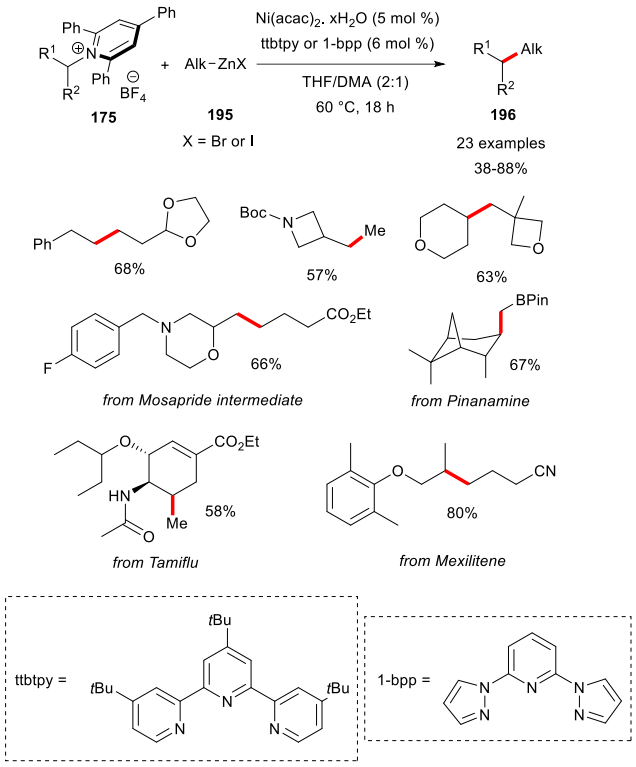

Scheme 76 Cross-coupling reactions between Katritzky salts and alkylzinc halides.

Other achievements have been accomplished in dual catalysis. Rueping and co-workers reported a Ni-catalyzed reductive cross-coupling of Katritzky salts **197** with aryl halides **198** (Scheme 77).[134] The reaction proceeds smoothly in the presence of $NiCl_2$ as the catalyst, Mn as reductant and DMA as solvent. An impressive reaction scope was reported with iodo- or bromobenzenes bearing electron-donating or electron withdrawing substituents, yielding products **199** mostly in good yields. Similar to Watson's work, the choice of ligand has a significant impact on the outcome of the reaction. Both cyclic and acyclic secondary alkylpyridinium salts were able to undergo this reaction smoothly. Notably, the use of 4,4',4''-tri-*tert*-butyl-2,2':6',2''-terpyridine (ttbtpy) was mandatory for effective coupling with the primary Katritzky salts, while the secondary pyridinium salts reacted in the presence of bipyridine (bpy) as a ligand.

The authors proposed a mechanistic explanation based on the Ni(0) species generated by reduction *in situ* with Mn. After oxidative addition, the arylNi(II) intermediate is reduced to arylNi(I) by the Mn salt. This newly formed Ni(I) complex is able to reduce the pyridinium salt by SET and the C-centered radical generated recombines with the Ni(II) intermediate leading to a Ni(III) species and then produces the expected product by reductive elimination. The Ni(0) species is regenerated by reduction with Mn.

It should be noted that at the same time, similar protocols involving Katritzky salts, aryl bromides and manganese have also been described by Watson's group[135] and Martin's group,[136] leading to the cross-coupling products in good yields.

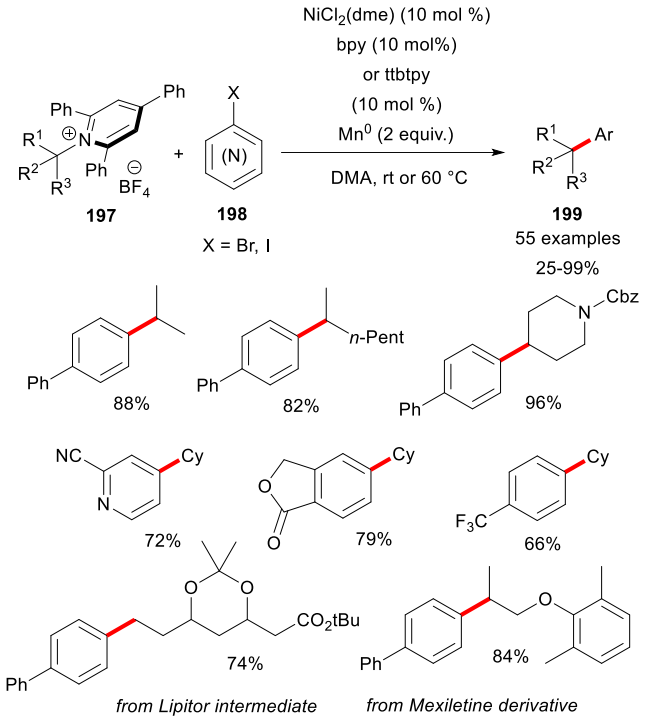

Scheme 77 Ni-catalyzed reductive cross-coupling of Katritzky salts with aryl halides.

Other electrophiles have also been engaged in this Ni-catalyzed cross-coupling reactions with Katritzky salts. For example, Matsuo,[137] Rasappan[138] and Watson and Weix[139] have independently reported the syntheses of ketones from pyridinium salts **175** or **200** (Scheme 78). Matsuo demonstrated that *N*-acylsuccinimides **201** react in the presence of $NiBr_2$ and 1,10-phenanthroline (1,10-phen) with the assistance of one equivalent of $MgCl_2$ as Lewis acid and Mn as reducing agent to afford ketones **202**. Similarly, Rasappan developed a protocol from acyl chloride **203** or by *in situ* activation of carboxylic acids **204** with di-tert-butyl dicarbonate (Boc_2O) for the synthesis of ketones **205**. Finally, Watson and Weix proposed a close system based on the activation of acyl fluoride **206** or 2-pyridyl ester **207** for the production of ketones **208**.

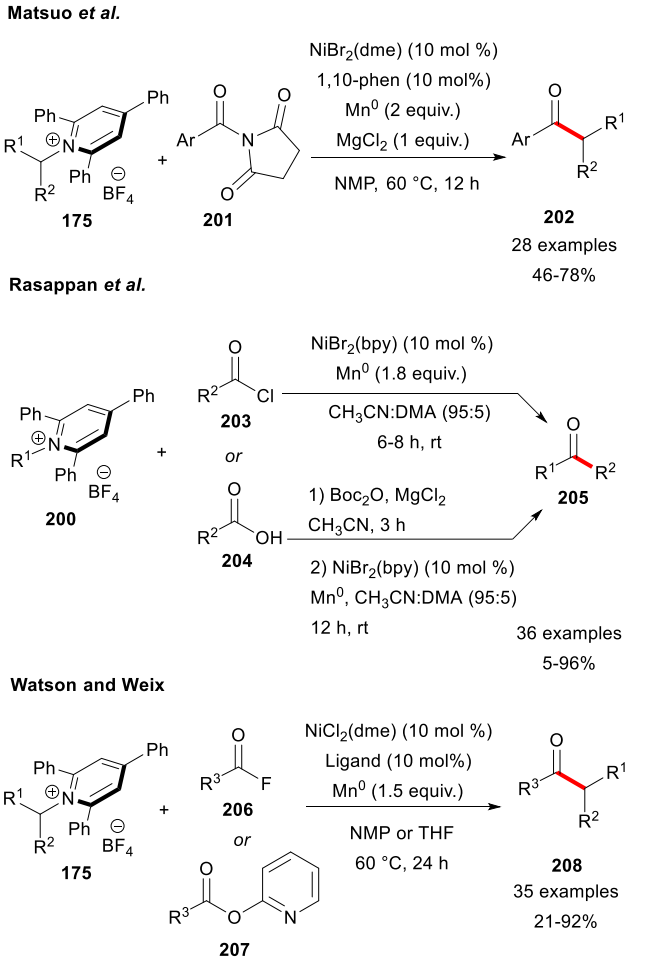

Scheme 78 Ni-catalyzed ketones synthesis from Katritzky salts.

In 2019, Molander reported the first Ni-catalyzed cross-coupling reactions between Katritzky salts **175** and aryl halides **209** (Scheme 79).[140] The authors found that the combination of the 4,4'-di-tert-butylbipyridine(dtbbpy)/$NiBr_2$ complex, 4CzIPN, and triethylamine in THF or DMA is optimal for effective cross-coupling reactions affording the cross-coupling products **210** in high yields. These very mild conditions avoided the use of external metal salts as a reductant and thus allowed the incorporation of sensitive chemical functions into the substrates.

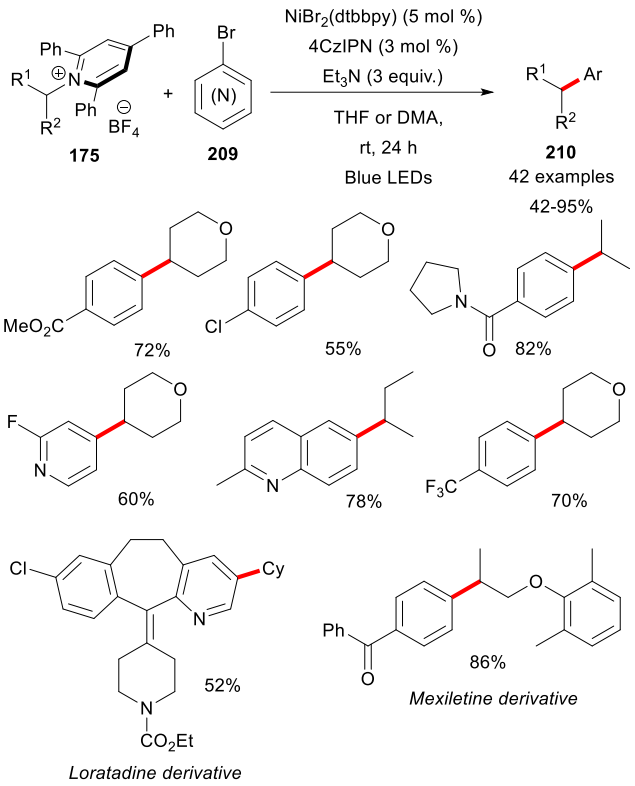

Scheme 79 Photocatalyzed Ni cross-coupling reactions between Katritzky salts and aryl halides.

Mechanistically, the photocatalytic cycle proposed by the authors involves a reductive quenching cycle where the photoexcited catalyst is reduced by triethylamine to form the radical anion 4CzIPN.-. This electron rich species is now able to reduce the Katritzky salt **175** and the Ni(I) species **F** during the catalytic cycle (Scheme 80). Combination of the generated alkyl radical and Ni(0) catalyst **G** led to a Ni(I) alkyl intermediate **H**. The latter undergoes oxidative addition with the aryl bromide **209** to give the Ni(III) intermediate **I**, which provides the desired product **210** after reductive elimination. The cycle is closed by reduction of the Ni(I)Br **F** salt regenerating the initial Ni(0) catalyst.

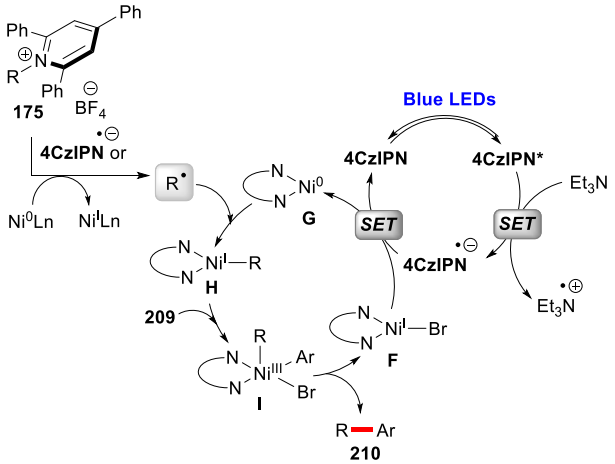

Scheme 80 Proposed mechanism for photocatalyzed Ni cross-coupling reactions between Katritzky salts and aryl halides.

An important milestone was reached with the work of the Aggarwal group on the radical borylation with Katritzky salts (Scheme 81).[141] In their research, Aggarwal and co-workers found that Katritzky salts **175** and bis(catecholato)diboron (B_2cat_2) in DMA as solvent underwent a deaminative borylation promoted by light but under catalyst-free conditions. The keystone of this protocol is the use of electron-rich B_2cat_2 enabling an electron donor-acceptor (EDA) complex with the electron-deficient pyridinium salts. This method displays a wide tolerance of functional groups and a broad scope of amines is reported furnishing the borylated products **211** in good to excellent yields. A further treatment with pinacol under basic condition leads to the corresponding ester **212** in good yields.

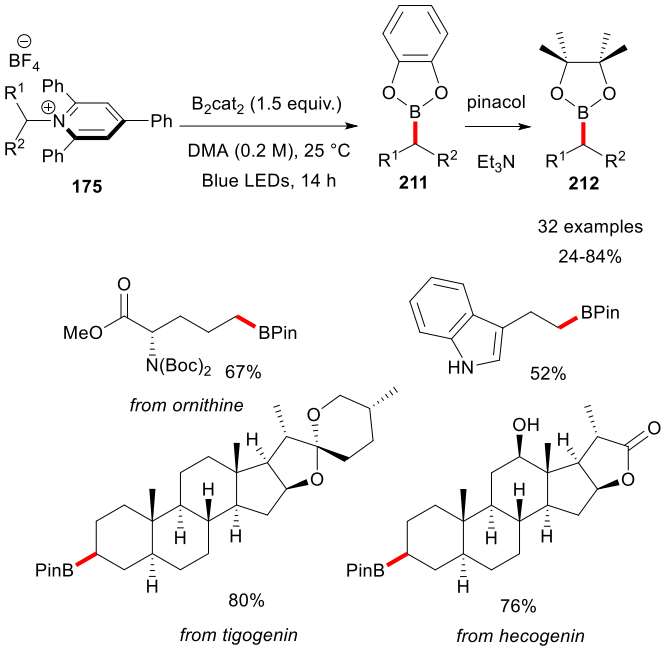

Scheme 81 Photoinduced deaminative borylation of Katritzky salts.

After a thorough study, the authors proposed a radical chain reaction mechanism as shown in scheme 82. First, an EDA complex **213** is formed *in situ* from pyridinium salt **175**, B_2cat_2 and DMA. The initiation SET step is induced by irradiation of the EDA complex **213** to give the radical ion pair **213a**. Fragmentation of **213a** gives the alkyl radical **214** and the boryl radical **215** as chain-propagating radicals, and the boron derivative **216** and triphenylpyridine (TPP) as by-products. The formed alkyl radical **214** reacts with B_2cat_2 to generate the radical intermediate **217**. After DMA complexation leading to **218**, fragmentation provides the expected boryl product **211** and boryl radical **215**. The latter reduces the Katritzky salt allowing radical chain propagation.

It should be noted that at the same time, the Glorius group disclosed a similar system for this deaminating borylation reaction.[142]

ARTICLE

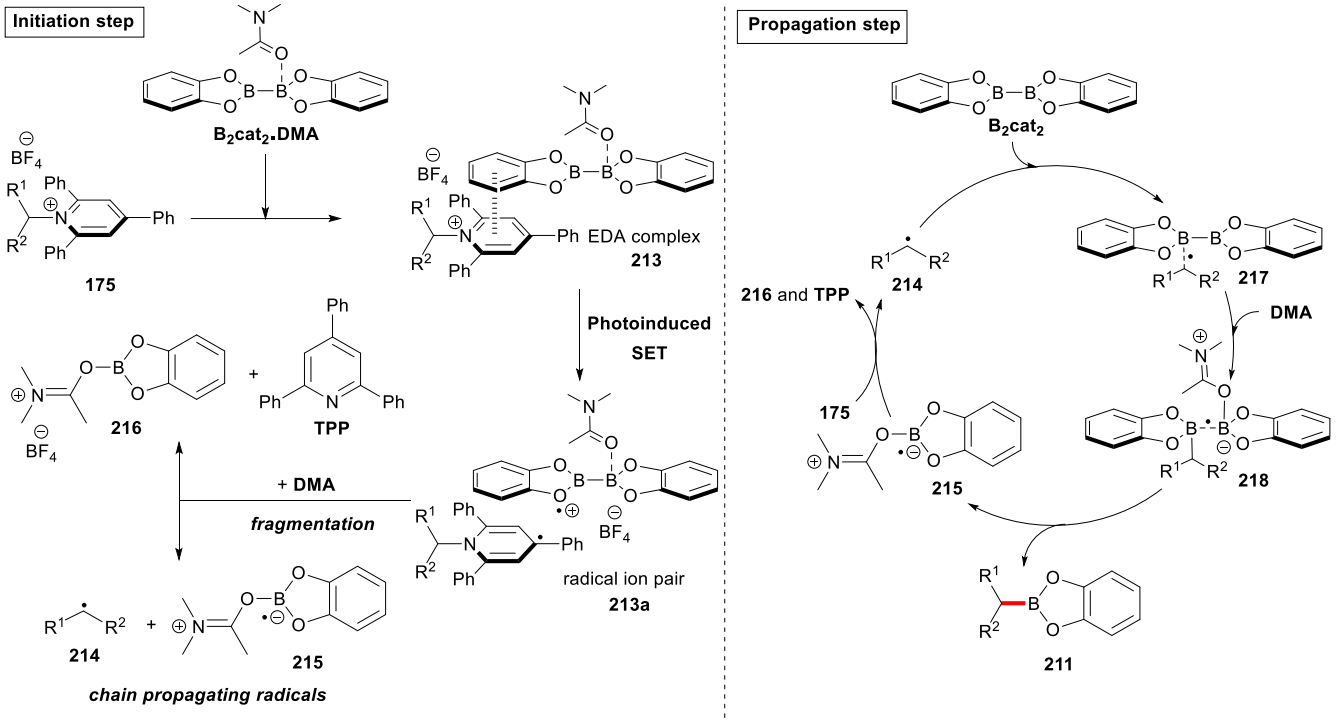

Scheme 82 Aggarwal's mechanism for EDA-mediated deaminative borylation.

In continuation of this research, Aggarwal and co-workers developed a photocatalyst-free deaminative method for Giese-type addition of Katritzky salt **175** onto activated alkenes **219** (Scheme 83).[143] Based on their previously reported work, the authors found that pyridinium salts combined with Hantzsch ester generate an EDA complex, which would undergo photo-induced SET under visible light irradiation. The generated alkyl radicals were successfully engaged in Giese-type addition leading to adducts **220**. This method was also applied to various transformations such as allylation, vinylation or alkynylation. A wide range of substrates with a high degree of functionalization was obtained, including the mexiletine derivative or the steroid tigogenin transformation.

A plausible mechanism, proposed by the authors, is described in scheme 84. The first step involves the formation of an EDA complex **221** between the Katritzky salt **175** and the Hantzsch ester. The photo-induced SET leads to the radical ion pair **222** which fragments to a C-centered radical **223** and the **TPP**. Subsequently, the alkyl radical adds to the electron-deficient alkene **219** to provide an intermediate **219a**, which would be converted to product **220** by hydrogen atom transfer with the dihydropyridine radical cation of the radical ion pair **222** or with the Hantzsch ester accompanied by the formation of pyridinium **224** or dihydropyridine radical **225**. It should be noted that the switch from Hantzsch ester to triethylamine gave the same result.

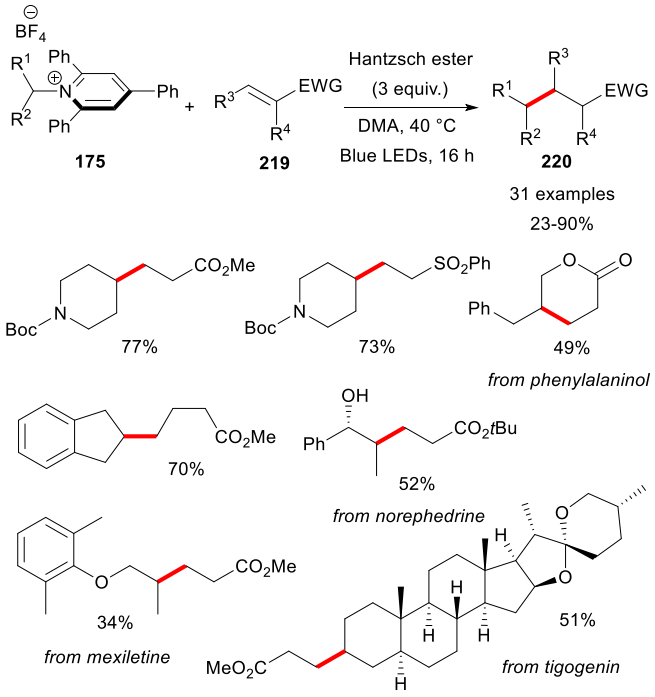

Scheme 83 Photoinduced deaminative Giese-type addition of Katritzky salts.

Other examples were subsequently disclosed. The Glorius group reported a similar system for the deaminative alkylation of electron-rich heteroarenes[144], Lou and co-workers developed a visible light-mediated alkylation of *N*-aryl tetrahydroquinolines[145], and Melchiorre and co-workers released a chemoselective alkylation of tryptophan-containing peptides. In each case, an EDA complex with Katritzky salts is involved.[146]

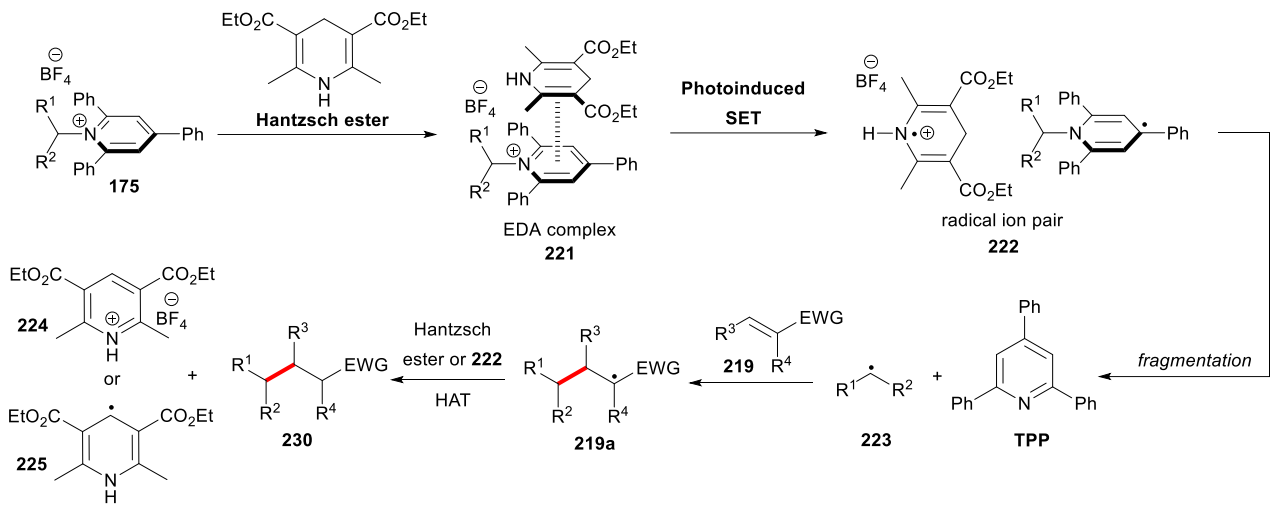

Scheme 84 Aggarwal's mechanism for photoinduced deaminative Giese-type addition of Katritzky salts.

D Sulphur-based alkyl derivatives

The development of sulfur precursors as a source of alkyl radicals is closely associated with the generation of the trifluoromethyl radical from the Langlois' reagent. The formation and use of this radical is the subject of a separate review in this special issue[147] and thus will not be discussed in this section. We will focus on recent sources of sulfur-based alkyl radicals.

D.1 alkylsulfinate salts

Alkylsulfinates represent an interesting reservoir of radicals. These salts are easily accessible or commercially available and have a low oxidative potential ($E_{1/2}^{red}$ = 0.595 V vs SCE for sodium 4-tetrahydropyran sulfinate) which makes them very attractive for an oxidation reaction. In 2017, Knauber and colleagues reported the photocatalyzed oxidation of alkylsulfinate salts as precursors of alkyl radicals.[148] The mechanism of this process was not established but it would follow a reductive quenching of the photocatalyst $Ru(bpy)_3Cl_2$ after photoexcitation with blue LEDs. SET between the photocatalyst and sulfinates leads to the generation of C-centered radicals after SO_2 extrusion, and the formed radicals could be engaged in a Giese-type addition. In addition, the alkylsulfinates were engaged in a metallaphotoredox catalytic process. The reaction of alkylsulfinate salts **226** and (hetero)aryl bromide **227** in the presence of $Ru(bpy)_3Cl_2$, $Ni(COD)_2$, and 2,2,6,6-tetramethyl-3,5-heptanedione (TMHD) under blue LEDs irradiation gave the desired coupling products

228 in moderate to good yields (Scheme 85). Mechanistically, a classical dual catalysis pathway is involved, where the Ni complex formed after oxidative addition traps the alkyl radical and furnishes the coupling compound.

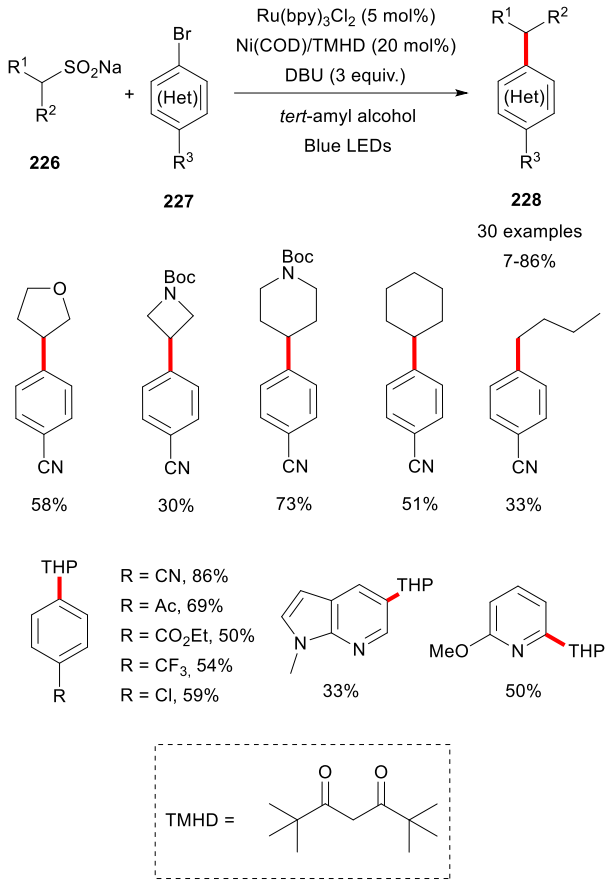

Scheme 85 Dual catalytic cross-coupling of (het)aryl bromides and alkyl sulfinates.

D.2 Alkylsulfinamides

In 2018, Quin demonstrated that alkylsulfinamide **229** could be engaged in a desulfurative strategy for the generation of alkyl radicals under photoredox conditions.[149] A large panel of alkyl radicals could be generated and successfully engaged into Giese-type addition on Michael acceptors **230** affording Giese adducts **231** in poor to excellent yields (Scheme 86).

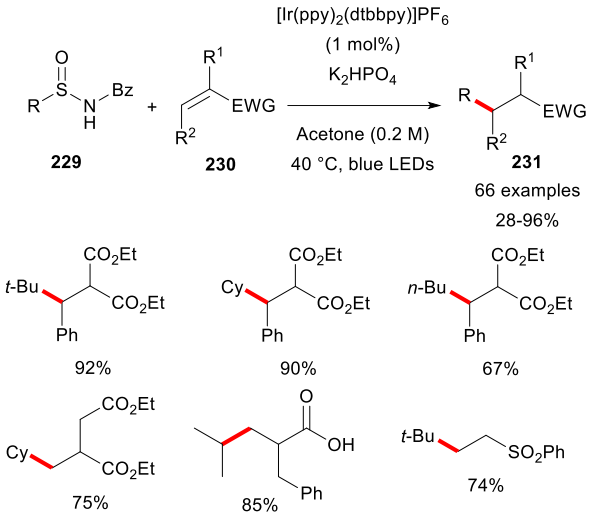

Scheme 86 Desulfurative Giese type addition of alkylsulfinamide.

To initiate the reaction, sulfinamides **229** were deprotonated with K_2HPO_4 to generate the corresponding sulfinamide anion **229a** (Scheme 87). The latter would be oxidized by the photoexcited photocatalyst $[Ir(dtbbpy)(ppy)_2]PF_6$ leading to the *N*-centered radical **229b** and the reduced $Ir^{(II)}$ species. Fragmentation of **229b** results in the formation of a C-centered radical that could add on the Michael acceptors **230**. The radical formed **230a** after addition is reduced by $Ir^{(II)}$ allowing the regeneration of the photocatalyst and the formation of the anion **230b** which is finally protonated to afford the desired product **231**.

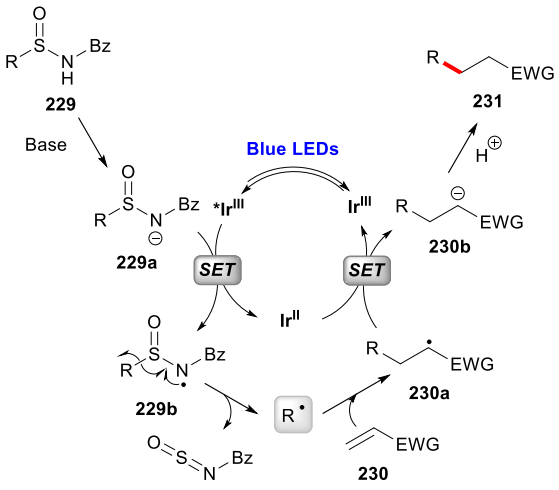

Scheme 87 Proposed mechanism for sulfinamide oxidation and the addition of alkyl radicals on Michael acceptors.

D.3 2-Mercaptothiazolinium salts

In 2019, Dilman introduced the use of 2-mercaptothiazolinium salts as a new source of alkyl radicals.[150] In contrast to the previous examples of sulphur based radical precursors, these electron-deficient salts exhibit low reductive potential ($E_{1/2}^{ox}$ = -0.82 V vs SCE for R = CH_2SiMe_3) suitable for

oxidative quenching. Methyl thiazolinium salts **232** could be prepared by direct methylation of the corresponding thiazolines with methyl triflate (Scheme 88, path a) or by reacting potassium 2-mercaptothiazoline with alkyl bromides followed by addition of methyl triflate (Scheme 88, path b). After screening the different reaction parameters, the authors found that thiazolinium salts **232** reacted smoothly with silyl enol ether **233** in the presence of $[Ir(dtbbpy)(ppy)_2]PF_6$ in DMPU as the solvent under blue LEDs irradiation to yield the alkylated ketones **234**.

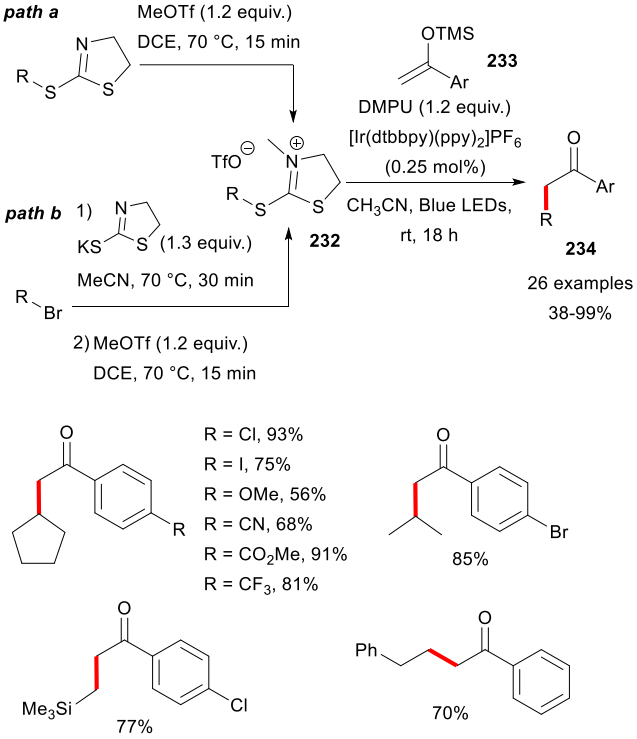

Scheme 88 Preparation of 2-mercaptothiazolinium salts and synthesis of alkylated ketones.

Upon photoexcitation, the $Ir^{(III)}$ complex ($E_{1/2}$ = -0.96 V vs SCE) in its excited state could reduce the thiazolinium salt **232** into the intermediate **232a** (Scheme 89). After C-S bond cleavage, the C-centered radical is generated and adds on enol ether **233**. The silyloxy radical **233a** is oxidized by the $Ir^{(IV)}$ species (or **232**) enabling the formation of the silyloxy carbocation intermediate **233b** and regenerating the photocatalyst in its ground state (or **232a**). Elimination of the trimethylsilyl group affords the addition product **234**.

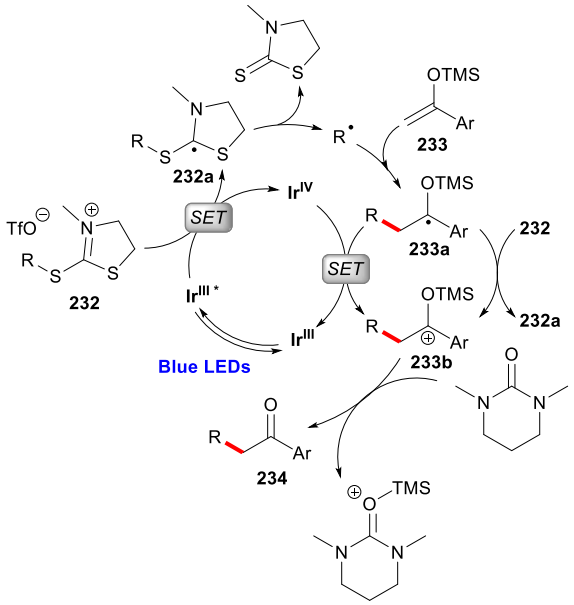

Scheme 89 Proposed mechanism for the reduction of 2-mercaptothiazolinium salts and ketone alkylation.

D.4 Alkyl tetrafluoropyridin-4-yl sulfides

In 2020, Dilman demonstrated that *gem*-difluoroalky tetrafluoropyridin-4-yl sulfides **235** can be used for the generation of *gem*-difluoroalkyl radicals.[151] The photoredox active group tetrafluoropyridine-4-thiol acts as an electron-deficient moiety exhibiting a low reductive potential (-1.36 V vs SCE for R = CH_2Ph). The preparation of **235** can be readily achieved by a photocatalyzed thiol-ene click reaction on difluorostyrenes with tetrafluoropyridine-4-thiol. After screening of reaction conditions, the authors have found that sulfides **235** reacted smoothly with silyl enol ether **236** in the presence of a photocatalyst in DMF as a solvent under blue LEDs irradiation to yield the alkylated ketones **237** (Scheme 90). The authors proposed two ways to promote this transformation from sulfides **235**. In method A, the high reducing organic photocatalyst 12-phenyl-12*H*-benzo[*b*]phenothiazine ($E_{1/2}^{red*}$ = -2.08 V vs SCE)[152] and zinc acetate were used. However, this method seems limited to electron-donor-substituted enol ethers. To overcome this drawback, a second system (Method B) involving the iridium-based photocatalyst $[Ir(dtbbpy)(ppy)_2]PF_6$ in combination with tetrabutylammonium iodide was developed.

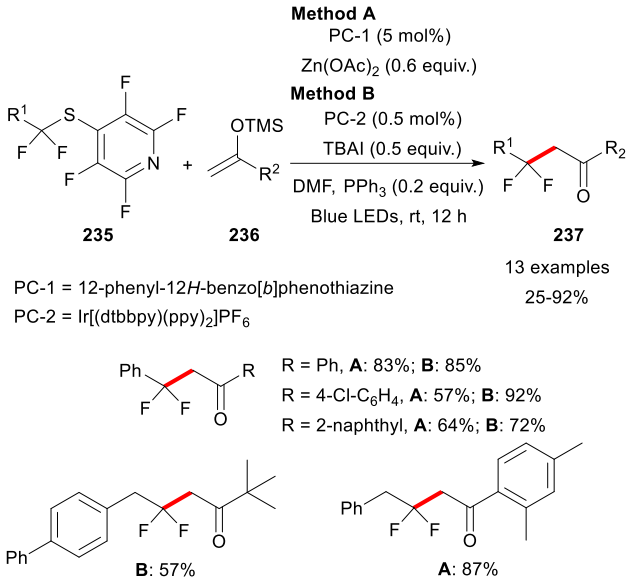

Scheme 90 Synthesis of difluoroalkylated ketones from *gem*-difluoroalkyl tetrafluoropyridin-4-yl sulfides **235**.

Note that an excess of borane pyridine complex in combination with *fac*-Ir(ppy)$_3$ can also be used as an alternative radical conditions. Activated alkenes such as acrylamides, acrylonitriles, acrylates or nitrones can be engaged leading to Giese-type addition products in good yields. However, this method is limited to *gem*-difluoroalkyl 4-tetrafluoropyridinyl sulfides.

Very recently, Dilman and co-workers developed an elegant approach for the synthesis of alkyl tetrafluoropyridin-4-yl sulfides **238** from unactivated alkanes and di-tetrafluoropyridin-4-yl disulfide *via* HAT process. As described for the *gem*-difluoroalkyl 4-tetrafluoropyridinyl sulfide anologues, the photoredox reaction occurred with enol ethers **239** in the presence of *fac*-Ir(ppy)$_3$ and zinc acetate under blue LEDs irradiation affording the alkylated ketones **240** (Scheme 91).[153] Other radical acceptors such as acrylamides, acrylates or heterocycles could be engaged affording the Giese-type and Minisci-type addition products respectively in moderate to good yields.

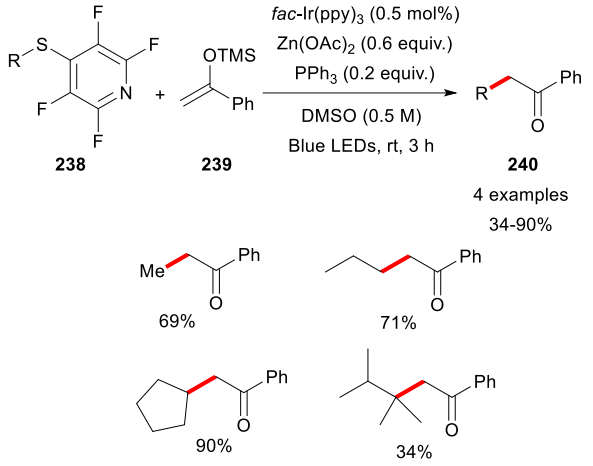

Scheme 91 Synthesis of alkylated ketones from alkyl tetrafluoropyridin-4-yl sulfides **238**.

D.5 Alkyl phenyl-tetrazole sulfones

In 2018, the Baran group introduced the use of alkyl phenyl-tetrazole sulfones **241** as a new source of alkyl radicals.[154] The phenyl-tetrazole sulfone represents the redox active group displaying an accessible potential ($E_{1/2}^{red}$ = -1.31 V vs SCE)[155] for oxidative quenching with low-valent metals or photocatalysts The authors demonstrated that sulfones **241** could be engaged with arylzinc chloride **242** in Negishi cross-coupling reaction in the presence of Ni(acac)$_2$ and bipyridine as a ligand (Scheme 92). An impressive reaction scope was disclosed with arylzinc reagents bearing electron-donating or electron-withdrawing substituents, giving products **243** in moderate to good yields. A series of successive syntheses using this method was reported as well as the late-stage synthesis of medicinal compounds.

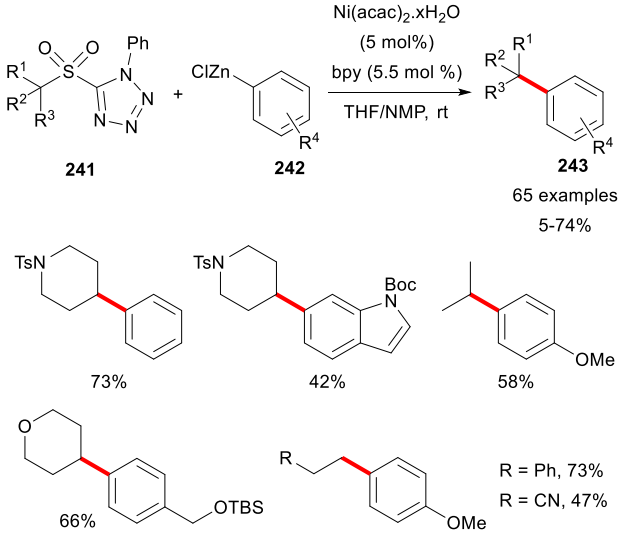

Scheme 92 Negishi cross-coupling reactions with alkyl phenyl-tetrazole sulfones **241**.

From a mechanistic point of view, the authors proposed a catalytic cycle similar to that described by Watson for the Suzuki-Miyaura cross-coupling reactions with $Ni(acac)_2$ and Katritzky salts (*vide supra*). A low valent aryl nickel complex can reduce the alkyl phenyl-tetrazole sulfone by SET and generate a radical anion intermediate that, after fragmentation, expels an alkyl radical, an ArNi(II) species and a sulfinic acid derivative. The two partners combine together and lead to a new ArNi(III) complex. Reductive elimination furnishes the desired cross-coupling product and restores an active Ni(I) intermediate.

D.6 Alkyl thianthrenium salts

Very recently, Shi introduced alkyl thianthrenium salts as a new and efficient source of alkyl radicals.[156] Thianthrenium salt can be readily obtained by nucleophilic substitution from thianthrene and triflate derivatives. Thianthrenium salts are electron-deficient structures with a reductive potential of -1.28 V vs $Ag/AgNO_3$.

During their investigations, Shi and co-workers found that thianthrenium salts **244** and bis(catecholato)diboron (B_2cat_2) in DMA as solvent underwent light-promoted desulfurative borylation but under catalyst-free conditions. As already mentioned for the borylation procedure with the Katritzky salts, the keystone of this protocol is the use of electron-rich B_2cat_2 enabling an electron donor-acceptor (EDA) complex with the electron-deficient thianthrenium salts. A wide range of substrates are reported, providing the borylated products **245** in good to excellent yields. Further treatment with pinacol under basic condition leads to the corresponding ester **246** in good yields (Scheme 93).

From a mechanistic point of view, the authors proposed a radical chain reaction as depicted in scheme 94. First, an EDA complex **247** is formed *in situ* from thianthrenium salt **244** and the B_2cat_2 / DMA adduct. The radical initiation step is induced by irradiation of the EDA complex **247** to give the alkyl radical, the boron derivative **248** and thianthrene as by-products. The formed alkyl radical reacts with B_2cat_2 / DMA adduct to generate the radical intermediate **249**. After fragmentation, the expected product **245** and the boryl radical **250** as chain-propagating radicals are generated. The latter reduces the thianthrenium salt **244** allowing radical chain propagation.

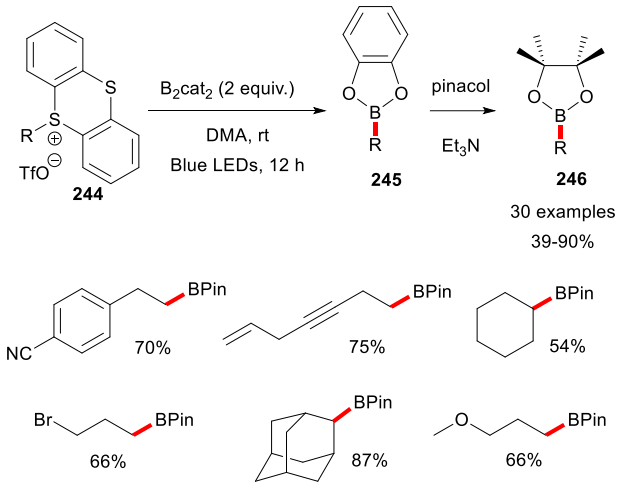

Scheme 93 Photoinduced borylation with thianthrenium salts.

As a promising perspective, Shi and co-workers successfully applied thianthreniums salts in Giese addition with acrylonitrile or vinyl phenyl sulfone in the presence of $[Ir(dtbbpy)(ppy)_2]PF_6$ as a photocatalyst and Hantzsch ester affording the 1.4-addition products in good yields. Encouraging results were also obtained in vinylation, alkynylation and Minisci reactions proving the high versatility of thianthrenium salts.

ARTICLE

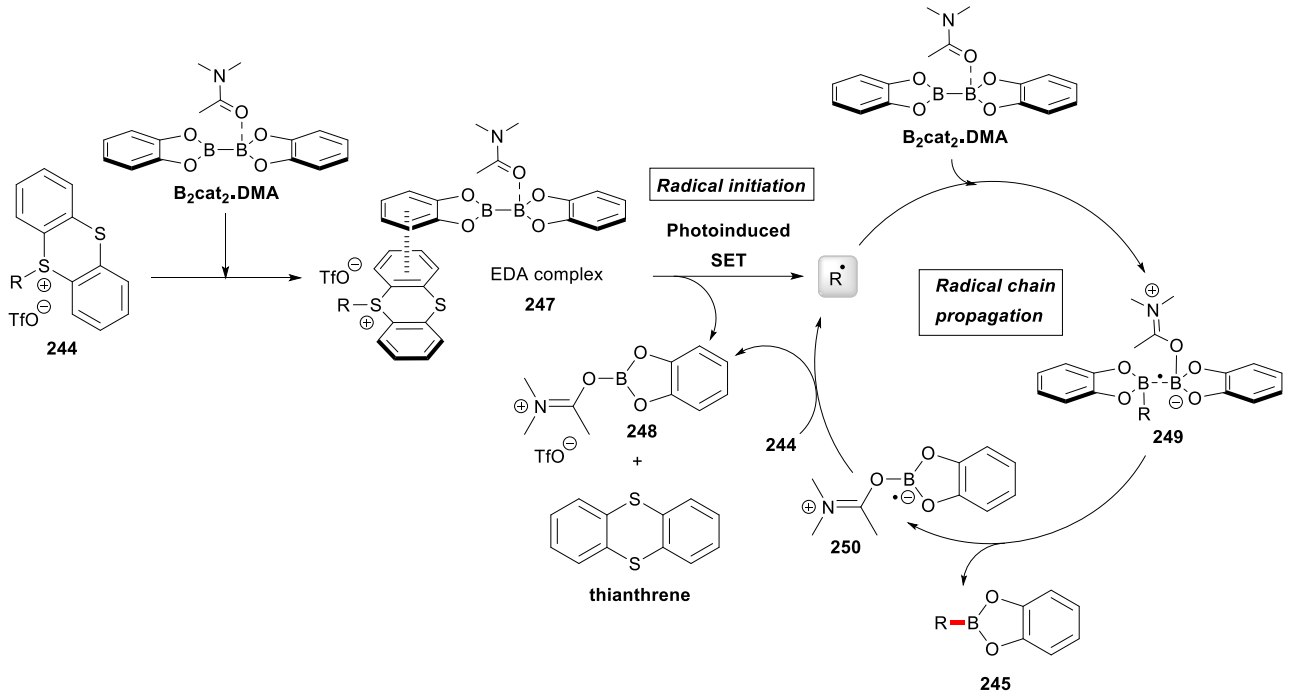

Scheme 94 Shi's mechanism for EDA-mediated borylation with thianthrenium salts **244**.

Conclusion

Focusing only on the chemistry of boron, silicon, nitrogen and sulfur derivatives for the generation of alkyl radicals by SET processes, mainly by photoredox, electrochemical or thermal means, it is clear how rich and versatile are the transformations that have been invented. This is reflected in the diversity of structures that have been generated, featuring notably alkynes, ketones, heterocycles, glycosides, fluorinated derivatives, cyclopropyl rings. Importantly, the generated alkyl radical could engage in a variety of transformation such as radical-polar cross over reactions, cross-coupling reactions via dual catalysis with nickel or palladium, asymmetric synthesis and late-stage functionalization. The speed and intensity of all these developments augur well for a future rich in new discoveries, in line with reinforced eco-compatibility specifications.

ARTICLE

Appendix

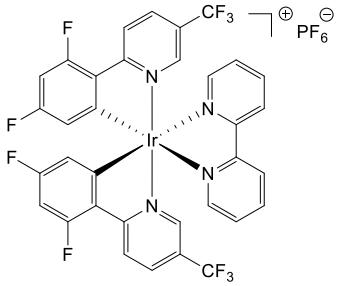

[Ir[dF(CF$_3$)ppy]$_2$(bpy)]PF$_6$

$E_{Ir(III)*/Ir(II)}$ = +1.32 V vs SCE

$E_{Ir(III)*/Ir(IV)}$ = -1.00 V vs SCE

λ_{max} excitation = 379 nm

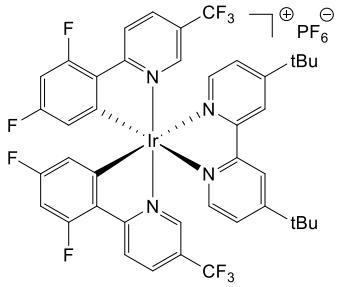

[Ir[dF(CF$_3$)ppy]$_2$(dtbbpy)]PF$_6$

$E_{Ir(III)*/Ir(II)}$ = +1.21 V vs SCE

$E_{Ir(III)*/Ir(IV)}$ = -0.89 V vs SCE

λ_{max} excitation = 380 nm

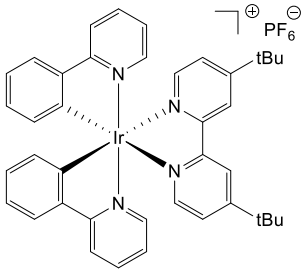

[Ir(dtbbpy)(ppy)$_2$]PF$_6$

$E_{Ir(III)*/Ir(II)}$ = +0.66 V vs SCE

$E_{Ir(III)*/Ir(IV)}$ = -0.96 V vs SCE

λ_{max} excitation = 380 nm

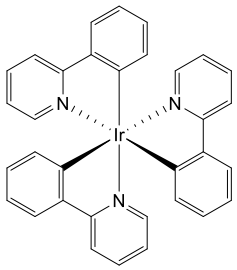

***fac*-Ir(ppy)$_3$**

$E_{Ir(III)*/Ir(II)}$ = +0.31 V vs SCE

$E_{Ir(III)*/Ir(IV)}$ = -1.73 V vs SCE

λ_{max} excitation = 375 nm

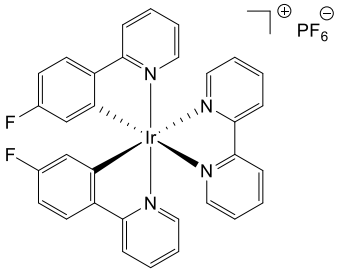

Ir(4-Fppy)$_2$(bpy)PF$_6$

$E_{Ir(III)*/Ir(II)}$ = +1.03 V vs SCE

$E_{Ir(III)*/Ir(IV)}$ = -0.89 V vs SCE

λ_{max} excitation = 380 nm

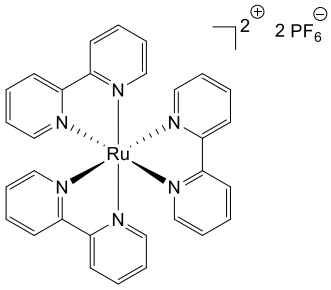

Ru(bpy)$_3$(PF$_6$)$_2$

$E_{Ru(II)*/Ru(I)}$ = +0.77 V vs SCE

$E_{Ru(II)*/Ru(III)}$ = -0.81 V vs SCE

λ_{max} excitation = 452 nm

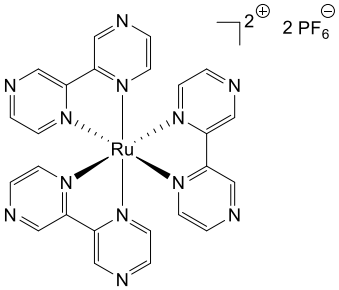

Ru(bpz)$_3$(PF$_6$)$_2$

$E_{Ru(II)*/Ru(I)}$ = +1.45 V vs SCE

$E_{Ru(II)*/Ru(III)}$ = -0.26 V vs SCE

λ_{max} excitation = 443 nm

Scheme 95 Structures and some photoredox properties of metal-based photocatalysts covered in this review.

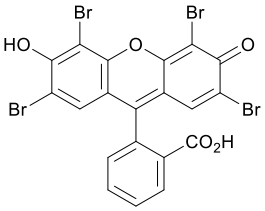

Eosin Y

$E_{PC^*/PC^{\bullet\ominus}}$ = +0.79 V vs SCE

λ_{max} excitation = 539 nm

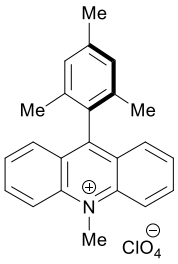

Mes-AcrClO$_4$

(Fukuzumi catalyst)

$E_{PC^*/PC^{\bullet\ominus}}$ = +2.06 V vs SCE

λ_{max} excitation = 430 nm

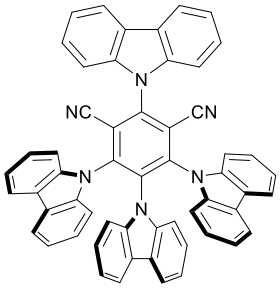

4CzIPN

$E_{PC^*/PC^{\bullet\ominus}}$ = +1.59 V vs SCE

λ_{max} excitation = 380 nm

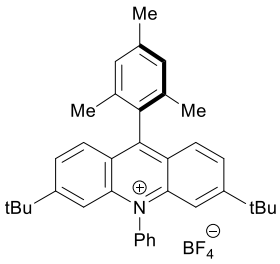

Di-tBu-Mes-AcrBF$_4$

$E_{PC^*/PC^{\bullet\ominus}}$ = +2.08 V vs SCE

λ_{max} excitation = 420 nm

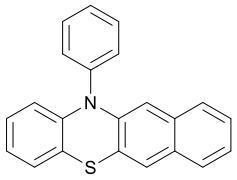

12-Ph-12*H*-benzo[*b*]phenothiazine

$E_{PC^*/PC^{\bullet\oplus}}$ = -2.08 V vs SCE

λ_{max} excitation = 376 nm

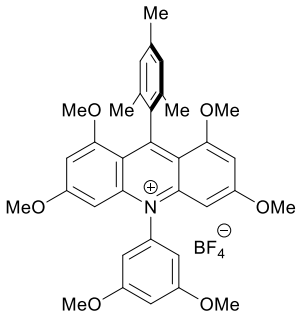

Mes-Acr-4-BF$_4$

$E_{PC^*/PC^{\bullet\ominus}}$ = +1.65 V vs SCE

λ_{max} excitation = 414 nm

Scheme 96 Structures and some photoredox properties of organic photocatalysts covered in this review.

Boron-based precursors

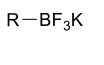

alkyl trifluoroborates

E^{ox} = +1.48 vs SCE

(for R = Cy)

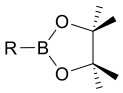

alkyl pinacol boronates

E^{ox} = N.A.

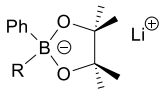

alkyl pinacol boronate / PhLi complex

E^{ox} = +0.31 V vs SCE

(for R = Cy)

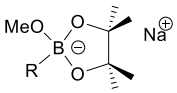

alkyl pinacol boronate / NaOMe complex

E^{ox} = +1.285 V vs SCE

(for R = Cy)

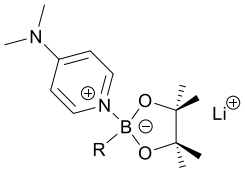

alkyl pinacol boronate / DMAP complex

E^{ox} = +0.81 V vs SCE

(for R = *p*-$MeOC_6H_4CH_2$)

alkyl boronic acids

E^{ox} > +2 V vs SCE

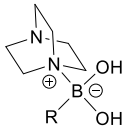

alkyl boronic acids / DABCO complex

E^{ox} = N.A.

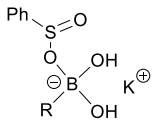

alkyl boronic acids / sulfinate complex

E^{ox} = +1.22 V vs SCE

(for R = Cp)

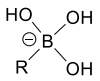

alkyl boronic acids / hydroxide complex

E^{ox} = N.A.

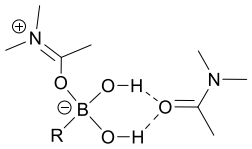

alkyl boronic acids / DMA complex

E^{ox} = +1.13 V vs SCE

(for R = $PhCH_2CH_2$)

Silicon-based precursors

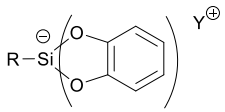

$Y^{\oplus}$ = $Et_4N^{\oplus}$, $K^{\oplus}$ [18-C-6], R'R"$_2NH^{\oplus}$

alkyl bis-catecholatosilicates

E^{ox} = +0.69 V vs SCE

(for R = Cy)

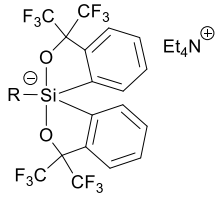

alkyl Martin's spirosilanes

E^{ox} = +1.47 V vs SCE

(for R = Cy)

alkyl pentafluorosilicates

E^{ox} = N.A.

alkyl trimethylsilanes

E^{ox} = +1.68 V vs SCE

(for R = Bn)

Nitrogen-based precursors

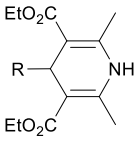

4-alkyl 1,4-dihydropyridines

E^{ox} = +0.89 V vs SCE

(for R = Bn)

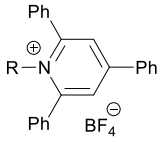

alkyl triphenylpyridinium salts (Katritzky salts)

E^{red} = - 0.93 V vs SCE

Sulfur-based precursors

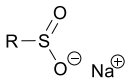

alkyl sulfinate salts

E^{ox} = +0.595 V vs SCE

(for R = 4-tetrahydropyran)

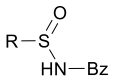

alkyl sulfinamides

E^{ox} = +0.43 V vs SCE

(for R = tBu)

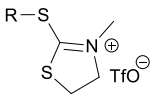

alkyl thiazolinium salts

E^{red} = -0.82 V vs SCE

(for R = Me_3SiCH_2)

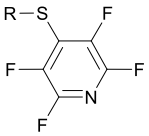

alkyl tetrafluoropyridin-4-yl sulfides

E^{red} = - 1.36 V vs SCE

(for R = Ph-CH_2-CF_2)

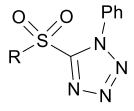

alkyl phenyl-tetrazole sulfones

E^{red} = -1.31 V vs SCE

(for R = *p*-F-C_6H_4-CH_2CH_2)

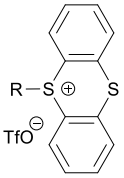

alkyl thianthrenium salts

E^{red} = -1.28 V vs $Ag/AgNO_3$

(for R = $PhCH_2$-CH_2)

Scheme 97 Structures and redox potentials of radical precursors covered in this review.

Author Contributions

The three authors share the writing of this review.

Conflicts of interest

There are no conflicts to declare.

Acknowledgements

The authors thank Sorbonne Université, CNRS and IUF for financial support.

Notes and references

1 G. Sorin, R. Martinez Mallorquin, Y. Contie, A. Baralle, M. Malacria, J.-P. Goddard and L. Fensterbank, *Angew. Chem. Int. Ed.*, 2010, **49**, 8721–8723.
2 Y. Nishigaichi, T. Orimi and A. Takuwa, *J. Organomet. Chem.*, 2009, **694**, 3837–3839.
3 C. Cazorla, E. Métay, B. Andrioletti and M. Lemaire, *Tetrahedron Lett.*, 2009, **50**, 6855–6857.
4 L. Chenneberg, C. Lévêque, V. Corcé, A. Baralle, J.-P. Goddard, C. Ollivier and L. Fensterbank, *Synlett*, 2016, **27**, 731–735.
5 S. Ding, S. Tian, Y. Zhao, Q. Ma, M. Zhu, H. Ren, K. Li and Z. Miao, *Synth.Commun.*, 2018, **48**, 936–945.
6 S. Ding, H. Ren, M. Zhu, Q. Ma, Z. Miao and P. Li, *Synth.Commun.*, 2021, **51**, 593–600.
7 S. Ding, Y. Zhao, Q. Ma, S. Tian, H. Ren, M. Zhu, K. Li and Z. Miao, *Chem. Lett.*, 2018, **47**, 562–565.
8 X. Jiang and P. Tang, *Org. Lett.*, 2020, **22**, 5135–5139.
9 Y. Yasu, T. Koike and M. Akita, *Adv. Synth. Catal.*, 2012, **354**, 3414–3420.
10 H. Huang, G. Zhang, L. Gong, S. Zhang and Y. Chen, *J. Am. Chem. Soc.*, 2014, **136**, 2280–2283.
11 D. Hanss, J. C. Freys, G. Bernardinelli and O. S. Wenger, *Eur. J. Inorg. Chem.*, 2009, **2009**, 4850–4859.
12 K. Miyazawa, Y. Yasu, T. Koike and M. Akita, *Chem. Commun.*, 2013, **49**, 7249–7251.
13 K. Miyazawa, T. Koike and M. Akita, *Adv. Synth. Catal.*, 2014, **356**, 2749–2755.
14 D. N. Primer, I. Karakaya, J. C. Tellis and G. A. Molander, *J. Am. Chem. Soc.*, 2015, **137**, 2195–2198.
15 T. Chinzei, K. Miyazawa, Y. Yasu, T. Koike and M. Akita, *RSC Adv.*, 2015, **5**, 21297–21300.
16 H. Huo, K. Harms and E. Meggers, *J. Am. Chem. Soc.*, 2016, **138**, 6936–6939.
17 H. Yan, Z.-W. Hou and H.-C. Xu, *Angew. Chem. Int. Ed.*, 2019, **58**, 4592–4595.
18 D. P. Plasko, C. J. Jordan, B. E. Ciesa, M. A. Merrill and J. M. Hanna, *Photochem. Photobiol. Sci.*, 2018, **17**, 1267–1267.
19 Y. Li, K. Zhou, Z. Wen, S. Cao, X. Shen, M. Lei and L. Gong, *J. Am. Chem. Soc.*, 2018, **140**, 15850–15858.
20 A. Hossain, A. Vidyasagar, C. Eichinger, C. Lankes, J. Phan, J. Rehbein and O. Reiser, *Angew. Chem. Int. Ed.*, 2018, **57**, 8288–8292.
21 J. Yi, S. O. Badir, R. Alam and G. A. Molander, *Org. Lett.*, 2019, **21**, 4853–4858.
22 J. A. Milligan, J. P. Phelan, V. C. Polites, C. B. Kelly and G. A. Molander, *Org. Lett.*, 2018, **20**, 6840–6844.
23 L. Zhang, Y. Chu, P. Ma, S. Zhao, Q. Li, B. Chen, X. Hong and J. Sun, *Org. Biomol. Chem.*, 2020, **18**, 1073–1077.
24 M. Roseau, N. Dhaouadi, C. Rolando, L. Chausset-Boissarie and M. Penhoat, *J. Flow. Chem.*, 2020, **10**, 347–352.
25 Z. Zuo, D. T. Ahneman, L. Chu, J. A. Terrett, A. G. Doyle and D. W. C. MacMillan, *Science*, 2014, **345**, 437–440.
26 J. C. Tellis, D. N. Primer and G. A. Molander, *Science*, 2014, **345**, 433–436.
27 O. Gutierrez, J. C. Tellis, D. N. Primer, G. A. Molander and M. C. Kozlowski, *J. Am. Chem. Soc.*, 2015, **137**, 4896–4899.
28 D. Takeda, M. Yoritate, H. Yasutomi, S. Chiba, T. Moriyama, A. Yokoo, K. Usui and G. Hirai, *Org. Lett.*, 2021, **23**, 1940–1944.
29 M. W. Campbell, J. S. Compton, C. B. Kelly and G. A. Molander, *J. Am. Chem. Soc.*, 2019, **141**, 20069–20078.
30 M. D. VanHeyst, J. Qi, A. J. Roecker, J. M. E. Hughes, L. Cheng, Z. Zhao and J. Yin, *Org. Lett.*, 2020, **22**, 1648–1654.
31 K. Nguyen, H. A. Clement, L. Bernier, J. W. Coe, W. Farrell, C. J. Helal, M. R. Reese, N. W. Sach, J. C. Lee and D. G. Hall, *ACS Catal.*, 2021, **11**, 404–413.
32 J. Khamrai, I. Ghosh, A. Savateev, M. Antonietti and B. König, *ACS Catal.*, 2020, **10**, 3526–3532.
33 K. Ohtsuka, S. Inagi and T. Fuchigami, *ChemElectroChem*, 2017, **4**, 183–187.
34 J. Luo, B. Hu, W. Wu, M. Hu and T. L. Liu, *Angew. Chem. Int. Ed.*, 2021, **60**, 6107–6116.
35 R. Rasappan and V. K. Aggarwal, *Nature Chem.*, 2014, **6**, 810–814.
36 C. Shu, A. Noble and V. K. Aggarwal, *Angew. Chem. Int. Ed.*, 2019, **58**, 3870–3874.
37 D. Kaiser, A. Noble, V. Fasano and V. K. Aggarwal, *J. Am. Chem. Soc.*, 2019, **141**, 14104–14109.
38 F. Clausen, M. Kischkewitz, K. Bergander and A. Studer, *Chem. Sci.*, 2019, **10**, 6210–6214.
39 D. Shi, C. Xia and C. Liu, *CCS Chem.*, 2020, **2**, 1718–1728.
40 F. Lima, M. A. Kabeshov, D. N. Tran, C. Battilocchio, J. Sedelmeier, G. Sedelmeier, B. Schenkel and S. V. Ley, *Angew. Chem. Int. Ed.*, 2016, **55**, 14085–14089.
41 F. Lima, U. K. Sharma, L. Grunenberg, D. Saha, S. Johannsen, J. Sedelmeier, E. V. Van der Eycken and S. V. Ley, *Angew. Chem. Int. Ed.*, 2017, **56**, 15136–15140.
42 F. Lima, L. Grunenberg, H. B. A. Rahman, R. Labes, J. Sedelmeier and S. V. Ley, *Chem. Commun.*, 2018, **54**, 5606–5609.
43 A. J. J. Lennox, J. E. Nutting and S. S. Stahl, *Chem. Sci.*, 2018, **9**, 356–361.

44 Y. Sato, K. Nakamura, Y. Sumida, D. Hashizume, T. Hosoya and H. Ohmiya, *J. Am. Chem. Soc.*, 2020, **142**, 9938–9943.
45 S. Ren, J. Fu, D. Cheng, X. Li and X. Xu, *Tetrahedron Lett.*, 2021, **66**, 152829.
46 F. Yue, J. Dong, Y. Liu and Q. Wang, *Org. Lett.*, 2021, **23**, 2477–2481.
47 Y. Iwata, Y. Tanaka, S. Kubosaki, T. Morita and Y. Yoshimi, *Chem. Commun.*, 2018, **54**, 1257–1260.
48 P. Ranjan, S. Pillitteri, G. Coppola, M. Oliva, E. V. Van der Eycken and U. K. Sharma, *ACS Catal.*, 2021, **11**, 10862–10870.
49 X. Li, M.-Y. Han, B. Wang, L. Wang and M. Wang, *Org. Biomol. Chem.*, 2019, **17**, 6612–6619.
50 M. Liu, H. Huang and Y. Chen, *Chin. J. Chem.*, 2018, **36**, 1209–1212.
51 Y. Yuan, Y. Zheng, B. Xu, J. Liao, F. Bu, S. Wang, J.-G. Hu and A. Lei, *ACS Catal.*, 2020, **10**, 6676–6681.
52 Claude. Chuit, R. J. P. Corriu, Catherine. Reye and J. Colin. Young, *Chem. Rev.*, 1993, **93**, 1371–1448.
53 Y. Nishigaichi, A. Suzuki and A. Takuwa, *Tetrahedron Lett.*, 2007, **48**, 211–214.
54 D. Matsuoka and Y. Nishigaichi, *Chem. Lett.*, 2014, **43**, 559–561.
55 V. Corcé, L.-M. Chamoreau, E. Derat, J.-P. Goddard, C. Ollivier and L. Fensterbank, *Angew. Chem. Int. Ed.*, 2015, **54**, 11414–11418.
56 A. Cartier, E. Levernier, V. Corcé, T. Fukuyama, A.-L. Dhimane, C. Ollivier, I. Ryu and L. Fensterbank, *Angew. Chem. Int. Ed.*, 2019, **58**, 1789–1793.
57 M. Jouffroy, D. N. Primer and G. A. Molander, *J. Am. Chem. Soc.*, 2016, **138**, 475–478.
58 C. Lévêque, L. Chenneberg, V. Corcé, J.-P. Goddard, C. Ollivier and L. Fensterbank, *Org. Chem. Front.*, 2016, **3**, 462–465.
59 N. R. Patel, C. B. Kelly, M. Jouffroy and G. A. Molander, *Org. Lett.*, 2016, **18**, 764–767.
60 N. R. Patel and G. A. Molander, *J. Org. Chem.*, 2016, **81**, 7271–7275.
61 B. A. Vara, M. Jouffroy and G. A. Molander, *Chem. Sci.*, 2016, **8**, 530–535.
62 M. Jouffroy, C. B. Kelly and G. A. Molander, *Org. Lett.*, 2016, **18**, 876–879.
63 C. Lévêque, V. Corcé, L. Chenneberg, C. Ollivier and L. Fensterbank, *Eur. J. Org. Chem.*, 2017, **2017**, 2118–2121.
64 H. Uoyama, K. Goushi, K. Shizu, H. Nomura and C. Adachi, *Nature*, 2012, **492**, 234–238.
65 C. Lévêque, L. Chenneberg, V. Corcé, C. Ollivier and L. Fensterbank, *Chem. Commun.*, 2016, **52**, 9877–9880.
66 F. L. Vaillant, M. Garreau, S. Nicolai, G. Gryn'ova, C. Corminboeuf and J. Waser, *Chem. Sci.*, 2018, **9**, 5883–5889.
67 J. Luo and J. Zhang, *ACS Catal.*, 2016, **6**, 873–877.
68 N. R. Patel, C. B. Kelly, A. P. Siegenfeld and G. A. Molander, *ACS Catal.*, 2017, **7**, 1766–1770.
69 S. T. J. Cullen and G. K. Friestad, *Org. Lett.*, 2019, **21**, 8290–8294.
70 J. P. Phelan, S. B. Lang, J. S. Compton, C. B. Kelly, R. Dykstra, O. Gutierrez and G. A. Molander, *J. Am. Chem. Soc.*, 2018, **140**, 8037–8047.
71 J. A. Milligan, K. L. Burns, A. V. Le, V. C. Polites, Z.-J. Wang, G. A. Molander and C. B. Kelly, *Adv. Synth. Catal.*, 2020, **362**, 242–247.
72 W. Luo, Y. Fang, L. Zhang, T. Xu, Y. Liu, Y. Li, X. Jin, J. Bao, X. Wu and Z. Zhang, *Eur. J. Org. Chem.*, 2020, **2020**, 1778–1781.
73 W. Luo, Y. Yang, Y. Fang, X. Zhang, X. Jin, G. Zhao, L. Zhang, Y. Li, W. Zhou, T. Xia and B. Chen, *Adv. Synth. Catal.*, 2019, **361**, 4215–4221.
74 J. A. Milligan, J. P. Phelan, V. C. Polites, C. B. Kelly and G. A. Molander, *Org. Lett.*, 2018, **20**, 6840–6844.
75 L. R. E. Pantaine, J. A. Milligan, J. K. Matsui, C. B. Kelly and G. A. Molander, *Org. Lett.*, 2019, **21**, 2317–2321.
76 E. Levernier, V. Corcé, L.-M. Rakotoarison, A. Smith, M. Zhang, S. Ognier, M. Tatoulian, C. Ollivier and L. Fensterbank, *Org. Chem. Front.*, 2019, **6**, 1378–1382.
77 A. Cartier, E. Levernier, A.-L. Dhimane, T. Fukuyama, C. Ollivier, I. Ryu and L. Fensterbank, *Adv. Synth. Catal.*, 2020, **362**, 2254–2259.
78 G. Ikarashi, T. Morofuji and N. Kano, *Chem. Commun.*, 2020, **56**, 10006–10009.
79 T. Morofuji, Y. Matsui, M. Ohno, G. Ikarashi and N. Kano, *Chem. Eur. J.*, , DOI:https://doi.org/10.1002/chem.202005300.
80 J. Yoshida, K. Tamao, T. Kakui, A. Kurita, M. Murata, K. Yamada and M. Kumada, *Organometallics*, 1982, **1**, 369–380.
81 T. Wang and D.-H. Wang, *Org. Lett.*, 2019, **21**, 3981–3985.
82 M. Uygur, T. Danelzik and O. G. Mancheño, *Chem. Commun.*, 2019, **55**, 2980–2983.
83 C. Ghiazza, L. Khrouz, T. Billard, C. Monnereau and A. Tlili, *Eur. J. Org. Chem.*, 2020, **2020**, 1559–1566.
84 N. Khatun, M. J. Kim and S. K. Woo, *Org. Lett.*, 2018, **20**, 6239–6243.
85 L. Ruiz Espelt, I. S. McPherson, E. M. Wiensch and T. P. Yoon, *J. Am. Chem. Soc.*, 2015, **137**, 2452–2455.
86 M. Silvi, C. Verrier, Y. P. Rey, L. Buzzetti and P. Melchiorre, *Nature Chem*, 2017, **9**, 868–873.
87 W. Dong, S. O. Badir, X. Zhang and G. A. Molander, *Org. Lett.*, 2021, **23**, 4250–4255.
88 P.-Z. Wang, J.-R. Chen and W.-J. Xiao, *Org. Biomol. Chem.*, 2019, **17**, 6936–6951.
89 C. Zheng and S.-L. You, *Chem. Soc. Rev.*, 2012, **41**, 2498–2518.
90 S. Fukuzumi, T. Suenobu, M. Patz, T. Hirasaka, S. Itoh, M. Fujitsuka and O. Ito, *J. Am. Chem. Soc.*, 1998, **120**, 8060–8068.
91 G. Li, R. Chen, L. Wu, Q. Fu, X. Zhang and Z. Tang, *Angew. Chem. Int. Ed.*, 2013, **52**, 8432–8436.
92 L. Cao, L. Zheng and Q. Huang, *J. Organomet. Chem.*, 2014, **768**, 56–60.
93 G. Li, L. Wu, G. Lv, H. Liu, Q. Fu, X. Zhang and Z. Tang, *Chem. Commun.*, 2014, **50**, 6246–6248.
94 W. Chen, Z. Liu, J. Tian, J. Li, J. Ma, X. Cheng and G. Li, *J. Am. Chem. Soc.*, 2016, **138**, 12312–12315.
95 K. Nakajima, S. Nojima, K. Sakata and Y. Nishibayashi, *ChemCatChem*, 2016, **8**, 1028–1032.
96 K. Nakajima, S. Nojima and Y. Nishibayashi, *Angew. Chem. Int. Ed.*, 2016, **55**, 14106–14110.
97 K. Nakajima, X. Guo and Y. Nishibayashi, *Chem. Eur. J.*, 2018, **13**, 3653–3657.
98 Á. Gutiérrez-Bonet, J. C. Tellis, J. K. Matsui, B. A. Vara and G. A. Molander, *ACS Catal.*, 2016, **6**, 8004–8008.
99 Á. Gutiérrez-Bonet, C. Remeur, J. K. Matsui and G. A. Molander, *J. Am. Chem. Soc.*, 2017, **139**, 12251–12258.
100 X. Chen, F. Ye, X. Luo, X. Liu, J. Zhao, S. Wang, Q. Zhou, G. Chen and P. Wang, *J. Am. Chem. Soc.*, 2019, **141**, 18230–18237.
101 J. Dong, F. Yue, W. Xu, H. Song, Y. Liu and Q. Wang, *Green Chem.*, 2020, **22**, 5599–5604.
102 H.-H. Zhang and S. Yu, *J. Org. Chem.*, 2017, **82**, 9995–10006.
103 H. Chen, D. Anand and L. Zhou, *Asian J. Org. Chem.*, 2019, **8**, 661–664.
104 Z.-Y. Song, C.-L. Zhang and S. Ye, *Org. Biomol. Chem.*, 2018, **17**, 181–185.

105 R. A. Angnes, C. Potnis, S. Liang, C. R. D. Correia and G. B. Hammond, *J. Org. Chem.*, 2020, **85**, 4153–4164.

106 S. O. Badir, A. Dumoulin, J. K. Matsui and G. A. Molander, *Angew. Chem. Int. Ed.*, 2018, **57**, 6610–6613.

107 A. V. Bay, K. P. Fitzpatrick, R. C. Betori and K. A. Scheidt, *Angew. Chem. Int. Ed.*, 2020, **59**, 9143–9148.

108 H.-H. Zhang, J.-J. Zhao and S. Yu, *J. Am. Chem. Soc.*, 2018, **140**, 16914–16919.

109 S. Xue, B. Limburg, D. Ghorai, J. Benet-Buchholz and A. W. Kleij, *Org. Lett.*, 2021, **23**, 4447–4451.

110 K. Zhang, L.-Q. Lu, Y. Jia, Y. Wang, F.-D. Lu, F. Pan and W.-J. Xiao, *Angew. Chem. Int. Ed.*, 2019, **58**, 13375–13379.

111 X. Huang and E. Meggers, *Acc. Chem. Res.*, 2019, **52**, 833–847.

112 L. Zhang and E. Meggers, *Acc. Chem. Res.*, 2017, **50**, 320–330.

113 G. E. M. Crisenza, A. Faraone, E. Gandolfo, D. Mazzarella and P. Melchiorre, *Nat. Chem.*, 2021, **13**, 575–580.

114 L. Buzzetti, A. Prieto, S. R. Roy and P. Melchiorre, *Angew. Chem. Int. Ed.*, 2017, **56**, 15039–15043.

115 C. Verrier, N. Alandini, C. Pezzetta, M. Moliterno, L. Buzzetti, H. B. Hepburn, A. Vega-Peñaloza, M. Silvi and P. Melchiorre, *ACS Catal.*, 2018, **8**, 1062–1066.

116 T. van Leeuwen, L. Buzzetti, L. A. Perego and P. Melchiorre, *Angew. Chem. Int. Ed.*, 2019, **58**, 4953–4957.

117 I. Kim, S. Park and S. Hong, *Org. Lett.*, 2020, **22**, 8730–8734.

118 C. G. S. Lima, T. de M. Lima, M. Duarte, I. D. Jurberg and M. W. Paixão, *ACS Catal.*, 2016, **6**, 1389–1407.

119 G. E. M. Crisenza, D. Mazzarella and P. Melchiorre, *J. Am. Chem. Soc.*, 2020, **142**, 5461–5476.

120 N. F. Eweiss, A. R. Katritzky, P.-L. Nie and C. A. Ramsden, *Synthesis*, 1977, **1977**, 634–635.

121 J. Grimshaw, S. Moore, J. Trocha-Grimshaw, K. Undheim, C. R. Enzell and K. Inoue, *Acta Chem. Scand.*, 1983, **37b**, 485–489.

122 F.-S. He, S. Ye and J. Wu, *ACS Catal.*, 2019, **9**, 8943–8960.

123 J. T. M. Correia, V. A. Fernandes, B. T. Matsuo, J. A. C. Delgado, W. C. de Souza and M. W. Paixão, *Chem. Commun.*, 2020, **56**, 503–514.

124 Y.-N. Li, F. Xiao, Y. Guo and Y.-F. Zeng, *Eur. J. Org. Chem.*, 2021, **2021**, 1215–1228.

125 C. H. Basch, J. Liao, J. Xu, J. J. Piane and M. P. Watson, *J. Am. Chem. Soc.*, 2017, **139**, 5313–5316.

126 F. J. R. Klauck, M. J. James and F. Glorius, *Angew. Chem. Int. Ed.*, 2017, **56**, 12336–12339.

127 M.-M. Zhang and F. Liu, *Org. Chem. Front.*, 2018, **5**, 3443–3446.

128 X. Jiang, M.-M. Zhang, W. Xiong, L.-Q. Lu and W.-J. Xiao, *Angew. Chem. Int. Ed.*, 2019, **58**, 2402–2406.

129 Z.-K. Yang, N.-X. Xu, C. Wang and M. Uchiyama, *Chem. Eur. J.*, 2019, **25**, 5433–5439.

130 F. J. R. Klauck, H. Yoon, M. J. James, M. Lautens and F. Glorius, *ACS Catal.*, 2019, **9**, 236–241.

131 M. Ociepa, J. Turkowska and D. Gryko, *ACS Catal.*, 2018, **8**, 11362–11367.

132 S. Plunkett, C. H. Basch, S. O. Santana and M. P. Watson, *J. Am. Chem. Soc.*, 2019, **141**, 2257–2262.

133 S. Ni, C.-X. Li, Y. Mao, J. Han, Y. Wang, H. Yan and Y. Pan, *Sci. Adv.*, 2019, **5**, eaaw9516.

134 H. Yue, C. Zhu, L. Shen, Q. Geng, K. J. Hock, T. Yuan, L. Cavallo and M. Rueping, *Chem. Sci.*, 2019, **10**, 4430–4435.

135 J. Liao, C. H. Basch, M. E. Hoerrner, M. R. Talley, B. P. Boscoe, J. W. Tucker, M. R. Garnsey and M. P. Watson, *Org. Lett.*, 2019, **21**, 2941–2946.

136 R. Martin-Montero, V. R. Yatham, H. Yin, J. Davies and R. Martin, *Org. Lett.*, 2019, **21**, 2947–2951.

137 C.-G. Yu and Y. Matsuo, *Org. Lett.*, 2020, **22**, 950–955.

138 F. T. Pulikottil, R. Pilli, R. V. Suku and R. Rasappan, *Org. Lett.*, 2020, **22**, 2902–2907.

139 J. Wang, M. E. Hoerrner, M. P. Watson and D. J. Weix, *Angew. Chem. Int. Ed.*, 2020, **59**, 13484–13489.

140 J. Yi, S. O. Badir, L. M. Kammer, M. Ribagorda and G. A. Molander, *Org. Lett.*, 2019, **21**, 3346–3351.

141 J. Wu, L. He, A. Noble and V. K. Aggarwal, *J. Am. Chem. Soc.*, 2018, **140**, 10700–10704.

142 F. Sandfort, F. Strieth-Kalthoff, F. J. R. Klauck, M. J. James and F. Glorius, *Chem. Eur. J.*, 2018, **24**, 17210–17214.

143 J. Wu, P. S. Grant, X. Li, A. Noble and V. K. Aggarwal, *Angew. Chem. Int. Ed.*, 2019, **58**, 5697–5701.

144 M. J. James, F. Strieth-Kalthoff, F. Sandfort, F. J. R. Klauck, F. Wagener and F. Glorius, *Chem. Eur. J.*, 2019, **25**, 8240–8244.

145 Y. Xu, Z.-J. Xu, Z.-P. Liu and H. Lou, *Org. Chem. Front.*, 2019, **6**, 3902–3905.

146 B. Laroche, X. Tang, G. Archer, R. Di Sanza and P. Melchiorre, *Org. Lett.*, 2021, **23**, 285–289.

147 H. Xiao, Z. Zhang, Y. Fang, L. Zhu and C. Li, *Chem. Soc. Rev.*, 2021, **50**, 6308–6319.

148 T. Knauber, R. Chandrasekaran, J. W. Tucker, J. M. Chen, M. Reese, D. A. Rankic, N. Sach and C. Helal, *Org. Lett.*, 2017, **19**, 6566–6569.

149 F. Xue, F. Wang, J. Liu, J. Di, Q. Liao, H. Lu, M. Zhu, L. He, H. He, D. Zhang, H. Song, X.-Y. Liu and Y. Qin, *Angew. Chem. Int. Ed.*, 2018, **57**, 6667–6671.

150 A. A. Zemtsov, S. S. Ashirbaev, V. V. Levin, V. A. Kokorekin, A. A. Korlyukov and A. D. Dilman, *J. Org. Chem.*, 2019, **84**, 15745–15753.

151 M. O. Zubkov, M. D. Kosobokov, V. V. Levin, V. A. Kokorekin, A. A. Korlyukov, J. Hu and A. D. Dilman, *Chem. Sci.*, 2020, **11**, 737–741.

152 D. Liu, M.-J. Jiao, Z.-T. Feng, X.-Z. Wang, G.-Q. Xu and P.-F. Xu, *Org. Lett.*, 2018, **20**, 5700–5704.

153 L. I. Panferova, M. O. Zubkov, V. A. Kokorekin, V. V. Levin and A. D. Dilman, *Angew. Chem. Int. Ed.*, 2021, **60**, 2849–2854.

154 R. R. Merchant, J. T. Edwards, T. Qin, M. M. Kruszyk, C. Bi, G. Che, D.-H. Bao, W. Qiao, L. Sun, M. R. Collins, O. O. Fadeyi, G. M. Gallego, J. J. Mousseau, P. Nuhant and P. S. Baran, *Science*, 2018, **360**, 75–80.

155 Y. Chen, N. McNamara, O. May, T. Pillaiyar, D. C. Blakemore and S. V. Ley, *Org. Lett.*, 2020, **22**, 5746–5748.

156 C. Chen, Z.-J. Wang, H. Lu, Y. Zhao and Z. Shi, *Nat Commun*, 2021, **12**, 1–9.